

天然水庫黏土（NRC）和 *S. pasteurii* 脲酶對水中重金屬鉛、鎘、砷

吸附及濁度之去除

林品芸¹、黃奕勛²、馬柔堤²、陳建易²

(1)中正大學化學暨生物化學系、(2)中正大學地球與環境科學系

重金屬鉛、鎘、砷為環境中持久且具有毒性的污染物，本研究利用天然水庫黏土與 *S. pasteurii* 產生的脲酶，降低水中重金屬鉛、鎘、砷濃度及濁度。實驗條件於 pH 7 條件下，用不同濃度的重金屬鉛、鎘、砷(20~1000 mg/L)，天然黏土 (0.01~0.7 g)，時間 (0~24 小時)，找出最佳去除對重金屬鉛、鎘、砷的條件，利用 X 射線螢光光譜儀(X-ray Fluorescence Spectrometer, XRF)及 X 射線衍射儀(X-ray Diffractometer, XRD)分析天然黏土主要成份為高嶺土及蒙脫石。重金屬吸附能力鉛>鎘>砷。吸附劑濃度 0.03 g 時，10 秒內可去除濃度 100 ppm 的鉛，60 秒內可去除 80 ppm 的鎘。在水中發現 *S. pasteurii* 脲酶能使水中濁度降低。結果顯示利用天然黏土與 *S. pasteurii* 脲酶能降低 99%以上的鉛，94%以上的鎘。以經驗常數($1 > n$)和吸附動力學(Langmuir 和 Freundlich)顯示，天然黏土吸附重金屬鉛和鎘，屬於單層吸附，較符合二階反應動力學。結果顯示天然水庫黏土與脲酶，能有效吸附重金屬並降低水中濁度。

中文關鍵字：重金屬去除、天然黏土、濁度、脲酶、等溫吸附、動力學

台灣西南海域冷泉系統中甲烷氧化菌之族群結構與甲烷消耗之關係

王韻茹¹、鄭資蓉²、陳貞年¹、塗子萱³、王珮玲²、林立虹¹

(1)臺灣大學地質科學系、(2)臺灣大學海洋研究所、(3)中山大學海洋科學系

台灣西南海域位於歐亞大陸板塊與菲律賓海板塊交界處，大陸邊緣受到板塊擠壓形成斷層構造，提供深部地層中甲烷向上移棲的管道，使此區域的海洋沉積物呈現高甲烷濃度及通量。根據 IPCC 於 2007 年的報告，海洋向大氣釋放的甲烷僅占大氣中含量 1~5%，顯示海洋沉積物中甲烷在擴散至海水層的過程中，存在著顯著的甲烷消耗機制。而甲烷氧化菌扮演著控制海洋與大氣中甲烷通量的重要角色。本研究利用勵進研究船於台灣西南海域四方圈合海脊及 G96 逸氣通道，以水下無人載具對甲烷滲漏區進行目標性的探勘觀測，並針對碳酸鹽礁、管蟲、貽貝與菌叢等冷泉生態系採集岩心。

根據間隙水甲烷與硫酸鹽資料，沉積物硫酸鹽-甲烷轉換帶深度約介於 5~10 公分內，與過去研究相比顯示，此區域存在高甲烷通量且存在甲烷消耗機制。利用次世代定序技術，對上述岩心樣本中所有微生物之 16SrRNA 基因與針對好氧甲烷氧化菌之 *pmoA* 基因以 97% 相似度進行群集組成分析，得到分屬於 90 種菌門的 147195 個操作分類單元，顯示環境中的微生物組成複雜，並存在高豐度的好氧與厭氧的甲烷氧化菌；透過及時定量聚合酶連鎖反應分析，近沉積物表層 1~8 公分處 *pmoA* 基因數量達峰值，而 ANME-1 與 ANME-2 的 16SrRNA 基因數量則隨沉積物深度增加，且與針對硫酸鹽還原菌之 *dsrB* 基因數量呈現正相關。經由樣本群集間 beta 多樣性的非度量多維度分析，顯示站點間群集組成差異大於站點內不同深度（高甲烷與硫酸鹽梯度）的群集組成差異。綜合上述，冷泉環境中沉積物微生物群集組成十分複雜且多樣，其豐度與組成除了反映現地地球化學的梯度，得以快速的代謝甲烷、硫酸鹽、有機質，亦受控於海床的特徵或位置，後續工作將進一步探討組成間的連動性與甲烷消耗機制的控制因子為何。

中文關鍵字：甲烷、甲烷氧化菌、冷泉、16SrRNA、*pmoA*

MIP 法製備高光催化性能之奈米氧化鋅生物白水泥砂漿

王敏峰¹、葉偉凡¹、黃奕勛¹、林品芸²、陳建易¹

(1)中正大學地球與環境科學系、(2)中正大學化學暨生物化學系

本研究主要利用 MICP(Microbial Induced Carbonate Precipitation)法於生物白水泥砂漿改良，並評估其應用於土木水利工程之探討。首先成功利用微生物誘導鋅沉澱方法填補白水泥材料中的微裂縫，可以降低其吸水率，並且成功結合水熱法合成出奈米氧化鋅。在吸水率方面，添加 2.5%四水硝酸鋅(鋅源)配比之生物白水泥砂漿與一般的白水泥砂漿相比可以下降 52.75%。在材料表面疏水性上，添加 2.5%的四水硝酸鋅配比之生物白水泥砂漿時，接觸角度高達 89.54°，相當接近疏水性材料之性質。在光催化性能方面，添加 2.5%的四水硝酸鋅配比之生物白水泥砂漿與一般的光催化白水泥砂漿相比，其光催化效率($\eta\%$)提升了 34.31%。在抗菌能力方面，含有鋅源配比之生物白水泥砂漿在模擬太陽光下具有 100%的抗菌效率。在成本方面，添加 2.5%的四水硝酸鋅配比之生物白水泥砂漿與一般的光催化白水泥砂漿相比，每立方公尺可以節省 149,531 元。實驗結果證明利用微生物誘導鋅沉澱技術結合水熱法製備生物白水泥砂漿，可成功改善白水泥砂漿特性，降低吸水率和親水性特性，防止水滲透所導致的問題，以及提高光催化能力以達到降解有機物和抗菌之成效。

中文關鍵字：微生物誘導沉澱、奈米氧化鋅、生物白水泥砂漿、光催化

利用微生物誘導碳酸鎘沉澱並經由鍛燒製備奈米氧化鎘

譚子翔¹、陳建易¹、黃奕勳¹、林品芸¹

(1)中正大學地球與環境科學系

使用 *SP* 與 *EC* 兩種不同的菌種，並經由微生物使水中鎘離子形成碳酸鎘沉澱，使用不同的溫度及時間鍛燒碳酸鎘沉澱物來製備奈米氧化鎘，經過 XRD、FTIR、SEM 及 TEM 分析經由不同溫度及時間鍛燒出的奈米氧化鎘，觀察晶格型態及差異。

中文關鍵字：氧化鎘



使用自製培養基改善微生物誘導碳酸鈣沉澱之技術並應用於

台中港揚塵防治

周郁翔¹、陳建易¹、黃奕勛¹、林品芸¹

(1)中正大學地球與環境科學系

台中港區域位於大甲溪出海口南側，由於此區域海流流向大多以西、北兩方向居多，會導致原本應該淤積於大甲溪出海口的河川漂沙被帶至台中港區域，再藉由北防波堤而停留在北側淤砂區。隨著淤積的灘地逐漸擴大，再加上此區域風向大多為東、北方向為大宗，這兩者引發揚塵並影響台中港及鄰近區域。

揚塵會對建築、農業、環境、人體等各方面造成威脅，為了抑制揚塵，本研究使用微生物誘導碳酸鈣沉澱（Microbial Induced Carbonate Precipitation, MICP）之技術來進行海沙固化，此種方法利用微生物新陳代謝的過程中伴隨產生尿素酶，並使用尿素酶加速尿素水解速度來生產銨根離子和碳酸根離子，並提供鈣源在土壤孔隙之間形成碳酸鈣結晶來達到固化的效果。不過此種方法目前成本較高，原因是在於細菌培養時使用的培養基價格較為昂貴，因此本實驗使用嘉義酒廠製酒過程中所產生之廢棄物酒糟，將其製作成培養基來取代原培養基，藉此在達到降低成本的同時又不影響固化效果。

本研究分為兩部分，第一部分為先驅實驗，對海沙樣本進行基本性質分析，包含粒徑分析、質地分析、孔隙率分析以及容積密度分析，與此同時，對微生物進行沉澱試驗和尿素酶實驗，確保微生物在酒糟培養基依然能生存，並生產尿素酶和形成碳酸鈣沉澱。在確認海沙和微生物性質後，即開始進行 MICP 防風定沙樣品製作，在此實驗中，我們以酒糟培養基來分別取代不同比例的 Tris-Yeast 培養基，並進行抗剪切強度與抗風蝕強度實驗，來確認降低成本並不會影響防風定沙的效果，之後進行後續驗證分析，包含場發射掃描式電子顯微鏡（Field Emission Scanning Electron Microscope, FE-SEM）、X 光粉末繞射儀（X-ray diffraction analysis, XRD）、碳酸鈣含量、數位偏光顯微鏡（Digital Polarizing Microscope）來確認是否有碳酸鈣結晶的形成，以確保防風定沙的效果是源自於 MICP 技術。

在先驅實驗的沉澱實驗中，我們發現以酒糟取代 Tris-Yeast 培養基並不會影響沉澱量太多，整體沉澱量大多維持在 1.4~1.9 g 之間；在抗剪強度實驗中，更可以發現完全以酒糟培養時，抗剪強度會大幅上升；在抗風蝕強度實驗中，不論以何種方式培養效果都差不多；而在之後的驗證分析中，不論是 FE-SEM，亦或是 XRD 皆有發現碳酸鈣結晶，並且碳酸鈣的含量確實有上升。由此可知，以酒糟作為培養基取代昂貴的培養基並應用於防風定沙是可行的。

中文關鍵字：微生物誘導碳酸鈣沉澱、揚塵、酒糟



微生物誘導沉澱應用於地下水中重金屬砷之去除研究

張伯宇¹、陳建易¹、黃奕勛¹、林品芸¹

(1)中正大學地球與環境科學系

因地下水中的重金屬含量通常皆會過高，根據行政院環境保護署公告之資料，地下水所含 10 種重金屬(砷、鎘、鉻、銅、鉛、汞、鎳、鋅、銻、鉬)，其中以砷的含量為最高，所以本研究選用優勢菌種簡稱為之 SP 細菌結合共沉澱技術，過濾工廠含砷廢水，根據不同細菌濃度及沉澱時間，以觀察沉澱物對於重金屬砷的淨化能力，使民眾平常使用的地下水所含重金屬含量降低，以保全民眾身體健康水，是人一生中不可或缺的物質，可以一日不食，卻不能一日不飲水，而根據行政院環境保護署公告之地下水所含重金屬高達 10 種，嘉義之地下水，其中以砷含量為最高，為使民眾盡可能的不使用到此種地下水，將使用專業技術試圖淨化水質。

中文關鍵字：細菌、共沉澱技術、砷、地下水



**Fold-thrust belt-related deformation bands in porous sandstone:
A study on the late Pliocene to early Pleistocene Cholan sandstone
downstream of Chichi weir, central Taiwan**

Nguyen Thi Lan Chi¹、Wen-Jeng Owen Huang²

(1)Graduate Institute of Applied Geology, National Central University、

(2)Department of Earth Sciences, National Central University

This study is concerned with the description, classification, analysis and interpretation of Chushiang fault-related deformation bands (DBs) based on field observation and microscopic observation. DBs are common structural elements that can be found in the late Pliocene to early Pleistocene Cholan sandstones distributed downstream of Chichi weir along the Zhuoshui River in the frontal part of the fold-thrust belt in central Taiwan. One fold train appears in the hanging wall of the east-dipping Chushiang left-lateral reverse fault and is composed of one tight asymmetric anticline to the east and the other gentle symmetric syncline to the west with a wavelength of hundreds of meters. The DBs occur in moderate sorted, fine to coarse sandstone layers. Most of the DBs is bounded by the two axial surfaces of the anticline and syncline and fall into three sets with orientations of 035°/45°SE, 135°/53°SW, and 000°/~80° W to 80°E, respectively. In addition, DBs that appear in the area between fault trace and syncline axial trace are obvious under microscopic but ambiguous on the outcrop and they evolve into becoming fractures. However, in the eastern limb of the anticline, the DBs sub-parallel to the bedding plane or close to some minor fault with orientation parallel to the fault trace. Based on my microscopic observation, these DBs are disaggregation bands and represent the result of the compaction regime. In contrast, DBs that appear in between the anticline axis and fault trace are cataclastic DBs. Such evidences (include DBs occurrences and microstructures) indicate the origin of these cataclastic DBs highly related to the Chushiang faulting. These preliminary observations show these DBs commonly appear in this fault or fault-affected zone and the factors controlling their development include lithology, proximity to the fault, and position on folds induced by faulting. In short, the DBs can serve as paleo-stress intensity indicator in this case.

Keywords: Chushiang fault, Cholan Formation, sandstone, deformation band

低速至高速旋剪儀實驗試體之鐵氟龍污染影響的量化

黃柏崴¹、董家鈞¹

(1)中央大學應用地質研究所

相較於過去傳統土壤剪力試驗(三軸、直剪試驗)，低速至高速旋剪儀可對試體進行長位移剪切之優勢。當研究試體為黏土粉末時，為防止試體粉末於旋剪試驗過程中溢出，試體粉末須以夾具包覆。選擇低摩擦性之鐵氟龍作為夾具降低其摩擦特性對旋剪試驗之影響。然而高速旋剪試驗中，鐵氟龍恐因摩擦熱變質或受剪磨損進而侵汙試體外圍，恐有影響實驗結果之疑慮。前人研究有將在經正向應力 1 MPa 以及滑移速度 1 m/s 下，使用高嶺土進行旋剪實驗後之受剪後試體做鐵氟龍汙染含量的量化分析，然而並未仔細考量鐵氟龍在試體中的汙染分布。故本研究採用經正向應力 1 MPa、滑移速度 1 m/s 旋剪試驗後之受剪氣乾高嶺土，進行試體外圍半徑 12.5-7.0 毫米的局部取樣及整個試體的均勻取樣，結合 X 光繞射儀及熱微差掃描分析儀以量化鐵氟龍於高嶺土粉末中之汙染含量，並比較均勻取樣及局部取樣的結果。均勻取樣之結果顯示，其鐵氟龍含量約在 1% 左右，未來將與局部取樣之結果進行比較，預期得到更高之鐵氟龍汙染含量。

中文關鍵字：旋剪試驗、氣乾高嶺土、鐵氟龍汙染



山崩潛感因子最適量測尺度探討－以石門水庫集水區為例

繆念澤¹、李錫堤¹

(1)中央大學應用地質研究所

良好的山崩潛感模型可提供適當的山崩災害預估，並作為製圖、工程選址、防災決策等依據，因此選取高效度潛感因子供建立潛感模型可謂重要。山崩潛感因子常取自於地形、地質等及區位尺度有關之因子，一般以潛感因子所使用之網格數值地形模型(DTM)及其他網格資料之網格解析度或網格大小定義尺度大小。從過往研究可知地形資料在不同的量測尺度下其輸出值會有所不同，這可能多少影響山崩潛感模型之表現。然而過往山崩潛感分析所使用的因子多為同一尺度，並未真正考量因子尺度對於山崩潛感模型之影響。

欲改變因子尺度時可內插產生較小之網格資料，或以重新取樣之方式產生較大之網格資料。但在實際運用上，近年國外學者是以不同大小的移動視窗先對原始DTM做平滑化，再以3x3核心產製各尺度因子，並分別評估各尺度因子之效度，以找出最適尺度之因子作為模型建立依據。本研究除了以平滑化移動視窗法建立不同尺度之因子外，試圖再以大核心網格法建立不同尺度之因子，做為比較之用。

本研究先在石門水庫集水區建立艾利(2004)、馬莎(2005)、辛樂克(2008)、蘇力(2013)等四個颱風事件誘發山崩目錄，找出各個颱風事件下，各個潛感因子的最適測量尺度，探討不同事件下最適測量尺度的異同，再利用各事件下最適尺度因子建立每一個事件的山崩潛感模型，比較每一個模型的成功率及預測率相較於原始模型的改善情形。最後將對因子最適量測尺度的方法學做成結論與建議。

中文關鍵字：大核心網格法、平滑化移動視窗法、潛感因子最適量測尺度

台灣板岩重力變形的控制因子分析

鐘暉翔¹、李錫堤¹

(1)中央大學應用地質研究所

台灣板岩帶的劈理位態大致呈東北-西南走向，向東南高角度傾斜。高角度劈理在重力作用下會發生下坡潛變現象；在順向坡處發生緩慢的拱彎變形(buckling)，而在逆傾坡處發生漸進式的撓曲變形(flexuring)。當變形持續累積時會使劈理角度變緩且岩體風化破碎，在豪大雨期間可能會有滑動致災之虞。板岩邊坡的調查研究在台灣已有多項計畫進行，累積了許多調查報告與資料，可供進行控制因子分析，但對於影響變形速率的各項因子尚未有深入探討及分析。

本研究利用中央地質調查所多年期大型崩塌調查計畫與農業委員會水土保持局大規模崩塌調查計畫中許多位於板岩坡的報告資料，整理出各鑽孔的滑動監測資料、岩心鑽探報告及水位監測資料等等，選取若干不同因子進行研究。所採用的岩體因子有：破碎程度、風化程度、板岩比例、劈理傾角等。地下水類因子有：地下水位深度、最大地下水位上升高度等。變形因子則包括：岩盤頂面變形速率，滑動面變形速率、變形最大深度等。整理完各項因子資料後，先針對各個控制因子與各個變形因子進行相關分析(correlation analysis)，挑選出相關性高的因子做為控制因子。最後運用多元迴歸方法建立板岩重力變形的潛感模型，供台灣各板岩坡重力變形程度之預估。

中文關鍵字：板岩、重力變形、控制因子、相關性分析、多元迴歸

以尤拉－拉格朗日耦合分析崩塌過程：以四川新磨崩塌為例

林亭妤¹、林冠璋¹

(1)成功大學地球科學系

近年來，有限元素分析常被運用於模擬崩塌的發生機制與運動過程，而傳統用於分析崩塌發生機制的有限元素分析常使用拉格朗日網格，其分析模型能承受之網格變形程度有限，無法模擬較大變形的情況。為模擬快速運動的大型崩塌，本研究採用尤拉-拉格朗日耦合分析，以尤拉網格分析排除拉格朗日分析於網格嚴重扭曲時無法進行計算的問題，並以 2017 年四川新磨村大型崩塌為例，模擬土石塊體崩落的過程及堆積狀況。土石材料在邊坡上的分布狀況也是影響崩塌運動過程的重要因素之一，本研究亦考量不同的材料分布情境，模擬崩塌過程的塊體運動行為。模擬結果顯示，當考量邊坡上有剝刮材料時，塊體最大運動速度達到 55 m/s。如果考量邊坡上有剝刮材料或邊坡下方具有舊崩積材料時，模擬之崩塌影響範圍便會最吻合實際崩塌後材料的堆積狀況。

中文關鍵字：數值模擬、尤拉-拉格朗日耦合分析、新磨崩塌



New evidence of high-pressure metamorphism in mafic schist from the Wanjung area, Yuli belt, eastern Taiwan

Enggar Wisnu Cahyaning Ratri¹、Chin-Ho Tsai¹、Yu-Wei Zhang¹、

Yui Kouketsu²、Yoshiyuki Iizuka³

(1)Department of Natural Resources and Environmental Studies, National Dong-Hwa University、

(2)Graduate School of Environmental Studies, Nagoya University, Japan、

(3)Institute of Earth Sciences, Academia Sinica, Taiwan

The Yuli belt is considered as a high-pressure (HP) metamorphic terrane, owing to the presence of glaucophane and omphacite in some rocks related to serpentinite. In the Wanjung area, metagabbro, serpentinite, and mafic schist are associated with metasedimentary schist. HP metamorphism in this area is only represented by omphacitic rock within serpentinite (Yui and Lo, 1989). In this study, we report a new finding of relict Na-amphibole in garnet-bearing mafic schist and amphibole-albite schist. The studied outcrop contains mafic schist with intercalated layers of garnet-bearing mafic schist (Type 1), amphibole-albite schist (Type 2), and barroisitic schist (Type 3). The peak mineral assemblages of these rock types are garnet + quartz + epidote + rutile ± glaucophane (Type 1), glaucophane + garnet + quartz + epidote (Type 2), and barroisite + garnet + quartz + epidote (Type 3). Centimeter-sized porphyroclastic garnet in Type 1 shows partially honeycomb texture in which thin garnet surrounds quartz grains. Honeycomb garnet is rare and commonly reported from HP/UHP rocks in some orogenic belts (Hawkins et al., 2007). Glaucophane only occurs as rare inclusions within albite. Amphibole compositional zoning in Type 2 from core to rim is glaucophane → barroisite → actinolite and in Type 3 is barroisite core to actinolite rim, suggesting retrograde recrystallization. We applied quartz Raman barometry (Enami et al., 2007; Kouketsu et al., 2014) and garnet-hornblende geothermometer (Graham and Powell, 1984) on Type 3, and obtained *P-T* conditions of 1.4-1.5 GPa and 495-503 °C, which indicate subduction metamorphism. Our finding suggests that HP metamorphism in the Wanjung area is not limited to omphacitic rock only.

Keywords: glaucophane, honeycomb garnet, subduction, Yuli belt

不同粒徑大小三水鋁石之熱行為與動力學探討

莊人豪¹、鄧茂華¹

(1)臺灣大學地質科學系

三水鋁石由氫氧化鋁所組成，經熱分解可產生氧化鋁與水，在工業上具有諸多應用，故為一種相當重要的礦物。然而，三水鋁石可能同時具有兩種不同的反應途徑：完全脫水形成 γ -氧化鋁、以及不完全脫水形成軟水鋁石。此性質由三水鋁石的粒徑大小所控制，粒徑越小則反應將趨向於單一。本研究即是利用不同粒徑之三水鋁石粉末進行熱重實驗，並藉由主導動力學曲線模型與 Avrami 方程式等兩種動力學模型探討三水鋁石熱分解反應之動力學性質。其中，主導動力學曲線模型以實驗數據為基礎，無須事先得知反應機制即可求得反應預測曲線，因此相當適合預測任意升溫歷程之反應；Avrami 方程式則為研究結晶過程之動力學模型，並可用於探討反應機制是否發生改變。

中文關鍵字：三水鋁石、粒徑大小、熱行為、主導動力學曲線模型、Avrami 方程式



台灣主要地層之熱導係數研究

華智祥¹、許鶴瀚¹、江協堂²

(1)臺灣大學海洋研究所、(2)宜蘭大學通識教育中心

前人的研究認為臺灣擁有相當高的地熱潛能，地層的熱導係數為評估地熱潛能的重要參數之一，本研究將有系統性的測量臺灣地層的熱導係數，過去一年來總計費時 21 天，於西部麓山帶、雪山山脈、脊樑山脈、海岸山脈、恆春半島等地質區的主要地層露頭，鑽取直徑 6 公分、長 10~30 公分的岩心或採集岩石樣本，共計於 40 個地層中採了 105 個樣本，樣本經磨平處理後，以 ISOMET 熱導係數儀測量其熱導係數。測量結果發現，熱導係數最大值($\sim 4.77 \text{ Wm}^{-1}\text{K}^{-1}$)為雪山山脈始新世時期的四稜砂岩，最小值($\sim 1.14 \text{ Wm}^{-1}\text{K}^{-1}$)為西部麓山帶中新世時期的南莊層，推測雪山山脈的四稜砂岩由於其礦物組成多為導熱程度高的石英組成，因此熱導係數偏高，西部麓山帶的南莊層可能因孔隙率高，因此熱導係數偏低。另外，海岸山脈地質區整體的熱導係數是所有地質區當中最底的($\sim 1.49 \text{ Wm}^{-1}\text{K}^{-1}$)，推測其岩石多為海洋性沉積物組成，膠結性差。若是以地理上做分類，會發現臺灣中央山脈的熱導係數皆大於海岸山脈，推測中央山脈的主要岩石多為石英含量高的沉積岩和變質岩，而海岸山脈的岩石多為雲母、黏土礦物這些導熱程度低的礦物組成。本研究所展示這些系統性的熱導係數量測結果，可提供未來研究臺灣熱流估算的參考。

中文關鍵字：熱導係數、地熱探勘、熱流、岩石熱傳導

Rock physics parameters estimations of gas-hydrate and free gas concentrations in Formosa Ridge, offshore SW Taiwan

Dipika Anggun Ardianti¹、How-Wei Chen¹

(1)Institute of Geophysics, National Central University

Rock physics parameters usually can be estimated through well log-based analysis approaches with various proposed models and empirical equations. We propose a strategy which treat seismic data as a pseudo-log then combine post- and pre-stack modeling and inversion efforts for rock physics study. The approach helps to identify gas hydrate, free gas and its host lithology with fluids existence in Formosa Ridge Off., Southwestern Taiwan. We developed four steps workflow. First, we refined velocity model suggested from conventional NMO stack with semblance analysis. Second, the synthetic CMP gathers are created by reflectivity and convolutional approach respectively. If synthetic and real gather are fit in both offset domains, then confirms the estimated parameters. Third, initial impedance model derived from convolutional and reflectivity method are used separately in post- and pre-stack procedure. Once we have the P- S-impedance model and source wavelets extraction from offset-dependent dataset, then post- and pre-stack inversion were implemented sequentially to extract the best resolvable models. Pre-stack inversion based on three assumptions (a) linearized approximation for reflectivity, (b) angle-dependent Fatti's equation and (c) linear relationship among P-, S-impedance and density. The inferred basic parameters including V_p , V_s and density are the key efforts for further rock physics estimations. The parameters including porosity, bulk-shear modulus, resistivity, and water saturation for understanding the lithology conditions can be obtained through empirical equations. The results can assist us to evaluate the interrelationships among the derived parameters through cross-plots and delineate the potential gas hydrate and free gas concentration zones. The proposed approach enables us to obtain petro-physical properties with the hope that additional feasibility evaluation and confirmation from borehole data will be available in the future.

Keywords: seismic inversion, post-pre-stack, rock physics, gas-hydrate, free gas, pseudo-logs

鐵鎂鋁榴石在高壓下之熱傳導率變化

洪瑜苹¹

(1)中央研究院地球科學研究所

地球內部的熱流影響著地球的熱結構、動力學甚至是地球演化，其中影響熱流的一項因素為物質的熱傳導率。我們長期的目標是希望藉由測量地球內部各類物質的熱導率以建構一完整的地球熱動力模型。本次研究對象為石榴子石群之鎂鐵鋁榴石，其熱導率在常溫壓下約為 $3 \text{ Wm}^{-1} \text{ K}^{-1}$ ，我們發現在壓力達到 23 GPa（約深 660 公里）時，會隨壓力上升達到 $7 \text{ Wm}^{-1} \text{ K}^{-1}$ 。當與鎂鋁榴石、鈣鋁榴石兩種不同端點成分之榴石做比對時，發現在壓力 16 GPa（約深 440 公里）以上，鎂鐵鋁榴石的熱導率上升速率較另外兩者為低。表示儘管深度與熱導率呈正相關，但含有鐵端鐵成分時，會使其熱導率上升趨勢變得緩慢。

中文關鍵字：石榴子石、鐵鋁榴石、高壓、熱傳導率



台灣東部變質岩區地熱地質構造之研究－以鹿野溪紅葉谷溫泉為例

張郁敬¹、葉恩肇¹、曾雅筑¹

(1)臺灣師範大學地球科學系

電力是人類不可或缺的生活必需能源，目前地球上主要的電力來源為燃燒化石燃料，在化石燃料轉換為電能的同時，會產生大量的二氧化碳以及粉塵，使得地球溫室效應和空氣汙染日趨嚴重。為了解決此一問題，未來發電應可利用綠色能源來取代部分化石燃料，地熱能為目前綠色能源轉換效率最高且相對環保的基載能源。世界上大多數地熱電廠皆是以鄰近火山地區作為地熱來源，臺灣雖為環太平洋火山帶中一小島，由歐亞板塊及菲律賓海板塊之交互運動驅使弧陸碰撞引發造山運動，但因國家公園之劃分，使得台灣之火山地熱無法探勘與開採，反觀台灣本島約三分之二面積的區域多出露變質岩，且文獻資料顯示中央山脈東翼變質岩區熱流值達百餘 mW/m^2 ，因此合理推測台灣東部具有極高的地熱發展潛力。

台東鹿野溪地區位處板岩區，具有較高的地溫梯度與多處溫泉出露，故本研究將以台東縣延平鄉鹿野溪紅葉谷溫泉地區進行研究。前人於本研究區內提出兩種構造模型，一模型為紅葉谷斷層，另一模型為紅葉谷背斜。紅葉谷溫泉的熱流機制是以斷層摩擦熱主控抑或是穹窿上升主控，其溫泉的熱水通道是否與地質構造相關聯，皆為本研究的主要探討重點。為協助台灣變質岩區地熱的探勘與開發，本研究將以空拍機進行鹿野溪三維數值模型建置及數值地形判釋，使用影像軟體產製高解析度正射影像作為地表地質調查底圖，並繪製此區域之路線地質圖及裂隙分布，採集岩石樣本以微構造分析地質構造型態和應力方向，以斷層擦痕反演古應力場方向，配合礦脈中液包體重建應力場方向、應力比值及液壓比值，回推礦脈形成之深度及溫度，且以碳質物拉曼光譜檢測最後一期構造形成時之最高溫度，藉此釐清中視地質構造之關係，探討地下熱源的成因及地理位置。

台東鹿野溪紅葉谷地熱地質構造之研究結果將可釐清變質岩區熱流機制，以利後續地熱電廠建置之工程設計，同時地熱電廠建置可提供更多的偏鄉工作機會，協助青年返鄉、留鄉，提供發展之空間，也有助於地方產業強化及發展。本研究之研究成果亦能作為全球變質岩區地熱開發之參考，提升全球地熱能源產量。變質岩區地熱探勘技術的一小步，將會是未來綠色能源的一大步。

中文關鍵字：地熱、板岩、地質構造

3D coseismic displacement field derived from SAR-based fusion method

Li-Chieh Lin¹、Ray Y. Chuang¹、Chih-Heng Lu²

(1)Department of Geography, National Taiwan University、(2)Research Center for Environmental Changes, Academia Sinica, Taiwan

Coseismic deformation is one of the keys to unveil the motion and mechanism of a seismogenic fault. A comprehensive 3D coseismic displacement field is also a helpful tool to identify the off-fault deformation and multi-fault triggering. Not only the distributed displacement pattern is well captured, but it also offers a good constrain on the slip vectors. However, it is sometimes difficult to obtain comprehensive 3D coseismic displacement field with high spatial resolution, coverage and accuracy. Terrestrial geodesy offers high accuracy measurements but with very limited spatial resolution. Optical satellite images can provide high spatial resolution and coverage, yet it is hard to invert the vertical displacement. Since the 90s, DInSAR has shown strong capability to capture the surface displacement due to different ground driving forces with high spatial resolution and coverage. Because SAR satellites are mainly polar orbits with side looking characteristics, surface displacement in the north-south direction is less constrained. To tackle this issue, several processing algorithms were developed to obtain the azimuth displacement. Therefore, surface displacements from at least three directions can be used to invert the true 3D displacement field. In this study, we take the 2018 Hualien earthquake as an example to test different algorithms to get enough surface displacements for the inversion of true 3D displacement field. We invert the 3D displacement field with results from DInSAR and Multiple Aperture Interferometry (MAI). The result shows that the newly obtained 3D displacement field has better spatial resolution comparing with result from combining DInSAR and Pixel Offset Tracking (POT). Since MAI requires less interpolation and have better accuracy and resolution than POT, it is convinced that MAI should be a significant component for inverting such 3D displacement map.

Keywords: coseismic deformation, SAR processing algorithms, 3D coseismic displacement, earthquake

Using PSInSAR technique to observe land subsidence in Pingtung coastal area

Ping-Chen Chiang¹、Ray Y. Chuang¹、Chih-Heng Lu²

(1)Department of Geography, National Taiwan University、(2)Research Center for Environmental
Changes, Academia Sinica, Taiwan

Land subsidence in Pingtung Plain is a severe problem in decades. The modern geodetic data indicated the velocity of land subsidence in Pingtung can be up 3.58 cm/yr. To date, ones can use soil strata well, leveling GPS, and SAR to monitoring land subsidence. Different from other methods, SAR can measure minor changes and slow deformation over a wide area. In this study, we processed 79 Sentinel-1 ascending images and 59 Sentinel-1 descending images with the persistent scatters InSAR (PSI) method to estimate the surface deformation of Pingtung Plain from 2016 to 2018. We split the whole time into 7 pairs by dry and wet seasons to estimate the seasonal deformation in this area. In addition, we analyze the spatiotemporal pattern of land subsidence in the PSInSAR timeseries to characterize subsidence migration.

Keywords: PSInSAR, land subsidence, GPS



利用精密水準資料解析現今臺灣西南部泥岩區的垂直地表變形特性

魯曜銓¹、景國恩¹、陳建良²

(1)成功大學測量及空間資訊學系、(2)中央地質調查所

根據過去地表變形研究工作顯示，臺灣西南部之地表應變速率遠大於台灣本島之平均值，然而此高應變速率可能是由於泥貫入體之持續發育所造成的。換言之，臺灣西南部地區之應變速率雖然很高，但是受到泥貫入體活動的影響並不容易累積能量並引發地震。本研究使用中央地質調查所自 2002 年至 2020 年設置之岡山至安坡及路竹至茂林兩條水準測線資料並進行資料濾除，接著篩選距水準測線較近且品質穩定之 GPS 連續站然後挑選出最佳的約制組合，並藉由 GPS 連續站之分析成果透過找到較佳時間以一地震兩事件修正震後效應對水準速度擬合的影響，獲得台灣西南部於甲仙地震前、甲仙至美濃地震間與美濃地震後相對於大陸邊緣之垂直速度場。由垂直速度場可知，背斜構造區域的東西側通常會有一速度梯度變化，其值大約為 3.6-10.2 mm/yr，而北端區域的速度變化趨勢大致呈後一時期較前一時期抬升速度增加，在中洲背斜甲仙地震前原本呈沉陷約 -6.8 mm/yr，在甲仙地震後變為抬升速度約 1.8 mm/yr，2016 年後更升至 6.2 mm/yr；小崗山背斜抬升速度變化約 6 mm/yr；古亭坑背斜速度變化約 3.3 mm/yr；車瓜林與旗山斷層北段所夾區域速度變化趨勢亦相似約為 3 mm/yr，在南端區域美濃地震前速度變化趨勢與前者相同，但在 2016 年後其速度均呈沉陷且較前一時期差約 7.9 mm/yr。同時，解析不同時期的垂直速度場梯度變化，以移動平均法對內插成等間距的垂直速度場進行平滑化達到高頻、低頻訊號的分解，預期可將斷層近地表潛移行為與泥貫入體活動造成之區域性的垂直地表變形型態進行區隔，並探究泥貫入體對地表垂直速度造成的影響與分布以及知悉與地震交互作用後不同時期的變形機制。了解泥貫入體對地表的變形機制有助於提升台灣西南部對於高估間震期垂直速度場的問題。

中文關鍵字：精密水準測量、GPS、泥貫入體、台灣西南部

利用 GNSS 和精密水準測量成果建立 2002 到 2019 年

臺灣同震位移場目錄

李柏逸¹、景國恩¹、蕭詩涵¹、陳建良²

(1)成功大學測量及空間資訊學系、(2)中央地質調查所

以 GNSS 連續站研究臺灣 2002 年以來發生重大地震事件的地表同震位移場成果已相當完整，然而 GNSS 連續站所能提供的仍是有限，對於垂直位移場的成果可靠度也有待提升。本研究因此嘗試利用中央地質調查所施測的 767 站 GNSS 移動站和 29 條精密水準測線的資料，來提升 2002 年以來重大地震事件：2002 年花蓮外海地震、2003 年成功地震、2006 年卑南地震、2006 年恆春地震、2010 年甲仙地震、2013 年瑞穗地震、2013 年 3 月南投地震、2013 年 6 月南投地震、2016 年美濃地震、2018 年花蓮地震和 2019 年花蓮地震的同震位移場空間解析力與垂直位移場可靠度。本研究將利用坐標時間序列分析來計算地表同震位移場，並分別將各重大地震事件之同震位移場彙整成表格和分布圖，接著引用前人已發表以 GNSS 連續站研究臺灣重大地震事件之同震位移場文章，並將其同震位移資料亦製作成表格與分布圖，以進行 GNSS 連續站、移動站和水準同震位移場空間分布之比對，確認其成果是否具一致性。其中，由於 GNSS 連續站的時間解析度為一天一筆觀測量，移動站和精密水準一年施測一次，且誤差較連續站大，所以前人發表的連續站同震位移場資料為重要的參考依據。有了同震位移場的資料，再利用斷層傾角、走向角、滑移角、深度、長度和寬度等幾何參數，以斷層滑移模型推出各個重大地震事件引發的斷層滑移分布，進而推得各斷層的構造型態。

中文關鍵字：GNSS 連續站、GNSS 移動站、精密水準測量、時間序列、同震位移場

Crustal deformation of the Kendeng Fault branches area from GNSS and InSAR data and its earthquake potential in Surabaya City, Indonesia

Raudlah Hawin Ayani¹、Ira Mutiara Anjasmara²、Yunung-Nina Lin³、
Reyhan Azeriansyah¹、Kuo-En Ching¹

(1)Department of Geomatics, National Cheng Kung University、(2)Institut Teknologi Sepuluh
Nopember、(3)Institute of Earth Sciences, Academia Sinica, Taiwan

The Kendeng fault is one of the active faults in East Java, which has two branches: the Surabaya fault and the Waru fault. It may pass through Surabaya city, the second-largest city in Indonesia. Understanding the earthquake potential is very important for seismic prevention in Surabaya city to evaluate the seismic hazard of the Kendeng fault. We integrated the data from the Global Navigation Satellite System (GNSS) and Interferometric Synthetic Aperture Radar (InSAR) for the crustal deformation monitoring in the study area. One hundred nine ascending images and one hundred twenty-six descending Sentinel-1A images from November 2014 to July 2020 and the 30-meter resolution SRTM DEM were used to generate the interferograms using Scientific Computing Environment ISCE software. Furthermore, we constructed the cumulative displacement time series using the Small Baseline Subset (SBAS) technique. The outlier detection and root mean square of residual phase estimation was applied to improve the InSAR time-series accuracy and reliability. The LOS InSAR velocities in ascending ranges between -14.8 mm/year and 9.5 mm/year, and the descending between -13 mm/year and 6.8 mm/year. In addition, data from 19 campaign-mode GNSS stations from 2017 to 2020 are collected and worked for time-series analysis and validate the LOS InSAR velocities. Horizontal velocities range between -23.18 mm/year and 47.88 mm/year toward to southeast. Most of the Surabaya city's vertical motions are subsidence ranging between -1.26 mm/year and -112.20 mm/year. These results also aim to detect the activity of Kendeng faults which can lead to potential earthquakes.

Keywords: earthquake potential, Surabaya fault, Waru fault, SBAS, GNSS

應用 SBAS-InSAR 觀測 2016-2020 台灣西南部構造活動性與

變形特徵

陳俊諺¹、胡植慶¹、譚諤²

(1)臺灣大學地質科學系、(2)中央研究院地球科學研究所

受到歐亞板塊前緣碰撞後隱沒到菲律賓海板塊之下，台灣西南部厚層泥岩中的活動構造常以潛變的形式發生，如龍船斷層、車瓜林斷層、右昌斷層與鳳山斷層等，利用合成孔徑干涉雷達技術 (InSAR) 來進行大面積地表變形監測，可以探討上述構造延走向方向的潛變行為，亦可以補足 GPS 觀測的不足。本研究應用小基線集法 (SBAS) 對升軌 L-band ALOS-1 2007-2011 與升降軌 C-band Sentinel-1 2016-2021 年的影像來分析西南部的地表變形，並利用擬合後的 GPS 連續站的觀測速度場，來對雷達觀測的結果進行約制。最後將雷達觀測到的地表變形投影至東西、升降方向作結果的討論。其中 20160206 美濃地震也提供了很好的材料用以來討論震前 (2007-2011)、震後 (2016-2017) 與間震 (2018-2020) 地表變形行為。以右昌斷層為例，在升軌與降軌在視衛星方向可以觀察到跨斷層 6 mm/yr 與 8 mm/yr 的變形。最後，則利用有限元素法軟體 DynEarthSol 建立概念模型，模擬活動構造可能造成的地表變形行為。

中文關鍵字：小基線集、合成孔徑干涉雷達、大地測量、有限元素法、右昌斷層

Horizontal coseismic displacements of the northernmost Chelungpu fault of the 1999 Chi-Chi earthquake

Yau-Hsuan Tsai¹、Ray Y. Chuang¹、Yu-Ting Kuo²

(1)Department of Geography, National Taiwan University、(2)Department of Earth and Environmental Sciences, National Chung-Cheng University

The distribution of surface deformation is important to understand the fault kinematics and fault geometry at depth. To learn the coseismic ground deformation, image geodesy can provide observations with good spatial coverage. For example, displacements derived from comparing pair images is spatially continuous. The 1999 $M_w=7.6$ Chi-Chi earthquake generated ~100-kilometer surface rupture in central Taiwan. Previous study has utilized subpixel correlation for SPOT images in the central segment of the Chelungpu fault. The displacement field of the northern segment, which has the maximum displacements of fault, has not been well studied. This research uses subpixel correlation for SPOT satellite images with the pixel resolution of 10 m to measure horizontal surface displacements along the northern segment of the surface rupture. The horizontal displacements are determined by merging SPOT offsets and GPS data. According to the result, we can see a very clear V-shape displacement boundary in the northern end of the surface rupture, which is parallel to the shape of the Chisui Shale on the surface. The horizontal coseismic displacements show that the average displacement is about 3~4 m (up to about 12 m) in E-W, about 4 m (up to about 12 m) in N-S, and both increase toward the fault trace.

Keywords: surface deformation, 921 Earthquake, Chinshui Shale, Tungshih Anticline

Seafloor crustal deformation and semidiurnal internal tides in northeast Taiwan deduced by GNSS-A measurements

Chi-Hsien Tang¹、Ya-Ju Hsu²、Horng-Yue Chen²、Ryoya Ikuta³、
Motoyuki Kido⁴、Hsin Tung²、Chin-Shang Ku²、Hsuan-Han Su²、
Hsin-Ming Lee²、Yi-Lin Jiang²、Yih-Min Wu⁵

(1)Institute of Earth Sciences, Academia Sinica, Taiwan、Department of Geosciences, National Taiwan University、(2)Institute of Earth Sciences, Academia Sinica, Taiwan、(3)Faculty of Science, Shizuoka University、(4)International Research Institute of Disaster Science, Tohoku University、
(5)Department of Geosciences, National Taiwan University

The dense land-based GNSS network has revolutionized our understanding of earthquake faults in Taiwan; however, due to the lack of offshore data, new tools are needed to address hazards associated with the subduction zone megathrusts and submarine fault systems. Active deformation at subduction zones mostly lies beneath the seafloor and relies on seafloor geodetic techniques. The Institute of Earth Sciences, Academia Sinica, has been developing the Global Navigation Satellite System-Acoustic ranging (GNSS-A) technique and carrying out field tests offshore northeast Taiwan since 2007. In this study, we analyzed the GNSS-A data in 2012-2019 collected at the OILN site, located in the southwestern part of the Okinawa Trough. We optimized (1) the geometry of the seafloor transponder array, (2) the relative displacements for each campaign, (3) the configurations of the shipboard transducer, and (4) the time-variant traveltime delay of the acoustic signal by using a nonlinear inversion. As a result, we extracted the three-dimensional positioning time series and velocities, which broadly agree with the clockwise rotation in northeast Taiwan influenced by the backarc rifting of the Okinawa Trough. Furthermore, the traveltime delay projected to the vertical direction (nadir total delay, NTD) shows a semidiurnal cycle. This feature is compatible with the sound speed profiles measured by CTD during the campaigns, indicating the strong semidiurnal internal tides in the study area. Our analysis shows that GNSS-A measurements are valuable to not only studying seafloor deformation but also physical oceanography.

Keywords: GNSS, acoustic ranging, seafloor geodesy, internal waves

Impact of Pleistocene ice sheets on European westerlies

Hsun-Ming Hu¹、Chuan-Chou Shen¹

(1)Department of Geosciences, National Taiwan University

The westerlies and winter cyclones are the most climate system in mid-latitude, which are essential modulators of the weather and its extremes. However, discrepancies among various climate models hamper adequate westerly winds forecasting for the next century, highlighting the need for a more complete understanding of the long-term dynamics of the westerlies. Here, we present ^{230}Th -based speleothem multi-proxy records from Basura cave, northern Italy. Our record spans from 480 to 235 thousand years ago (ka), which reveals sensitivity of the westerlies to precessional forcings and incipient retreats of the Fennoscandian Ice Sheet. Our results show that the westerlies are controlled primarily by insolation during interglacials. In glacial periods, however, the variable size of the Fennoscandian Ice Sheet significantly modulated the latitudinal position, direction and strength of the westerlies.

Keywords: westerlies, ice-sheet



中更新世西太平洋暖池 MD97-2140 岩芯次表層浮游性有孔蟲殼體

穩定碳氧同位素與鎂鈣元素比所反映之古海洋特性

朱家萱¹、羅立²、米泓生¹、莊智凱²、沈川洲²

(1)臺灣師範大學地球科學系、(2)臺灣大學地質科學系

地球氣候系統之冰期—間冰期週期在過去 120 萬至 70 萬年前之間，從約 41,000 年(41-kyr)，轉變以約 100,000 年(100-kyr)為主，稱為中更新世變遷(Mid-Pleistocene Transition, MPT, Lisiecki and Raymo, 2005)。本研究選定西太平洋暖池 MD97-2140 岩芯(2°02.586'N, 141°45.49'E, 水深 2547 公尺)深度 1700-2700 公分(年代約為 1200-580 ka)的次表層浮游性有孔蟲 *Neoglobobulimina dutertrei* (355 - 425 μm)，與數種底棲性有孔蟲(>250 μm)為研究材料。研究結果顯示底棲性有孔蟲殼體之穩定氧同位素數值(介於 2.61‰及 4.76‰間)，與全球底棲性有孔蟲綜合氧同位素曲線 LR04 數值皆相近，以此作為本岩芯年代模式微調之依據。*N. dutertrei* 殼體穩定氧同位素數值於-1.37‰與 0.87‰(VPDB)之間震盪，且振幅在 1200-900 ka 段落約為 0.50‰，而 900-600 ka 段落振幅增為約 1.50‰；於海洋氧同位素階(Marine Isotope Stage, MIS)第 16 階的平均氧同位素數值較其餘冰期數值多約 0.50‰；頻譜分析初步結果顯示浮游性有孔蟲 *N. dutertrei* 氧同位素數值具有顯著 100、4、23 kyr 之週期性。穩定碳同位素數值於 0.69‰及 1.74‰之間震盪，較無明顯冰期—間冰期週期變化。初步計算鎂鈣比轉換的次表層水溫度(介於 13.1°C及 22.0°C之間) 平均變化較不顯著，相鄰之冰期與間冰期最大溫差約 3.0°C。扣除溫度效應計算水體氧同位素數值，發現冰期段落之數值在 900 ka 前平均約 0.30‰，至 MIS 16 數值達約 1.50‰，顯示冰川體積在 900 ka 後漸增，對長期海水面變化亦會有所影響。

中文關鍵字：中更新世變遷、西太平洋暖池、次表層浮游性有孔蟲

Tectonic geomorphology analysis in Hsinchu area by using historical aerial photos and SfM technique

Chin-Yi Lin¹、Ray Y. Chuang¹

(1)Department of Geography, National Taiwan University

Geomorphic features are useful tools to identify active structures in tectonically-active areas. Because the island of Taiwan is located at an active plate boundary, the study of tectonic geomorphology is very important for assessing seismic hazards. In Taiwan, Hsinchu is one major urban area with a large population and a high-technological industry development area (Hsinchu Science Park), which is at high seismic because it is located in between the Hsinchu fault and Hsincheng fault. To better understand the fault geometries and slip rates, the studies of river terraces displaced by the faults are required. However, the geomorphic features in current high resolution DEMs may disappear because of rapid industrialization and urbanization. Therefore, historical photos provide an opportunity for us to clearly see the geomorphic features before the modification by the urban development. Compared with aerial photogrammetry, the Structure from Motion (SfM) technique requires fewer photo parameters and the DEM generated by historical aerial photos with SfM technique has higher spatial resolution of about 1 m. Therefore, historical photos with SfM technique could be more suitable for analyzing tectonic geomorphology. Thus, this study aims to analyze tectonic geomorphology via high resolution 3D model derived from historical aerial photos and the SfM technique. The SfM-generated 3D model will be connected to real coordinate system through Ground Control Points (GCP) established by reference maps and 5 m DEM. In this research, we map and correlate terraces of Touchien River and identify suspected fault scarps and estimate the displacement of the terraces on the same step. Finally, we examine how the SfM-generated DEMs and the GCP settings perform in this case.

Keywords: mapping geomorphological feature, Structure from Motion, fluvial terrace, fault scarp

Topographic changes due to erosion of Lichi Badland by using archival aerial photos and SfM technique

Zi-Xin Lee¹、Ray Y. Chuang¹

(1)Department of Geography, National Taiwan University

In this study, we estimate topographic changes of Lichi Badland by using archival aerial photos and Structure from Motion (SfM) method. Archival aerial photos, which were taken since 1940s in Taiwan, provide valuable visual interpretation for surface analysis and datasets for generating topographic data. However, it may be difficult to assess all camera parameters for historic aerial photos and the coordinates of ground control points, making topography reconstruction through traditional photogrammetry almost impossible. With the development of computer vision-based SfM photogrammetry in recent years, it becomes possible to reconstruct old topography without complicated procedures and parameters. In eastern Taiwan, Lichi Badland is one famous geotourism area with rugged topography under high erosion of the Lichi Mélange. The erosion pattern of the Lichi Mélange is less understood. Therefore, we aim to generate high resolution 3D model by archival aerial image and SfM technique of the Lichi Badland. This model will be constrained by ground control points (GCPs) derived from recent DEM and orthomosaic image. Then, we will examine the accuracy of the model and test the ability and limitation to detect land cover changes of the Lichi Badland by using archival aerial photos and Digital Elevation Models of Difference (DoD) method.

Keywords: Structure from Motion, Digital Elevation Models of Difference, archival aerial photos, change detection

利用二維地電阻法推估蘭陽平原扇頂淺層地下水位面及比出水率

謝孟勳¹、嚴精明¹、張竝瑜¹

(1)中央大學地球科學系

蘭陽平原位於台灣東北部，東鄰太平洋，西側與南側接雪山山脈及中央山脈。本研究地區位於蘭陽溪至羅東河之間一大隱地區，此區位於扇頂補注區的礫石層範圍內，在水文地質方面，屬於非拘限含水層分布區域，適合地下水區。為了瞭解蘭陽平原大隱地區之地下水文特性，遂利用二維地電阻法調查並計算淺層地下水位深度及比出水率隨季節之變化情形。在研究區域內，每次布設十條二維地電阻測線，並於測區內之大隱地下水觀測井附近進行試驗，以利進行推估地下水位面之比較，而後將調查所得電阻率資料帶入 Archie's Law 轉換成相對含水量，並藉由 Van-Genuchten 保水曲線推估地下水位深度，以及利用飽和及殘餘含水量計算比出水率，最後將所得結果繪製成地下水位高程分布圖。本研究區域其比出水率約 0.08 至 0.15 之間，並發現地下水位由西南向東北遞減趨勢，與羅東溪流向大致一致，推測本區受山區及河流補注影響。

中文關鍵字：地電阻剖面法、保水曲線、比出水率



Finite-difference time-domain simulation of magnetotelluric data

許耀文¹

(1)中央大學地球科學系

有限差分時域 (Finite-Difference Time-Domain, FDTD) 或 Yee 方法 (以華裔美國應用數學家 Kane S. Yee 的名字命名) 是一種電磁場計算領域的數值分析技術。這是一種時間域的分析方法, 可以通過一次模擬運行就覆蓋很寬的頻率範圍, 應用範圍可由極低頻(接近直流電)至極高頻(如可見光)。本研究以 MATLAB 語言開發了時域有限差分法來模擬大地電磁法於一維地層中的電磁波行為, 可模擬產生任意位置觀測到的時間序列資料, 吸收邊界條件 (absorbing boundary conditions, ABC) 採用 Mur's ABC。經過驗證, 一維模型在此吸收邊界下數值模擬產生的時間序列準確度高。本研究模擬不同的大地電磁法野外觀測位置, 例如地表、河底、海底, 產生時間序列資料, 可計算大地電磁法常用的物理量, 如阻抗 (impedance)、視電阻率 (apparent resistivity) 及相位 (phase)。另外, 本研究可作為寬頻大地電磁法資料蒐集儀器設計的重要參考, 用於評估河底、海底的訊號強度進而設計最佳的資料蒐集方案。

中文關鍵字：有限差分時域，大地電磁法模擬。



應用地電阻影像法於海岸廢棄物測勘之研究

顏麒書¹

(1)中央大學地球科學系

本研究應用地電阻影像法 (Electrical resistivity tomography, ERT) 於桃園市大園區新街溪出海口，對地表下可能埋藏之廢棄物進行測勘。2020 年 9 月 3 日及 9 月 4 日於桃園新街溪出海口左岸進行野外施測，布置兩條長度 96 公尺、電極間距 1.5 公尺的交錯測線 (L1 測線與 L2 測線) 及一條長度 64 公尺、電極間距 1 公尺的測線 (L3 測線)。使用自行開發之地電阻監測儀器—多波道直流電阻法與自然電位法全自動監測系統(Remote Resistivity Monitoring System, R2MS)，進行多電極波道測勘。施測所得的資料，使用阻尼最小平方法 (Damped least squares inversion)，進行非線性逆推解算。並且，將逆推結果繪製成電阻率剖面圖，配合阿爾奇定律 (Archie's law)，對比兩條測線間之孔隙率及含水率差異，藉此判釋地質構造、地下材料特性，對海岸地下構造進行完整的分析。成果為：

一、依照最佳的逆推模型，各測線下方之電性構造呈現明顯的層狀構造，與常見的海岸地下構造吻合，容易判別地電阻異常區域。

二、地層岩石之電阻率受含水量、滲透水成分影響，L1 測線與 L2 測線位於潮間帶，為海水滲透之地層，含水量較大，電阻率普遍較低；L3 測線靠近陸地，為淡水與海水滲透的交界帶，含水量較小，電阻率較高，符合阿爾奇定律。

三、根據 L1+L2 測線及 L3 測線之地電阻剖面圖、中位數剖面圖，在測量範圍內皆無發現電阻率異常區域。並且，對比 L1+L2 測線與 L3 測線在各深度之平均電阻率、孔隙率及含水率，數值十分相近，不存在大範圍的電阻率異常。因此，評估該場址範圍內無掩埋之廢棄物。

中文關鍵字：地電阻影像法、阿爾奇定律、海岸廢棄物

Effect of rainfall infiltration processes on subsurface using time-lapse electrical resistivity tomography in Liyutan area, Northern Taiwan

Tran Van Huu¹、Chien-Chih Chen¹

(1)Department of Earth Sciences, National Central University

Rainfall infiltration has a substantial effect on the subsurface, especially soil stability. It can penetrate through the soil layer, and contribute to the water table level as a whole. In our research, we evaluated the changes of a hillslope under the effect of rainfall infiltration in the Liyutan area, Northern Taiwan. The rainfall infiltration causes the changes in resistivity values of the rock. Therefore, we used the time-lapse Electrical Resistivity Tomography (ERT) method to investigate its effect. Data were collected from May to August 2019 and included apparent resistivity data from electrical resistivity tomography measurements, rainfall precipitation, and groundwater level from 7 wells in the research area. In order to determine rainfall effects, time-lapse resistivity sections were obtained from apparent resistivity data after applying the inversion process. Based on the changes in resistivity distribution, the research area can be divided into 5 subzones. The spatial and temporal effects of rainfall events were estimated by three types of further analysis. First, we compared the precipitation with the mean resistivity value of each zone to evaluate the effect of rainfall. Second, the relationship between groundwater table level and median resistivity value was set. Finally, normalized water content was established from resistivity data. Results have proved the effects of rainfall infiltration on the subsurface in the study area. The rainfall water infiltrated into the subzones after one hour. This causes the changes in median resistivity in each zone. Rainfall can virtually penetrate to the deeper part of zone D. The results of the normalized water content show the fluctuations over the investigated period because of precipitation.

Keywords: rainfall precipitation, electrical resistivity tomography, Taiwan, groundwater, normalized water content

折射震測與多波道表面波分析法研究澎湖東吉嶼的沉積地層

楊子誠¹、謝秉燁¹、張永孚¹、汪良奇¹

(1)中正大學地球與環境科學系

澎湖縣位於台灣與中國大陸的中間，是研究兩岸環境變遷的重要指標，而沉積物往往是研究環境的要素，土壤剖面能提供長時間尺度的植群變遷紀錄，本研究的目的就是希望擔任研究沉積物厚薄分布的起頭，利用折射震測法與多通道表面波分析法(MASW)去分析澎湖南方四島東吉嶼的地層分布情形，以非破壞性的方式，繪製出完整的地層剖面，以利將來得以重建南方四島過去的自然環境變遷與探索人類活動的證據，建立起兩岸環境變遷的橋樑。

中文關鍵字：澎湖南方四島國家公園、折射震測、多通道表波分析法(MASW)



New approach in multi-scale adaptive mesh construction of 2D/3D Taiwan models and traveltimes tomography

M. Syahdan Akbar Suryantara¹、How-Wei Chen¹

(1)Department of Earth Sciences, National Central University

Traveltimes tomography has been used for years. However, low resolution features due to structured mesh system usually prohibit its applicability of accommodating realistic suggestion and potentially large error involved during interpretation stage. Therefore, to avoid this limitations, unstructured adaptive mesh system is needed. A new approach for seismic traveltimes tomographic inversion or potentially suitable for other geophysical problems is tested. The goal is to reduce the geophysical uncertainty when merge different types of data which carry various degree of errors while incorporate accurate geographic information into the model. Shortest path ray tracing is implemented for unstructured Delaunay triangulation mesh system. Un-structured mesh system is designed follow Adaptive Mesh Refinement (AMR) scheme with intension to preserve multi-scale features of the model including topography, bathymetry, geological boundary, active fault traces, sensor location and available information of different velocity models. We show that such an unstructured adaptive mesh system can preserve detailed features of 2D Earth surface and then extend to 3D model of Taiwan. The implementation strategy in mesh generation process follow atomic meshing algorithm. Atomic lattice construction algorithm uses designate control points, its density distribution and cell size to perform refinement within particular regions to preserve discontinuous features. Automatic initialization of control points is based on the nominal distance field that derived from the gradient of a particular physical feature such as velocity or topography variations. In the region where the gradient is high, the cell size become smaller than those regions where gradient is low. Forward seismic ray tracing for such mesh system also shows better coverage and accuracy. Consequently, incorporate all proposed approaches can produce more reliable traveltimes inversion result at the end.

Keywords: unstructured mesh, adaptive mesh system, atomic meshing, seismic ray tracing, traveltimes inversion

應用地電阻法判釋古大員市鎮於現今區域海陸交界

毛重仁¹、樂鎔・祿樸峻岸¹、鍾國風²

(1)成功大學地球科學系、(2)成功大學考古研究所

台江內海原址是荷據時期重要的對外貿易港口，荷人亦在此發展出繁榮一時的大員市鎮。但隨著曾文溪的改道帶入大量沉積物，古安平港逐漸淤積失去了港口功能。沉積環境也從原本泥岩轉換成砂岩沉積。然而對安平地區的歷史多為人文紀載及口述歷史傳承，鮮少有針對此地的地球物理測勘研究。根據地調所地質調查及鑽探岩心分析顯示，安平地區近地表多為砂岩沉積地層。但其原址為台江內海，較早期沉積環境以泥岩為主。故本研究將藉由地層組成物質與含水量的不同，呈現出不同的導電特性(一般以電阻率表示)，以地電阻試驗搭配地電阻影像剖面法(Resistivity image profile, RIP)來呈現地表以下地層電阻率的分布情形。

本研究採用地電阻儀來做施測，建立地表下視電阻率模型，利用逆推程式來反演實際地層電阻率的模型。將以模型判釋泥岩與砂岩分布，再搭配考古成果及土地利用之歷史資料研究做比對以此劃定古大員市鎮海陸交界分布、舊港口水道位址及推算出台江內海沉積速率。

經過多次的野外地電阻施測與建立反演模型，搭配考古資料佐證，大致已將古大員市鎮疆域做出劃定，北起西門國小；南至林默娘公園一帶；東達石門國小一帶。沉積地層除去表面的人為回填層，多以穩定的海象或濱海相沉積之泥沙岩為主，而透過泥岩層的分佈深度，推測出此地的沉積速率約為每年 0.5 公分。

中文關鍵字：古大員市鎮、地電阻影像剖面法、海陸交界，沉積速率

利用 Kriging 插值觀測地層下陷中心移動以及壓縮狀況

邱淳銓¹、倪春發¹

(1)中央大學應用地質研究所

地層下陷是台灣的國土安全不容忽視的問題，除沿海低窪地區因地層下陷所產生之淹水問題外，台灣高鐵路線上之下陷嚴重區，造成交通安全層面上的疑慮，是刻不容緩的重要議題。目前高鐵路線上所經過之下陷區屬濁水溪沖積扇為最嚴重，其中以虎尾、土庫、元長及褒忠等鄉鎮為主要下陷區。地層下陷的觀測方法有許多種，其中精準度最高且分布最廣的觀測資料為水準測量，但此方法之缺點是監測頻率過長，而地層下陷影響主因為地下水，地下水會隨著旱季或雨季而有水位的高低起伏，因此以年的觀測頻率是明顯不足的。為解決各種觀測資料在時間、空間上精度與頻率差異，所產生資料無法直接互補之問題，本研究使用 kriging 插值，假定採樣點之間的距離或方向可以用於反映插值結果的空間相關性，利用水準測量資料與 GNSS 資料進行融合，結合兩者的優點，並以 kriging 插值出每月的地表沉陷分布，用以分析地下水位與地層下陷的關係。藉由磁環式監測井與水準樁的觀測資料進行融合，插值出較淺層地區的壓縮量，分析地表下 300M 之壓縮量，並與地表沉陷分布做分析比較。

中文關鍵字：克利金插值、地層下陷、地層壓縮、地下水

應用多變量統計分析歸納蘭陽平原地下水水質特性之研究

蔡秉諺¹、劉雅瑄¹

(1)臺灣大學地質科學系

蘭陽平原為雪山山脈及脊梁山脈包夾而朝東面海的沖積平原，接受自兩山脈攔截的水氣並由扇端補注地下水層。由於地下水水量豐沛且水位高，蘭陽平原之用水需求依賴地下水源之比例甚高，以農業及養殖漁業為主要的需求方，民生用水亦多仰賴地下水。因此，蘭陽平原地下水的水質深深地影響該地區之人類活動，故需受嚴格檢視。根據過往檢測紀錄，蘭陽平原於多處具有多個監測項目，曾有超過監測標準甚至管制標準的情形。然而，地下水系統龐大且複雜，涵蓋為數眾多卻難以全面瞭解的物理及化學進程，導致我們面對監測值異常時，若無確鑿的證據，則難以找出污染源。

本研究藉由行政院環保署全國環境水質監測資訊網之公開資訊，提取蘭陽平原地下水監測活動自 1993 年至今二十餘載的紀錄。以此資料集為基礎，本研究利用統計學的數據分析、階層式分群(Hierarchical Clustering, HA)及主成份分析(Principal Component Analysis, PCA)進行資訊統整。透過數據分析結果，協助本研究探討蘭陽平原於空間及時間上的地下水水質交互作用關係，進而逐步歸納複雜的蘭陽平原地下水系統，並解釋各區域的水質特性及變化，以解決地下水系統因物理及化學性質而錯綜複雜的問題。根據分析結果，蘭陽平原之地下水井可分為五類。第一類：包含大隱、廣興、頭城及礁溪四井，代表沉積顆粒受侵蝕風化較多且呈氧化環境的山麓帶；第二類井取自職訓中心、內城、萬富及大洲，係屬於與海水無關之上游段；而第三類屬大同、七賢、五結及公館，為受到較少污染的群集，應與蘭陽溪之大流量有關；宜蘭高商、員山、龍德及冬山等井具代表性，為還原環境導致 As、Fe 及 Mn 釋出所致，屬第四類；第五類受人為活動影響較為明顯，竹林及古亭總有機碳含量高。

中文關鍵字：蘭陽平原、地下水、群集分析、主成份分析

HYDRUS-2D 模式應用於地下水熱傳遞之研究

秦淑娟¹、倪春發¹

(1)中央大學應用地質研究所

溫度作為示踪劑可反映地下水流及熱傳遞的動態過程，與化學示踪劑相比，溫度示踪劑可以減少對環境的負面影響，為增進推估含水層內水流及溫度傳遞行為之精確度，本研究通過砂箱實驗以及 HYDRUS-2D 數值模式模擬，分析水溫、水流及熱傳輸的過程，探討 HYDRUS 模式之水流、溫度傳輸模型及其反推估模式。砂箱試驗所填充之材料土壤特徵參數及熱傳導性質透過室內實驗取得，包含水力傳導係數、非飽和土壤 van Genuchten 特徵曲線、熱導率及比熱容，再將參數帶入 HYDRUS-2D 內進行反推估計算，以校正與水流相關之參數。再將校正後參數輸入數值模式，模擬地下水流與溫度變化。砂箱試驗於室內恆溫環境下進行，砂箱尺寸為 $155*55*2\text{ cm}^3$ ，砂箱左右各有一水槽調節水位，使左右邊界皆為定水頭，分別為 40 公分及 20 公分，砂箱中的水溫接近於室內溫度約 18 度，在離左水槽水平距離 35 公分、離砂箱底部垂直距離 25 公分處，以單點的方式注入熱水，使用蠕動馬達以流量每秒 0.642 立方公分持續注水 5 小時，以觀察相對高溫水注入相對低溫水中的熱傳遞軌跡。

中文關鍵字：溫度示踪劑、van Genuchten 特徵曲線、HYDRUS-2D、砂箱實驗

A two-dimensional analytical model for multispecies transport with rate-limited sorption

Nguyen Thi Thu Uyen¹、Jui-Sheng Chen¹

(1)Institute of Applied Geology, National Central University

In recent years, most studies using an analytical model for multispecies assume relationship between dissolve phase and sorbed phase was equilibrium controlled. However, some previous researches developed one-dimensional model for rate-limited sorption demonstrated that the rate-limited sorption process can affect the accurate prediction of contaminant concentration in the subsurface environment. Nevertheless, a multidimensional model would be more suitable in practice and have more applications. This study introduces an analytical model for the two-dimension transport of degradation contaminants under the action of rate-limited sorption. The system of partial differential equations has been analyzed into linear algebraic equations through the sequential application of the Laplace transforms, the finite Fourier transform, generalized integral transform and their inverses. The contaminant concentration of each species is calculated based on this linear algebraic equation. This study determined transport of the contaminants with different sorption rates of 0.05 year⁻¹, 0.5 year⁻¹, 5 year⁻¹ and 20 year⁻¹, respectively. The results of the analytical model have been compared with numerical model, with high similarity proving the accuracy and reliability of the new model. In addition, the sorption rate affects the range of spread of the contaminants. With a high sorption rate, the extent of the plume is narrowed and the concentration level also decreased. Moreover, the lower the sorption rate is, the higher the concentration predicted for pollutants is expected. The results of the rate-limited sorption model approach the equilibrium-controlled sorption model when the sorption rate reaches 20 year⁻¹.

Keywords: analytical model, rate-limited sorption, multispecies transport, advection-dispersion equation

A geological exploration of the unexpected normal faulting in the Zhongliao tunnel area, southwestern Taiwan

Kai-Fong Chen¹、Maryline Le Béon²、Yi-Wei Chiou²、Yu-Cheng Hsu²、
Chang-Chih Chen²

(1)Department of Earth Sciences, National Central University、(2)Institute of Applied Geology,
National Central University

According to geodetic data, we learned that there is a significant ground displacement across the Chishan fault, near the north end of the Highway 3 Zhongliao tunnel, leading to a serious damage on the tunnel. Footwall uplift and fault-parallel component reach up to 80 mm/yr and 15 mm/yr, respectively. The current deformation corresponds to normal faulting with a right-lateral component, which contradicts the traditional knowledge of the Chishan fault, as an east-dipping thrust that brings the Miocene Wushan sandstone on the Plio-Pleistocene Gutingkeng mudstone. Because geodetic data has limited spatial coverage and time span, this study is based on geological field survey and geomorphologic analysis to look for evidence for long-term deformation and explore the fault zone characteristics. Several outcrops with brittle fault mirrors and ductile deformation are found. The principal shear zone reaches up to 50 m in width, with an average attitude N48E/67E. We are also able to interpret slickenlines and sheared mud with ductile C-S structures as an evidence of right-lateral normal faulting. The shear zone width and the presence of ductile structures imply that the unexpected normal faulting is more than a transient deformation: it is a relatively long-lived phenomenon that resulted in permanent deformation. The fault line is sometimes associated with anomalies in the topography, such as SE-facing counter-slope escarpments, that would also be consistent with sustained normal faulting. The mechanism behind this phenomenon still remains uncertain. Understanding the relation between this unexpected fault zone and the other active tectonic structures in the region will be the primary focus of this research in the future.

Keywords: Chishan fault, Zhongliao tunnel, fault zone, structural geology, active fault, geomorphology

2006 年屏東外海地震誘發之恆春斷層慢滑移事件

蕭詩涵¹、景國恩¹、蔡佩京²、李劍珩³、張文和⁴、陳建良⁵

(1)成功大學測量及空間資訊學系、(2)綠環工程技術顧問有限公司、(3)K2 Management、

(4)中央大學地球科學系、(5)中央地質調查所

本研究藉由中央地質調查所於恆春半島設置之 7 個 GNSS 連續站、37 個移動站及 2 條精密水準測線 2002 年至 2016 年間之觀測資料發現，2006 年屏東外海 M_L 7.0 地震發生後，恆春半島之地表運動型態產生了明顯的轉變，且首次觀察到臺灣地區之慢滑移事件。為了釐清此區域慢滑移事件之活動型態及其在恆春斷層上能量累積與釋放的模式，本研究除了分析時間序列獲得地表速度場外，更透過基線反演模型與斷層錯位模型，推估斷層面上滑移虧損速率與滑移速率之分布型態及數值，再結合地質調查結果進行綜合探討。根據時間序列分析結果，恆春半島之地表速度場以 2006 年屏東外海地震及 2010 年 4 月為界，可區分為 3 個時期：相對於 S01R 測站，2006 年屏東外海地震發生前，西南側水平速度於約 53-58 mm/yr 向西北，垂直沉降速度約 8-15 mm/yr；東側水平速度於約 47-55 mm/yr 向西北西，垂直沉降速度約 5-18 mm/yr。2006 年屏東外海地震發生後至 2010 年 4 月，西南側水平速度於約 53-56 mm/yr 向西南西，垂直沉降速度約 3-10 mm/yr；東側水平速度於約 45-53 mm/yr 西北西，垂直速度轉為抬升為主約 3-9 mm/yr。2010 年 4 月至 2016 年，西南側水平速度於約 50-54 mm/yr 向西南西，垂直沉降速度約 3-8 mm/yr；東側水平速度於約 43-53 mm/yr 西北，垂直速度轉回沉降為主約 1-6 mm/yr。基線反演模型與斷層錯位模型結果則指出，恆春斷層為具有左移分量之逆衝斷層，其於 2006 年屏東外海地震發生前，具有南北兩個地栓（asperity）；且地震發生後，能量並未停止釋放，而是持續於此兩個地栓由南往北遞進釋放。此外，根據地質調查研究結果，鄰近恆春斷層區域直至 2017 年仍有地表裂隙產生，亦為此區域震後持續潛移之佐證。綜上所述，本研究推論：(1) 恆春半島地表運動型態的改變是由 2006 年屏東外海地震所誘發；(2) 恆春斷層上盤垂直速度之變化與地質調查研究結果顯示，斷層面上所累積之能量於地震後仍持續緩慢釋放中，亦即此區域有慢滑移事件之發生；(3) 恆春斷層之位置可能位於目前劃定範圍之東側約 1-2 公里之位置。

中文關鍵字：恆春斷層、2006 年屏東外海地震、慢滑移事件、斷層滑移虧損速率

卑南溪流域河水之生物性碳轉換

陳培恩¹、塗子萱²、林立虹³、王珮玲¹

(1)臺灣大學海洋研究所、(2)中山大學海洋科學系、(3)臺灣大學地質科學系

調控大氣二氧化碳的諸多機制中，岩石風化作用扮演了關鍵的角色。過去探討風化作用的研究中，大都聚焦於運用大河系統中的河水溶質或同位素特徵，推論無機風化作用的形式、速率與影響因子，往往忽略了其生地化作用，亦可能對大氣二氧化碳收支產生的重要貢獻。特別是於造山帶的小河系統中，河水滯留時間短，並有大量溶質與沉積物輸送至河道，提供豐沛的岩石源礦物質與有機質，作為河域自營作用和異營作用可能的基質，分別消耗和釋出二氧化碳，過去卻鮮有研究探討此兩種代謝形式，對於流域二氧化碳收支的影響。

有鑑於此，本研究選擇於台灣東部擁有最高沉積物輸出通量與高化學風化速率之卑南溪流域，收集不同季節上至下游的河水樣本，添加標定 ^{13}C 同位素之無機碳與有機碳源進行培養實驗，量測自營與異營作用速率，並進行生地化和分子生物分析，釐清相關控制因子和參與作用的微生物族群組成。初步結果顯示，相較於河川上游，全年在卑南溪出海口皆有最高的自營作用速率，約 $0.55\sim 2.32\text{ mg C m}^{-3}\text{ h}^{-1}$ ，且在濕季時較高，可達乾季時的 4 倍，與河川之硝酸鹽濃度呈顯著正相關；異營呼吸作用速率約為 $16.4\sim 79.0\text{ mg C m}^{-3}\text{ h}^{-1}$ ，雖呈現明顯的區域性和季節性差異，卻未有上下游或普遍性的乾濕季系統性變化。在環境中複雜的微生物族群組成，亦有 *Cyanobacteria* 與 *Campilobacterota* 等菌門豐度在時空上的變化，可能在其中扮演重要角色。總結來說，於卑南溪上游、支流至下游出海口，全年異營代謝產生二氧化碳速率高於自營生物合成消耗的速率，可知卑南溪流域屬於異養河川系統，對大氣二氧化碳為淨輸出。未來期望能統合各項成果，提供卑南溪流域完整的生物性碳轉換過程與貢獻。

中文關鍵字：自營作用、異營作用、 ^{13}C 同位素標定

Morphotectonics of the Houjing Tableland Area, Kaohsiung, TaiwanChiming Tung¹、Yu Wang¹

(1)Department of Geosciences, National Taiwan University

In this study, we use topo maps in the 20th and 21st century, post-WW2 aerial photos, and digital elevation models in the 21st century to map the active tectonic features within the Houjing Tableland area before the urban development. Houjing Tableland is a NE-SW trending tableland in the Kaohsiung area with surface elevations of about 18-20 m. The top surface of the tableland is mantled by the Holocene sediments (Wu, 2000; Wu et al., 2002), and Sun (1964) suggest its northwestern and southeastern edge is bounded by the Youchang Fault and the Shoushan Fault, respectively. Along the NW edge of the tableland, our result suggests the Youchang Fault can be separated into three sections: the Ciaotou section, the Lantian section, and the Youchang section, from NE to SW. The orientations of the escarpments are $\sim N60^{\circ}E$ to $\sim N45^{\circ}E$ in the Ciaotou section, $\sim N25^{\circ}E$ to $\sim N7^{\circ}E$ in the Lantian section, and $\sim N30^{\circ}E$ in the Youchang section. The distribution of these escarpments suggests the left-stepping reverse fault geometry of the Youchang Fault. Our result of the Shoushan Fault at the southwestern edge of the tableland suggests the Shoushan fault contains less clear tectonic escarpments than the Youchang Fault. This indicates vertical activity of the Shoushan Fault is much less than the Youchang Fault since the formation of the Houjing Tableland. We also find at least four levels of fluvial terraces along the Houjing River, transecting through the Houjing Tableland. The distribution of the terrace suggests the persistent and differential land-level changes across the tableland. By adapting the previous published radiocarbon dating results, and the regional sea-level change history, together with our mapping result, we suggest the currently geometry of the Houjing Tableland is primarily controlled by the vertical throw of the Youchang Fault. The average uplift rate of the Houjing Tableland is about 3 mm/year in about the last 4 thousand years.

Keywords: Youchang Fault, Shoushan Fault, active fault, tectonic geomorphology

Dynamic modeling of the multi-fault rupture of the 1906 Mw 7.1 Meishan, Taiwan, earthquake: Constraints on frictional behavior and stress

Chen-Ray Lin¹、Sebastian von Specht²、Kuo-Fong Ma³、Yi-Wun Liao⁴

(1)Department of Earth Sciences, National Central University; Earthquake-Disaster & Risk Evaluation and Management (E-DREaM) Center, National Central University、(2)Earthquake-Disaster & Risk Evaluation and Management (E-DREaM) Center, National Central University; Institute of Earth Sciences, Academia Sinica, Taiwan; Helmholtz Centre Potsdam GFZ German Research Centre for Geosciences, Potsdam, Germany、(3)Department of Earth Sciences, National Central University; Earthquake-Disaster & Risk Evaluation and Management (E-DREaM) Center, National Central University; Institute of Earth Sciences, Academia Sinica, Taiwan、(4)Earthquake-Disaster & Risk Evaluation and Management (E-DREaM) Center, National Central University; GNS Science, Lower Hutt, New Zealand

The March 17 1906 Mw 7.1 Meishan earthquake marks one of the most devastating events in Taiwan. Previous studies regarded the Meishan earthquake as a right-lateral strike-slip event related to the coseismic surface rupture along the Meishan fault. Liao et al. (2018) discussed a scenario where rupture on a blind thrust fault triggered the preexisting weak zone on the Meishan fault. They validated their model by comparing three Omori seismographs records from Taiwan with synthetic waveforms. We investigated this multiple segment rupture scenario from a dynamical modeling perspective for various fault system configurations in the Meishan earthquake region. Model parameters are constrained within physically reasonable ranges by incorporating stress mechanics related to the frictional limit, fluid pressure, rheology, and the Wallace-Bott hypothesis; horizontal stress orientations are taken from the World Stress Map and stress drop ranges within globally observed values. We considered both hydrostatic fluid pressure and fluid overpressurization. The static friction coefficient ranges from $\mu_s=0.4$, (Kidder et al., 2012) and $\mu_s=0.7$ (Byerlee's law). We created pure brittle and brittle-ductile models based on rock strength curves. The linear slip-weakening model is run on a 3D finite element mesh in a homogeneous half-space. Our rupture simulations show reasonable slip distributions for low μ_s (0.4 to 0.5), implying that Byerlee's law does not hold in the region. Rupture in the brittle models is limited within the predefined fault patches while in models with brittle-ductile models, rupture does not extend beyond the brittle-ductile transition zone. Fluid overpressurization reduces rock strength resulting in larger slip. The Omori records are comparable to the synthetic waveforms from various scenarios, indicating that the 1906 Meishan earthquake can be reasonably explained as a multiple-segment rupture system, but not from a single segment rupture.

Keywords: 1906 Meishan earthquake, multiple segment rupture, frictional behavior, physical stress constraints



臺東鹿野地區河流地形作用與山崩事件之交互影響

蔡加洛¹、徐濤德¹

(1)臺灣大學地質科學系

河流作用是地表侵蝕與堆積最主要的營力之一，因此河流地形之相關研究長期以來皆是地質學家所重視的議題之一；另一方面，活躍造山帶中，山崩事件是影響地形演育的重要地表作用，主控了侵蝕作用與河流系統的沉積物供應。臺灣地處活躍造山帶，因此山崩對河流系統的影響是臺灣中低海拔地形演化的主要因素之一。臺東鹿野地區的鹿野溪與卑南溪匯流處附近，有一系列發育良好的河階地形，地形上同時顯示過去曾有一個規模極大的古山崩事件（鸞山山崩），過去雖然曾經有針對兩者分別進行的研究，但並未詳細探討河流地形變化是否與山崩事件的發生具有因果關係，或是山崩事件崩落後對該處河流系統是否造成影響。有鑑於此，本研究目的為藉由山崩與周圍河流階地的地形幾何、層位關係、以及其相對年代，來釐清鹿野地區河流系統的演育歷史，瞭解這些地表作用在河流演育的過程中其交互的影響。本研究利用即時動態定位(RTK-GPS)與雷射測距儀在野外進行山崩堆積物與其底岩間界面的高程測量，再透過高精度數值地形模型進行地形分析，得到過去山崩未發生前的古地形面。結果發現兩千多年前山崩事件發生前，卑南溪主流古河道可能流於目前河道東側數百公尺處，此河道於山崩發生時遭到山崩堆積物掩埋，使得河流改道至現今卑南溪河道所在位置，並下切形成外成峽谷。另一方面，綜合前人的觀察與資料，本研究認為兩千多年前此山壁內的古河道也並非是長久以來卑南溪所流經的位置，而可能是當鹿野溪發育大規模的龍田沖積扇階地時，大量的沉積物加積使得兩千多年前之卑南溪河道向東遷徙數百公尺，流到了現今山壁內本研究所發現的古河道處。其後又由於這個側向遷徙造成海岸山脈西翼邊坡過陡，而引發了鸞山山崩事件。整體來說，鹿野地區河流地形作用與山崩事件經過一系列的相互影響，才形成了目前所見的面貌。

中文關鍵字：河流地形作用、山崩、沖積扇、鹿野地區、卑南溪

Using groundwater flow and land subsidence simulations to assess the geological model uncertainty

Nguyen Quoc Cuong¹、Shih-Jung Wang¹、Duc Huy Tran¹、

Yonatan Garkebo Doyoro²

(1)Institute of Applied Geology, National Central University、(2)Department of Earth Science,
National Central University; International Graduate Program for Earth System Science between
National Central University and Academia Sinica

Land subsidence is a phenomenon that currently attracted great noticed around the world, especially in populated and large building areas. Studies and predictions of land subsidence rate and understanding the factors that cause soil compaction are widely studied and understood. However, the uncertainty in the geological model, as well as the parameters, which may affect the groundwater flow and subsidence are less considered in the literature. The software GMS (Groundwater Modeling System) was used to operate the groundwater flow and land subsidence simulations to quantify the geological model uncertainty. A synthetic geological model was constructed as the original model. Different numbers of borehole data extracted from the original model and a combination of the data from resistivity tomography and borehole were conducted to build several new 3D geological models. 3D transient groundwater flow model (MODFLOW) and subsidence model (SUB) are developed based on the constructed geological models. The root mean square error (RMSE) and coefficient of determination (R-Square) using the reconstructed models' results compared to those of the original model were calculated to assess the geological model uncertainty. The results showed that using resistivity tomography data with the correction of boreholes data showed the best result than only using different numbers of borehole data. The results revealed an acceptable RMSEs (2 mm) and R-square value (approximate 0.9) in land subsidence simulation. The results also indicated that the prescribed boundary condition dramatically affects the results of subsidence simulation, as well as the value of hydraulic conductivity significantly affects the delay behavior in compaction calculation. Based on these results, geologists can assess the appropriate number of boreholes and combine the geophysical results to mitigate the geological model and parameter uncertainties to a specific study area.

Keywords: geological model uncertainty, land subsidence, groundwater flow,
borehole number, geophysical and geological fusion.

辨認卑南溪沉積物的有機地化特徵

楊沁文¹、林玉詩¹、黃美惠¹、王珮玲²、蘇志杰²、張詠斌¹

(1)中山大學海洋科學系、(2)臺灣大學海洋研究所

臺灣位於歐亞板塊與菲律賓海板塊的碰撞邊界上，活躍的造山運動造就許多高聳的山脈，也造成臺灣較高的地震發生頻率及較為破碎的地質條件。而在東亞季風及颱風的影響下，臺灣降雨量相對豐沛，在強降雨或颱風事件發生時，沉積物混雜風化的岩石、植物碎屑進入河川，進一步向外海輸送，若有條件形成濁流，則會在海洋沉積物中形成所謂的快速沉積層(事件層)。為了瞭解物質傳輸的過程，分析陸源沉積物的特徵是不可或缺的。由於木質素普遍存在維管束植物中，加上結構穩定，較不易被生物降解，在前人研究中多作為植物有機碳來源的示蹤劑。為了釐清這些經由河川攜帶至深海埋藏的沉積物特性，本研究使用多項有機碳代用指標，包含碳氮比、穩定有機碳同位素以及生物指標中的木質素，分析標本包含卑南溪河床沉積物、懸浮沉積物以及集水區內土壤。分析結果中，從穩定有機碳同位素約-22‰至-30‰的偏負數值，可以推估有機碳有高比例來自浮游植物及C3植物的貢獻，在木質素的S/V比和C/V比結果上，發現主要來自於被子植物的貢獻。利用木質素酸醛比的資料，可進一步推斷木質素受降解作用影響的程度，研究結果發現土壤標本比起河床沉積物具有更高的酸醛比值，顯示降雨沖刷土壤所帶至河川的有機質中，具有較多降解成熟的木質素，可能為岩石風化所產生及土壤中微生物活動所影響。而河床沉積物中的木質素，則有較高比例來自於集水區內的現生植物碎屑，受到降解作用影響較低。結合各項指標結果的討論，有助於釐清木質素是否能做為指示深海沉積物事件層成因的有效指標，並可作為後續研究海洋沉積事件層的重要依據。

中文關鍵字：卑南溪、顆粒態有機碳、木質素、降雨事件

運用高精度空載光達地形探討 2016 年紅葉崩塌後續地形演育

區雪儀¹、林冠瑋¹、林志交²、鄧嘉欣²、吳俊龍³、陳奕中⁴、陳柔妃⁴

(1)成功大學地球科學系、(2)中興測量有限公司、(3)行政院農委會水土保持局、

(4)臺北科技大學材料及資源工程系

2016 年 9 月莫蘭蒂強烈颱風帶來累積雨量超過 600 mm 的豪大雨，導致位於台東縣延平鄉紅葉村邊坡發生大面積崩塌，其後續產生的大量土石，導致土石流、破壞村莊內道路與民宅。由於大規模崩塌具破壞力強、影響範圍大之特性，且通常伴生土石流等複合型災害之發生，紅葉村土石流掩埋事件更再次喚起國內對大規模崩塌災害的重視與關注。由於崩塌邊坡先天的地表特性及地質模式，是瞭解崩塌發生條件的根本基礎，然而在崩塌後期邊坡的地形發育更是鮮少為人探討。為瞭解紅葉崩塌事件後續的地形演育，本研究利用 2020 年 0.5 公尺高精度空載數值地形模型，藉由產製坡度圖、紅色地圖等基礎資料，瞭解大規模崩塌邊坡之地形演變，並配合多期數值地形模型進行崩塌特徵、線性構造比對，以及土方量體計算等，再配合野外現勘進行比對室內分析結果。本研究初步成果顯示，紅葉村北方邊坡上的蝕溝發育，受到區域構造影響，其岩體弱面是主要控制崩塌面雙溝同源的因素，而莫蘭蒂颱風強降雨則是誘發大規模崩塌的外在因素，以致於造成大面積岩屑崩滑並引發土石流災害。為了探討崩塌前後地表變形特徵，本研究後續將加入多時序合成孔徑雷達干涉技術(Multi Temporal InSAR, MT-InSAR)配合 2007-2011 年 ALOS 以及 2014-2021 年 ALOS-2 雷達衛星，產製多時序地表變形資訊，配合數值模擬方法針對紅葉崩塌邊坡的活動性與破壞機制，進行更深入的探討與分析。

中文關鍵字：地表地質作用、空載光達數值地形模型、地質災害、紅葉滑坡

探究降雨與地震力對於中大規模崩塌觸發之影響

曾文奕¹、趙韋安²、張睿明³

(1)陽明交通大學土木工程學系、(2)陽明交通大學土木工程學系/陽明交通大學防災與水環境研究中心、(3)臺灣大學地質科學系

降雨為坡面地質災害的主要觸發因子之一，利用歷史災害事件的降雨資訊與背景雨量資料結合統計的方法可求得該地區不同降雨產生災害的機率，進而導入降雨門檻警戒值之概念。現今臺灣地區在豪雨期間之降雨警戒值主要為水土保持局之土石流降雨警戒值，以及國家災害防救科技中心之坡地災害降雨警戒值兩種，但歷史災害之時間不確定性會使上述之降雨警戒值產生誤差，而坡地災害所產生的地動訊號確有助於釐清災害所發生之準確時間點。故本研究利用 2007 年至 2013 年間崩塌面積介於 11,100 與 502,739 平方公尺共 30 個非莫拉克期間之坡地災害目錄，經由地動訊號來確認精準的崩塌時間，將降雨強度開始大於 4 毫米/小時視為雨場的開始時間，進一步計算產生坡地災害之累積雨量與平均降雨強度來檢核土石流與坡地災害降雨警戒值。本研究結果顯示有些許的坡地災害其發生當下的累積雨量小於兩單位的降雨警戒門檻，該現象可能受到前期地震之影響使得降雨警戒門檻下降，因此更進一步利用地震目錄各地震之對數地震矩經距離修正後，計算其地震影響力，結果顯示低於降雨警戒門檻值之坡地災害，在其發生之前地震影響力明顯有偏高的趨勢；然而，以同樣的方法針對莫拉克颱風期間面積介於 200,000 至 2,487,000 平方公尺的 40 個深層崩塌事件進行分析，則無此現象發生。故本研究認為大型的坡面災害主要的致災因子為大量降雨所導致(>200,000 平方公尺)，而較小型的坡面災害則易受到地震影響力與降雨的複合作用而發生。因此除了考慮降雨以外，背景地震影響力的作用於未來也應納入坡地災害的警戒的考量因素，以提升中小規模且發生頻率高的崩塌事件之預警準確性。

中文關鍵字：降雨警戒值、坡地災害、地震影響力

Seismic recognition of small-to-large sized landslide and earthquake with deep-learning method

Kuo-Pin Chou¹、Wei-An Chao²

(1)Department of Civil Engineering, National Yang Ming Chiao Tung University、(2)Disaster

Prevention and Water Environment Research Center, National Yang Ming Chiao Tung University

Seismic signals induced can help us to know the information on when, where, and how landslide event occur. However, how to quickly and effectively distinguish seismic signals between earthquake and landslide is still a big challenge for real-time monitoring purpose. Previous study has used convolutional neural network (CNN) to train the spectrogram features, which related to the distribution pattern of spectral power, time and frequency, for the discrimination of signals from earthquake and tectonic tremor. Based on the machine learning processing, the Random Forest classifier was developed to identify landslide seismic signals. However, aforementioned results are limited in application because their training dataset do not cover wide ranges of landslide types. In this study, we first collect the information (occurrence time, location, size, lithology) of landslide events with a collapse area ranging from 100 m² to 2-million m², and then the seismic signals of landslides can be found from the broadband seismic network. A total number of landslide events used in this study is over than 60. Since the machine learning method such as the support vector machine and decision tree cannot well identify the signals corresponding to variable sized landslides, we further use CNN method to train the landslide recognizer based on the image features. Here, five parameters, including the signal duration (SD), skewness (SK), kurtosis (KT), magnitude ratio between local magnitude and duration magnitude (MR), and spectral amplitude ratio between low-frequency and high-frequency (SRLH), can be extracted from seismic time series data, are used to construct the image shape (radar image). Radar image of different event types is 200×200 pixels with gray-color image. Our proposed landslide recognizer not only identifies the signals generated by earthquakes and landslides in accuracy but also can distinguish the landslide signals with different event magnitude and source types.

Keywords: seismic signals, landslide, convolution neural network, radar image

運用雷達極化與空載光達地形特徵評估自動化崩塌圈繪之可行性

李銘泓¹、李恩瑞¹、陳柔妃²、陳奕中²

(1)成功大學地球科學系、(2)臺北科技大學材料及資源工程系

台灣為世界少數之複合性自然災害地區，除了地狹人稠、過度開發外，地質條件複雜、岩體脆弱以及全年降雨事件集中等，都是造成山崩災害的主要因素。以 2009 年莫拉克獻肚山山崩為例，在 72 小時之內下超過全年度的降雨，邊坡土壤含水量達到飽和、誘發山崩。期間崩塌量體在楠梓仙溪形成大型堰塞湖，爾後河水高漲造成潰堤、沖毀小林部落，造成四百餘人罹難。為避免憾事再度重演，如何快速、有效地掌握崩塌區域、影響範圍等，尤為重要。

傳統上崩塌地的劃定多半使用各種載具搭配光學影像儀器，利用事件前後影像之變異程度進行崩塌判釋研究。然而災後天氣通常不佳、雲層覆蓋率高，不利於快速取得災區之光學衛星，了解崩塌地現況。合成孔徑雷達則是利用雷達微波偵測地表，其全時、全天候的影像拍攝，較不受天候及雲層覆蓋影響，得以取得更多災後立即資料，更適用於災後判釋及協助救援。

本研究使用日本宇宙航空研究開發機構(JAXA, Japan Aerospace Exploration Agency)於 2006 年發射之 ALOS/PALSAR 衛星，透過衛星雷達影像的雙極化成像(Dual-polarization)，將水準極化(Horizontal polarization)與垂直極化(Vertical polarization)之水平發射水平接收(HH)和水平發射垂直接收(HV)偏極化影像進行融合。為了增強雷達影像極化特徵，本團隊發展一套數值分析模式，透過提取每一像素之極化值，針對不同地表特徵物進行極化值分析，透過統計可快速分辨植被覆蓋區及裸露地。

以旗山溪流域為例，利用莫拉克風災前後雷達極化影像，可快速識別出絕大多數明顯裸露地，提取該裸露地範圍之極化影像、坡度圖、紅色地圖等地形特徵。嘗試尋找合適門檻值，建立符合該區域裸露地篩選模式，作為未來新生裸露地快速篩選之依據。同時結合雷達影像雙極化與高精度數值地形模型，為進一步進行深度學習中自動化判釋邊坡崩塌提供良好前置資料。

中文關鍵字：合成孔徑雷達、雙極化、ALOS/PALSAR、崩塌判釋、深度學習

Evaluating logistic regression and random forest for nowcasting modeling of earthquake-triggered landslides in Taiwan

Jay Liu¹、Ray Y. Chuang¹、Bing-Sheng Wu²

(1)Department of Geography, National Taiwan University、(2)Department of Geography, National Taiwan Normal University

Earthquake-triggered landslides can cause severe hazards, especially for plate boundary zones like Taiwan where has a lot of earthquakes occur every year. Thus, it is important to monitor and to predict earthquake-triggered landslides in such areas. In order to rapidly estimate landslide locations in near real-time, nowcasting is an effective way to provide possible landslide distributions when an earthquake happened. In this study, we aim to assess the predictive ability of two models, which were built by logistic regression and random forest methods. We use landslide data induced by the 1999 Chi-Chi earthquake as training data, and the Jueili earthquake-triggered landslide as the validation dataset. First, we compile parameters from the literature and produce these variable data at the spatial resolution of 40 m. Second, we access different combinations of parameters in the logistic regression and decide how many trees and how many variables will be taken in a tree in random forest. Third, we use indicators of model performance to evaluate the models. We use sensitivity and AUC to evaluate model performance. According to our result, the sensitivity in training data is 0.93 for logistic regression and is 0.94 for random forest. For the validation, the sensitivity is 0.83 for logistic regression and is 0.65 for random forest. The results show that the logistic regression model has its advantages for the nowcasting, and the random forest approach may not be as good as logistic regression based on the validation.

Keywords: near real time, seismic-induced, machine learning

Developing the building exposure inventory for seismic risk assessment in Taipei

Ming-Kai Hsu¹、Kuo-Fong Ma²、Chung-Han Chan¹

(1)International Graduate Program for Earth System Science between National Central University and Academia Sinica, Taiwan; Earthquake-Disaster and Risk Evaluation and Management Center, National Central University、(2)International Graduate Program for Earth System Science between National Central University, Taiwan; Earthquake-Disaster and Risk Evaluation and Management Center, National Central University; Institute of Earth Sciences, Academia Sinica, Taiwan

Development of building exposure for seismic risk assessment has been a focus topic for urban development and future design to understand societal capacity and strengthen resilience. An exposure database includes building parameters, including locations, taxonomy, height (number of floor), construction times and usage. These end-to-end hazard and risk assessment will increase the resilience of society to extreme earthquake events by identifying the factors critical to society in the earthquake scenarios or/and seismic assessment in probability. Departing from some exposure databases with grid-based resolution, we have constructed building-based exposure database. We first obtained the geometry of each individual building from the National Land Survey and Mapping Center. Then we acquired corresponding building parameters (such as address, taxonomy, number of floor, construction times and usage) according to the government tax data from finance statistics database. Address of each building was converted to corresponding coordinate through the Taiwan Geospatial One Stop (TGOS). Based on the geometry and coordinate, parameters from various sources can be integrated. Such high-resolution database would contribute crucial information for subsequent risk assessment, such as risk from fault displacement hazard; implementing specific response spectra based on the height (or number of floor) of each building.

Keywords: seismic risk, exposure model, building inventory

Probabilistic fault displacement hazard analysis: Review and case study in Taiwan

Jia-Cian Gao¹、Chung-Han Chan²、Kuo-Fong Ma³、Chyi-Tyi Lee¹

(1)Earthquake-Disaster and Risk Evaluation and Management Center, National Central University / Institute of Applied Geology, National Central University、(2)Earthquake-Disaster and Risk Evaluation and Management Center, National Central University / Department of Earth Sciences, National Central University、(3)Earthquake-Disaster and Risk Evaluation and Management Center, National Central University / Department of Earth Sciences, National Central University / Institute of Earth Sciences, Academia Sinica, Taiwan

Coseismic surface displacements associated with large earthquakes could result in significant damage to structures located on or near a fault. Thus, a probabilistic fault displacement hazard analysis (PFDHA) has been proposed to estimate expected levels of slip on a fault due to surface rupture. However, the dataset that contributed to this analysis is rare due to infrequent events of this kind. An earthquake with M_w 6.4 occurred in Hualien, Taiwan, on 6 February 2018, which caused surface ruptures associated with the Milun Fault with a maximum offset of 30 cm, resulting in damage. Field investigations were immediately carried out with good compilations of the data, which provided additional important test data for the PFDHA. In addition to validating the PFDHA, we first implemented the empirical prediction equations for fault displacement, variability of displacement, and other variables that are the key to implementing a PFDHA from the available global dataset, and proposed a new fault displacement prediction equation (FDPE) for the principal fault based on an existing prediction form. We used the derived prediction equations and their variability to calculate the fault displacement hazard and handle epistemic uncertainties through a logic tree formulation. Using the surface rupture data (with free field data and other possible artifact data in the fields) of the 2018 Hualien earthquake, we validated the credibility of the FDPE that we selected, and the investigation on the fault displacement hazard. The comparison shows that 86% of the free field data of the Hualien event is within one deviation, whereas about 65% for other datasets having artifacts. Our study shows a possible establishment of a Taiwan fault displacements hazard map, which is helpful to the government and public for understanding the fault displacement hazard and the potential hazard level for major facilities.

Keywords: probabilistic fault displacement hazard analysis

台灣南部隱沒帶地震地動預估式之研究

劉妍希¹、李錫堤¹

(1)中央大學應用地質研究所

地動預估式是用來評估地動值隨距離衰減的公式，為地震危害度分析中重要的一環，藉由地動預估式可估算場址可能受到的地動值大小，進而作為工程設計上的考量。

台灣位於歐亞大陸板塊與菲律賓海板塊的碰撞帶上，兩板塊的碰撞作用在台灣外海形成兩個隱沒帶構造，分別是位於東北部外海的琉球隱沒帶和西南部外海的馬尼拉隱沒帶。不同的震源類型其震波特性和衰減模式不盡相同，現今針對台灣隱沒帶地震所建立的地動預估式是以東北部的地震資料來建立。過去在進行地震危害度分析時，兩個隱沒帶地震之皆採用相同的地動預估式，但南部隱沒帶地震與東北部隱沒帶地震的震源特性和衰減特性有所不同，加上近幾年來南部隱沒帶的地震資料也已足夠，故本研究針對南部隱沒帶地震建立地動預估式，以臺灣強地動觀測網 1991 年至 2018 年的資料，進行基線校正與濾波並計算反應譜，透過混合效應的非線性迴歸分析建立台灣西南部隱沒帶地動預估式供地震危害度分析應用。

中文關鍵字：地動預估式、台灣南部隱沒帶地震、地震危害度分析、非線性迴歸分析

Horizontal deformation caused by groundwater withdrawal in central Taiwan based on GNSS observation analysis

Reyhan Azeriansyah¹、Kuo-En Ching¹、Pei-Ching Tsai²

(1)Department of Geomatics, National Cheng-Kung University、

(2)Green Environmental Engineering Consultant Co., Ltd.

Although the horizontal deformation related to the land subsidence has been proposed in the USA, only the vertical deformation resulted from the groundwater pumping was considered in central Taiwan so far and this information is an efficient coefficient to manage the groundwater withdrawal. However, the discrepancy of geodetic surface subsidence rate larger than compaction rate from monitoring well indicates that the compaction at the aquifer deeper than 300 m is possible. To clarify this enigma, a horizontal deformation pattern may help to resolve the compaction located at the aquifer deeper than 300 m. In general, central Taiwan moves toward NW relative to the Eurasian plate due to plate convergence. However, the directions of horizontal velocities in the land subsidence region are relatively random. Because the velocities are generally less than 10 mm/yr in this area, this random orientation is usually proposed as the measurement error. But the study in Los Angeles, USA indicates that the random orientations of horizontal velocities result from the groundwater pumping. We, therefore, re-visited the horizontal velocity field in central Taiwan in this study. The GNSS observations were first used to estimate the horizontal velocities around the land subsidence region based on the coordinate time-series analysis. To extract the signals of land subsidence from the raw horizontal motion, the velocities out of the land subsidence region will be used to evaluate the tectonic-driven velocities in the land subsidence region by two methods: the spatial interpolation and tectonic block model. After removing the tectonic-driven velocities, the land subsidence-related horizontal velocities will be obtained and used to evaluate the layer depth and its compaction rate using the dislocation model.

Keywords: land subsidence, secular velocity field, tectonic block model, spatial interpolation, dislocation

Developing low-cost portable scanner with raspberry Pi for surface grain size distribution of riverbed and its application

Yao-Chen Yang¹、Wei-An Chao²

(1)Department of Civil Engineering, National Yang Ming Chiao Tung University、(2)Disaster

Prevention and Water Environment Research Center, National Yang Ming Chiao Tung University

Grain-size distribution of riverbed is crucial parameter for not only understanding geomorphic metric of gravel- and boulder-bed river but also studying the river sediment transport. Most typhoons hit Taiwan during summer, causing the obvious change in grain size distribution of riverbed. Thus, an efficient way for grain size survey is urgent needed. The traditional measurement methods, including manual counting and sieving, are useful but they are limited in spatial survey area of 1-10 m² scale, and are time and human-consuming. With advancing in feature recognition, the image-based grain sizing approach can do work rapidly on determining grain size. In this study, we first test the open-source python-based program, *PebbleCountsAuto*, which is a fully automated scheme for the edge detection based on Sobel, Canny and Top-hat processing from photographs. Then, Raspberry Pi and Pi-camera were used and embedded with the *PebbleCountsAuto* program to develop the low-cost portable scanner. We also build a webserver in Raspberry Pi for displacing result in field. The downstream of Zhenwen River and Putunpunas River are selected to be the testing sites, and the artificial large-scale dam break experiment is used as application site. In the case of Yufong Bridge, the median diameter (D₅₀) estimated by the scanner and derived from the manual counting are 42.3 mm and 81.2 mm, respectively. Result determined by the scanner is the surface grain size instead of the particle size, causing the aforementioned discrepancy in the value of D₅₀. In general, low-resolution images can deduce the computing time but result the underestimated in grain size. Finally, our proposed was applied to the dam break experiment, which can investigate the spatial distribution of riverbed eroding and accumulating rapidly. We demonstrated that our scanner can survey the grain size distribution of riverbed with larger cover areas without time consuming.

Keywords: grain-size distribution, low-cost portable scanner, dam break experiment

漫天徹地-運用 ERT 結合 InSAR 探討滾水坪泥火山活動跡象

陳宗霆¹、樂鎔·祿璞峻岸¹、吳劭威²、葉佳鴻²、陳奕中³、陳柔妃³

(1)成功大學地球科學系、(2)臺灣世曦工程顧問股份有限公司、

(3)臺北科技大學材料及資源工程系

台灣西南部海底早期的快速沉積作用，使沉積物尚未充分壓密膠結，在西部麓山帶一系列褶皺逆衝帶中，發達發育良好的泥貫入體構造，藉由斷層或裂隙等線性構造出露於地表形成大小規模不同的泥火山。滾水坪泥火山位於高雄市燕巢區及橋頭區之交界，其鄰近龍船斷層向西南延伸之車瓜林斷層。由經濟部中央地質調查所五萬分之一地質圖旗山圖幅，可將本區地層劃分為：現代沖積層、階地堆積層、崎頂層、古亭坑層等，其中滾水坪泥火山之泥漿噴發物經由化學分析後，結果為古亭坑層之產物(林啟文等，2013)。本研究使用地電阻影像剖面法(Electrical Resistivity Tomography, ERT)，藉由 ERT 深入地表下取得地層間不同岩性電阻率之特性，繪製滾水坪泥火山地層電阻率分布圖，並搭配 3DERT 建置泥火山地下構造，推測泥漿庫所在位置。同時，結合多時序合成孔徑雷達干涉技術(Multi Temporal InSAR, MT-InSAR)，監測地表變動之變形量及變動頻率之特性，獲得泥火山地表高程變化資料，最後利用多期地表變形量進而探討滾水坪泥火山噴發口之地表活動情形。本研究藉由這兩方法取得地表下泥漿庫通道、地層間含水量多寡與泥火山噴發口變動頻率相互關係，此兩種不同技術可相輔相成，達成泥火山地區地球物理與衛星遙測聯合探勘之實務應用。

誌謝 本研究計畫承蒙 台灣世曦工程顧問股份有限公司「橋頭科學園區泥火山公園三維地表地質及地電阻(含地聲觀測)整合調查及分析」計畫案提供研究經費 謹致謝忱。

中文關鍵字：地電阻影像剖面法、多時序合成孔徑雷達干涉技術、滾水坪、泥火山

The effect of groundwater fluctuations on accumulative subsidence of aquifer layers based on a fluid - mechanical model in Choushui River alluvial fan.

Nguyen Thi My Tien¹、Chuen-Fa Ni¹

(1)Institute of Applied Geology, National Central University

In Taiwan, the Choushui River alluvial fan is a severe land subsidence area due to groundwater extraction in the past decades. Unexpectedly, the subsidence area has been moved from the coastal to the central of Choushui River alluvial fan where the Taiwan High-Speed Rail constructed can threaten its safety. Previous studies found that the land subsidence and layer settlement were consistent with the groundwater level variations. However, the average of groundwater variations changes from stable to increasing over time while cumulative subsidence continuously increases if we consider observation wells around Taiwan High-Speed Rail. The dynamics of groundwater fluctuations might affect the land subsidence on the surface and in the aquifer layers. In this study, numerical simulations of pumping wells in the shallow and deep aquifer were conducted to investigate which factor has a superior influence on the subsidence. The finite-difference model in FLAC3D was used to simulate the fluid-mechanical interaction when pumping. The predicted layer settlements will be compared to observed data to verify the numerical model performance. The preliminary results indicate that shallow aquifer pumping will not only influence shallow aquifer but also deeper aquifer. The factor affecting the subsidence might be the combination of seasonal groundwater fluctuations and dynamic loading of Taiwan High-Speed Rail. Based on the understanding of the local variation process of the land subsidence, we could carry out an efficient management plan to mitigate subsidence in the Choushui river Alluvial fan. We will simulate subsidence induced by deep aquifer pumping and apply dynamic loading to the model to analyze the response of groundwater and aquifer layers to pumping in near future.

Keywords: Choushui River, groundwater fluctuations, fluid-mechanical interaction, FLAC3D.

中臺灣海峽近岸區淺部地層之流體特徵辨識及分布

曾湧翔¹、許鶴瀚¹、陳憶萍²、楊懿丞²、王明²、劉家瑄²

(1)臺灣大學海洋研究所、(2)臺灣大學海洋中心

沉積物液化與地層中流體移棲皆為海床不穩定因子。在淺海具有快速沉積作用發生的區域，特別是高孔隙率的砂質沉積環境，常會有流體填充在孔隙當中，當極端事件發生且造成地層擾動時，這些超孔隙水壓地層孔隙之間因富含流體，故顆粒間摩擦力較小，即有機會發生沉積物液化，並且孔隙中流體可能沿著壓力梯度方向移棲，形成流體移棲特徵，進而造成海床與地層不穩定。本研究探討臺灣海峽東側彰濱外海近岸區淺部地層之流體特徵及分布，研究區鄰近濁水溪出海口。濁水溪為全台沉積物供應量最大的河流(30~60 Mt/yr)，河口的淺海環境中堆積大量砂質沉積物，且因臺灣地震、颱風、洪泛等極端事件發生頻繁，大量沉積物於短時間內輸入彰濱外海，快速沉積作用有利於流體封存於地層中，一旦地層受到擾動，容易觸發流體移棲與沉積物液化作用。本研究利用火花放電(sparker)震測調查得到的地層剖面，透過震測相分析，根據流體造成的震波性質改變來辨識彰濱外海地層中的流體，例如：頂部強振幅、低頻、極性反轉、內部振幅衰減與垂直貫穿水平地層等特徵。震測剖面顯示研究地區有廣泛分布的楔型體(clinoform)，其震測相呈現下覆至下部地層，上部整合，內部呈傾斜狀排列與反白特徵，深度約為海床下十到二十公尺，厚度則介於數公尺到十多公尺，水平延伸達數百公尺到數公里，其發育可分為兩期並皆向海進積，且在其下方亦觀察到透鏡狀反白特徵。因其分布鄰近古濁水溪出海口，故推測為過去於高水位時期古濁水溪輸入大量陸源沉積物進入彰濱外海，因快速堆積而沉積出的富含流體地層。綜觀震測剖面中顯示的流體特徵，本研究將彰濱外海近岸區的流體分為兩大類型，分別為水平富集型與垂直移棲型。水平富集型的流體在空間上呈連續性分布，主要分布在楔型體內部、楔型體下方與東彰雲砂脊下方；垂直移棲型可依震測相中出現的流體指示特徵，分為 Pa(反極性)、Pb(無反極性)、Pc(頂部連結麻坑)三種，大多位於淺部地層且皆移棲至海床下十公尺左右，有少數幾個突破海床。這些垂直移棲通道直徑皆介於數公尺到一百公尺間，其中 Pa 有觀察到極性反轉的特徵，推測當中可能含氣體；Pc 則表示流體向上移棲冒出海床而形成麻坑或古麻坑。垂直移棲型主要分布於古濁水溪口與現今濁水溪口外，故推測是因濁水溪輸入大量砂質沉積物，快速沉積後，流體被封存於一定深度地層中，可能因之後的擾動事件，使其向上移棲。根據彰濱外海近岸區的流體特徵與分布，我們認為此區的流體移棲與富存可能與古代及現今的濁水溪出海口位置有所關聯，濁水溪的快速堆積作用是影響彰濱外海地層中流體封存的重要機制之一，而封存的流體受極端事件的擾動後，即可能造成沉積物液化，亦可能促使流體移棲發生，造成海域地質災害。近年來台灣積極發展離岸風電，彰濱外海正是重要潛力場址之一，希望透過本研究對此處淺部地層流體特徵的辨識與分佈位置的探討，能夠對流體造成

的相關地質災害風險有更進一步的了解與掌握，以提升海域工程安全，也能對日後離岸風場的建設及營運有所幫助。

中文關鍵字：流體移棲、沉積物液化、震測、火花式放電、離岸風力發電



Tectonics of the Hualien Ridge and offshore extension of the Milun Fault

Lien-Kai Lin¹、Shu-Kun Hsu¹、Ching-Hui Tsai²、Yi-Ching Yeh¹、

Shiou-Ya Wang¹、陳冠廷¹、陳松春³、林筱珊²

(1)Department of Earth Sciences, National Central University、(2)Center for Environmental Studies, National Central University、(3)Central Geological Survey, MOEA, Taiwan

Located in eastern Taiwan, the Longitudinal Valley is generally considered as the collisional suture between the Philippine Sea and the Eurasian plates. To the northeast, the Philippine Sea Plate is generally considered to have subducted beneath the Ryukyu Arc. The corner between the eastern Taiwan and the Ryukyu Arc system is the transition from the plate collision to plate subduction of the Philippine Sea Plate. In consequence, the tectonics is complicated and the earthquakes are rather frequent. In this study, we use marine geophysical data to study the submarine Hualien Ridge that is situated in this plate collision/subduction transition. The Hualien Ridge is the offshore portion of the inland Milun Tableland; the Milun Tableland is uplifting and is bordered in the west by the active Milun Fault. Our results show that the Hualien Ridge can be tectonically divided into the active southern Hualien Ridge and the inactive northern Hualien Ridge. Several active faults trending $\sim N30^{\circ}E$ exist in the southern Hualien Ridge; some faults could be linked to the active faults in the Milun Tableland. The structures in the southern Hualien Ridge and the Milun Tableland display a pop-up structure that is subject to the oblique compression from the northwestward collision of the Philippine Sea plate. Moreover, the $\sim N30^{\circ}E$ trending structural faults are the results of the transpressional fault system. However, the Milun Fault, the western boundary of the fault system, probably terminates near $24^{\circ}04'N$, where a pronounced bathymetric structure trending $N300^{\circ}$ exists. On the other hand, in the northern Hualien Ridge we can only observe several blind normal faults covered by ~ 100 m thick sediments. Overall, the distinct separation of tectonic activity in the Hualien Ridge marks the transition from the actively plate colliding (convergence) to inactively convergence or partially subduction of the Philippine Sea Plate relative to the Eurasian Plate.

Keywords: Hualien ridge, collision, subduction, sparker reflection seismic, Milun Fault

臺灣北方海域棚坡區海床形貌的成因探討

鍾承峻¹、許鶴瀚¹、張日新¹、楊懿丞²、陳姿婷¹、劉家瑄²、
林依蓉³、陳松春³

(1)臺灣大學海洋研究所、(2)臺灣大學海洋中心、(3)中央地質調查所

海床的形貌反應了不同地質及構造作用影響，臺灣北方海域地處東海陸棚與陸坡區，平均水深小於 300 公尺，東南側與南沖繩海槽接鄰，西、北側是平緩的東海陸棚。過去研究指出，此區大地構造由臺灣造山帶的後造山垮塌及沖繩海槽弧後擴張所主導，但其細部地形特徵與地體構造的關聯性卻少有討論。本研究利用多音束水深及多頻道反射震測資料，進行地形與震測相分析，嘗試了解海床的構造型態，並將臺灣北方海域區分為基隆內陸棚區、基隆外陸棚區與北方三島區進行探討。在基隆外陸棚區，水深資料顯示海床線型特徵皆為東北-西南向，延伸長度可大於 10 公里；在震測剖面上，海床線型特徵大多有可對應的斷層構造，而斷層構造鄰近的反射則有強振幅、混亂相等特徵。在基隆內陸棚區，海床上不但有東北-西南向以及西北-東南向兩組不同走向的線型特徵，尚有環狀特徵的分布；在震測剖面上，除了亦可觀測到與海床線型特徵相對應的斷層構造、以及斷層構造周圍強振幅與混亂相等特徵之外，也有觀察到噴出火山構造之特徵。在北方三島區，則以西北-東南向(長度<10 公里)的線型特徵以及環狀特徵為主；在震測剖面上，除了強振幅與混亂相的反射特徵不限於斷層構造周圍，以及噴出火山構造特徵之外，我們同時發現有部分區域的深部地層影像被近海床之訊號遮蔽。根據水深與震測資料的分析結果，我們推測海床上的線型特徵主要反映切穿海床的斷層構造，走向上以東北-西南向為主、西北-東南向為次；而根據線型特徵在走向和長度上的差別，則可能為主要斷層構造以及因其相互接續所造成的次生構造。環狀特徵則可能與崩塌有關，推測是受斷層錯動或是破火山口機制所導致。而剖面中強振幅、混亂相與訊號遮蔽區域推測為火成岩體及熔岩流覆蓋海床造成。我們的觀察說明了臺灣北方海域之海床與地層正受到活動斷層與火成作用的影響。

中文關鍵字：臺灣北方海域、海床構造形貌、多頻道反射震測、多音束水深資料

利用海底形貌與震測特徵探討棉花峽谷的沉積型態

黃靖芸¹、許鶴瀚¹、張日新¹、林亮甫²、陳姿婷¹、劉家瑄²、
陳松春³、林依蓉³

(1)臺灣大學海洋研究所、(2)臺灣大學海洋中心、(3)中央地質調查所

棉花峽谷位於臺灣東北外海，其上游有東西兩支流，在峽谷中段匯合為一主流，然而過去因資料限制，對於棉花峽谷的地形、地層特性與相關構造對峽谷演化的作用仍未能完全瞭解。本研究藉高解析水深與多頻道反射震測資料，檢視棉花峽谷的地形與構造特徵，並討論峽谷地形受沉積及構造作用的影響。棉花峽谷自西支流頭部至陸坡底部全長約 136 公里，且東西兩支流形貌差異大：東支流長約 22 公里，由水深 600 公尺處發育，寬約 1.2 至 5 公里，下切深度約 120 至 380 公尺，頭部的數個小分支皆從一崖狀地形發育，其下段有小型曲流、數個半月型崩面及階地的分布，屬陸坡限制型峽谷；西支流長約 86 公里，由水深 200 公尺處發育，寬約 0.6 至 4 公里，下切深度僅 35 至 207 公尺，支流上段下切淺、地勢起伏小且流徑蜿蜒，屬陸棚嵌入型峽谷。東支流的震測剖面顯示少量沉積物堆積，谷壁兩側的地層多被截切，有許多斷層與斷塊分布在東支流以及兩支流交匯處底下，在東支流的兩側亦可發現被掩埋的古峽谷；西支流的震測剖面中，沉積物幾乎沒有堆積，在支流中段可能因熔岩流分布造成海床堅硬，使得訊號難以穿透至下部地層，在震測剖面上呈反白震測相；相較於東西兩支流，主流軸部水道兩側堆積了大量沉積物，應為多期的自然堤。本研究藉地形及震測資料的分析，推測東支流及頭部的數個分支可能是沿斷層間的斷塊或由斷層所觸發的塊體運動所形成，以旺盛的侵蝕作用為主，沉積物堆積較少；西支流上段可能為沿海床熔岩流造成的局部起伏所形成，但因地層堅硬而無法深切，支流下段無熔岩流分布，亦以侵蝕作用為主，才形成現今的峽谷形貌；主流兩側除了有厚層沉積物堆積，還有數個階地與崩移塊體分布，顯示主流目前以堆積作用為主。初步的成果也顯示被掩埋的古峽谷與現今峽谷的分布範圍並不相同，然而對於古峽谷的成因與現今峽谷的演化還需要近一步的分析與討論。

中文關鍵字：海底峽谷、多音束水深、反射震測、棉花峽谷、臺灣東北海域

利用海底地震儀與多頻道反射震測資料分析臺灣海峽中段之沉積層

P 波速度構造

蘇永祥¹、Sebastian Wege¹、王天楷¹、戚務正²

(1)臺灣海洋大學地球科學研究所、(2)中央研究院地球科學研究所

臺灣海峽中部的沉積構造，包括臺西盆地，南日島盆地，澎湖盆地等，都有活躍的斷層構造，值得研究。這項研究的目的是了解斷層的分佈，並協助對臺灣海峽中部深海(大於 50 公尺深)風電場的海底工程進行地質評估。首先，從 2017 年在臺灣海峽中部收集的多頻道反射震測和海底地震儀資料，以建立 P 波速度和斷層的沉積構造。根據海底地震儀資料走時反演烏坵凹陷與澎湖台地之間的 P 波速度-界面模型發現基盤上下錯動造成約 0.8 公里落差的正斷層帶，推測為濱海斷裂帶。位於烏坵凹陷西北側與金門隆起的交界發現 P 波速度(5 公里/秒)低速帶，形成不對稱的半地塹構造。我們認為臺灣海峽中部的濱海斷裂帶不但有右移走滑斷層，並重新激發先前存在的正斷層。此外，分析 2020 年 6 月新海研二號 007 航次跨越南日島盆地的 8 部海底地震儀資料折射和反射波走時反演 2 公里深的 P 波速度-界面模型與 9 條多頻道反射震測剖面，我們發現淺層沉積層(0.1-0.9 公里深)的 P 波速度為 1.5-2.3 公里/秒，較深層(0.8-1.5 公里深) P 波速度則為 3.5-4 公里/秒。此反演模型也顯示位於南日島盆地東南側深度 0.8-1.5 公里的 P 波速度(4 公里/秒)較高，可能是緊鄰東南側的邊界斷層所導致。南日島盆地西北側淺層(0.5-0.7 公里深)沉積層 P 波速度(2.5 公里/秒)高速帶，則可能是受到通過沉積層的正斷層影響。

中文關鍵字：斷層構造、前陸盆地、濱海斷裂帶、南日島盆地

利用多頻道反射與海底地震儀震測資料分析臺灣海峽北部之沉積層

P 波速度構造

王政揚¹、王天楷¹、魏格¹、馬仙古¹

(1)臺灣海洋大學地球科學研究所

本研究分析 2019 年 6 月在臺灣海峽北部觀音台地(新北市西北外海)收集的十條多頻道反射震測剖面及 6 部海底地震儀震測資料，以建立橫跨觀音台地之沉積層 P 波速度-界面模型。由於 2019 年收集的反射震測資料頻道數(12 頻道)較少，故先比較 2018 年在觀音台地北部收集的 24 頻道反射震測資料，並以此輔助震測資料處理與解釋。海底地震儀震測資料處理則是先進行海底地震儀定位，之後根據多頻道震測剖面的反射面建立初始模型的界面，再進行海底地震儀資料折射波與反射波走時選取。利用逐層反演修正折射波與反射波走時誤差後，建立沉積層 P 波速度-界面模型。從臺灣海峽北部中線附近的十條多頻道反射震測剖面顯示許多分段的正斷層，且在橫跨觀音台地雙程走時 0.52-0.63 秒處探測到前陸基底不整合面。一般而言，觀音台地東南部的前陸基底不整合面深度較觀音台地北部的深度深。在觀音台地的東北側（靠近新北市）也發現一些走滑斷層的花狀結構。從海底地震儀資料折射波和反射波走時反演橫跨觀音台地北部的沉積構造觀測到在前陸基底不整合面附近的 P 波速度（1.9-2.1 公里/秒）有較大的側向變化，其中幾條正斷層在較深的構造穿過前陸基底不整合面。此外，從海底地震儀震測 P 波速度模型可發現觀音台地表層(海床下約 100 米處)P 波速度(1.5-1.6 公里/秒)較小，可能為較鬆軟的淺層沉積層，故不適宜進行海底工程。我們收集的反射與折射震測資料和完成的 P 波速度-界面構造，將有助於臺灣海峽北部的海上風電場，海底電纜和海底隧道的地質評估。

中文關鍵字：前陸基底不整合面、花狀構造、觀音台地、走時反演

由海底地震儀資料探討南沖繩海槽之熱液活動特性

黃安婕¹、林靜怡¹、K.I. Konstantinou¹

(1)中央大學地球科學系

沖繩海槽是琉球弧溝系統作用所造成的弧後擴張盆地，在這樣張裂性的地質作用區域內常有活躍的火成和熱液活動。在過去的研究中，利用地球物理(震測、重力和磁力)、地質(岩石採樣)和實際水下觀測方法，也在南沖繩海槽內發現許多有潛力的熱液活動場址，包含火龍火山 1、火龍火山 2、石林隆堆、蓬萊斷層帶及第四與那國海丘場址等。但這些方法對於熱液相關活動分析所能涵蓋區域通常較小或是無法長期持續觀測。海底地震儀，具備一個水聽器及三分量的地動儀，可以用來持續監測天然地震及各種地動訊號，本研究即希望利用海底地震儀資料分析，來對於這些熱液活動資訊有更進一步了解。本研究分析了 2017 年 OR2-2231 航次於南沖繩海槽佈放的 6 個海底地震儀資料，記錄時間從 2017 年 4 月 7 日至 4 月 18 日，共 12 天。資料時頻分析顯示其中 3 個海底地震儀有記錄到諧波震顫(harmonic tremor)，一種常被認為與流體在火山內部的共振或火山氣體的排放有關的訊號。在測站距離小於 4 公里的情況下，諧波震顫只被單一個海底地震儀記錄，推測諧波震顫應該是由局部的活動造成。為了瞭解諧波震顫的震源特性，本研究也透過火山震顫模擬測試不同物理參數下產生的不同火山震顫，結果顯示諧波震顫在火山氣體週期性供應時才會產生。透過訊號來源定位分析搭配前人研究南沖繩海槽內部的噴氣構造位置，發現諧波震顫訊號來源與海槽內噴氣構造及海底火山的位置對應良好，且相同時段發生的諧波震顫不一定來自同一個方向，可能是熱液系統內流體遷移造成的結果。

中文關鍵字：沖繩海槽、諧波震顫、熱液活動、海底地震儀

Seismic source studies of Mindanao earthquakes using finite fault inversion

Wei-Yu Zhang¹、Po-Fei Chen¹

(1)Department of Earth Sciences, National Central University

The Mindanao island in South Philippines represents a completion stage of northward propagation of arc-arc collision by the divergent double subduction of the Molucca Sea plate (Chen et al., 2020). Here, the NE dipping subduction of the Cotabato Trench to the west, the west dipping of the Philippine Trench to the east, and the left-lateral strike-slip faults (Cotabato and Philippine) in the island together absorb the Philippine-Sundaland relative motions. Recently, a few strong ($M > 6.0$) earthquakes at least three in Oct. and one in Dec., 2019 - occurred in close proximity to each other on the Cotabato fault. Intrigued by causative relationships of these earthquakes, we conduct a finite fault inversion in this study to investigate the slip distributions as a function of time for aforementioned events. In the inversion schemes, the overall fault plane is divided into subfaults with which the Green's functions of teleseismic body waves (1Hz low-pass filter) to observatory stations calculated. The optimal slip amplitude, rake angle, initial rupture time, and rise time of each subfault are then determined by minimizing the discrepancy between those superposed from each subfault and those from observations. The comparison is made on wavelet amplitude variations that apply wavelet transform both on synthetics and observations. The optimization scheme is simulated annealing algorithm that approximates the global minimum of a given function through a probabilistic technique (Ji et al., 2002). Having determined the source characteristics of these earthquakes, we will look into their spatial and temporal relationships and potential tectonic implications.

Keywords: Mindanao, finite fault inversion

台灣地震對與重複地震關聯性與其潛在活動構造區域

林育璿¹、樂鎔・祿璞峻岸¹

(1)成功大學地球科學系

台灣人口密度高且地質活動頻繁，這兩項因素亦是影響地質災害模型的重要參數，如何在災害性地震下降低危險是台灣人民保護自己最重要的課題。藉由地震對的地震特性來了解發震區域特徵，並利用此因素建造符合災害風險的建築和制訂適宜法規。本計畫使用氣象局地震目錄並利用時間與空間特性剔除餘震後篩選出地震對，並探尋其發震區域分布及其特性，和發震區內事件時間間隔。此外並探究重複地震(特定地震群重複在同一斷層上，並且具有相似發震機制、波形相似度、規模大小)與地震對(相似規模、相近距離、彼此互非餘震)的關聯性，輔助解釋地震對可能的地體構造成因，且補充台灣活動構造分布模型。

中文關鍵字：地震對、重複地震、孕震構造



New insight into tectonics of Taiwan Strait from focal mechanisms and geophysical data

Chieh-Chen Lee¹、Tai-Lin Tseng¹、Pei-Ru Jian²、Bor-Shouh Huang²

(1)Department of Geosciences, National Taiwan University、

(2)Institute of Earth Sciences, Academia Sinica, Taiwan

Earthquakes in Taiwan Strait, on a passive margin, are infrequent and sometimes lack of well constrained focal mechanisms due to station coverage. To better understand the earthquake generations and crustal structures associated in Taiwan Strait, we analyzed the focal mechanisms of 21 moderate earthquakes from 1996 to 2018. All the moment tensor solutions were inverted using refined velocity models and waveforms of the best available stations. By combining results of previous studies, we compile a total of 44 well-constrained focal mechanisms in Taiwan Strait and compare them with magnetic data. There is a sequence of extremely shallow thrusting events in the offshore Miaoli area of Taiwan that are likely associated with the deformation front formed by collision. In the offshore region of southwestern Taiwan, both strike-slip and normal events are present. The latter is related to bending caused by gravity load on the continental margin. As for Tainan Basin, where the 1994 Mw 6.5 earthquake occurred, its vicinity remained seismically active in the past two decades. Earthquakes there are mostly normal faulting with minor strike-slip component with focal depth ranging from upper to lower crust (majority 15-25 km). The distribution correlates with the belt of high positive magnetic anomaly (100-250 nT). Previous studies interpreted the source of high magnetic anomaly to be magma intrusions into lower crust during the final rifting and early spreading of South China Sea. Therefore, we propose that a heterogeneity of crust beneath this area caused the concentration of stress and clustering of earthquake, a scenario analogous to the lower crustal rift-pillow as an explanation for the New Madrid seismic zone. The focal mechanisms near the Binhai Fault are variable. The 2018/11/25 Mw5.7 Taiwan Shoal earthquake sequence show high angle strike-slips and shallow centroid depth of 11-21 km. The inferred fault plane is E-W striking, also consistent with the previous study.

Keywords: Taiwan Strait, focal mechanisms, moment tensor inversion

Using multi-size unit tsunami method to build the tsunami early warning system in Ryukyu subduction zone

Yu-Chuan Chou¹、Po-Fei Chen¹、Tso-Ren Wu²

(1)Department of Earth Sciences, National Central University、

(2)Institute of Hydrological and Oceanic Sciences, National Central University

The Ryukyu subduction zone offshore NE Taiwan with its along-strike length nearly 1000 km is potentially for the occurrence of mega-earthquakes ($M_w > 9$) that will inflict significant tsunamis hazards in Taiwan. It is thus essential to establish a regional tsunami early warning system, which heavily relies on tsunami simulations. Among the three stages - Generation, Propagation, Run-up - of tsunami simulations, the propagation is the most time consuming stage and we adopt unit tsunami method to circumvent the real-time calculation of tsunami propagations. In this method, the seafloor of potential source region is divided into pixels. With each pixel, a one meter initial wave height was assigned and the propagation to tidal gauge stations was calculated using COMCOT (Liu et al., 1998) with results (unit tsunamis) stored in database. In the case of a real earthquake, the tsunamis at tidal stations generated by the earthquake are synthesized by linear combinations of unit tsunamis pulled out from database with coefficients equivalent to the average vertical seafloor displacement of the corresponding pixel caused by the earthquake. It is a trade-off between the number of pixels and the spatial resolution of seafloor displacements. Here, we employ a multi-size approach to cope with the broad coverage of the Ryukyu subduction zone. In the future, we will apply the same approach to establish tsunami warning systems for other tsunami-prone regions, such as Indonesia.

Keywords: Ryukyu subduction zone, unit tsunami method, tsunami early warning, COMCOT

Vp and Vs of shallow oceanic crust constrained by body-wave polarization analysis

Yu-Wen Fang¹、Ban-Yuan Kuo²、Justin Yen-Ting Ko¹

(1)Institute of Oceanography, National Taiwan University、

(2)Institute of Earth Science, Academia Sinica, Taiwan

Body-wave polarization provides a new and inexpensive way to constrain shallow oceanic crust structure. This method will be applied to the data from the Marine Observations of Anisotropy Near Aotearoa (MOANA) experiment to estimate Vp and Vs of shallow oceanic crust beneath ocean bottom seismometers (OBSs) array installed off both coasts of the South Island of New Zealand from late January 2009 to early February 2010. The P-wave polarization angle has no sensitivity to Vp but only to Vs, while the S-wave polarization angle has sensitivity to both Vp and Vs. In this study, both local and teleseismic events will be used. We expect to see frequency dependence of P-wave polarization that is sensitive to Vs at different depths.

Keywords: body wave, shallow oceanic crust, MOANA.



利用體波極化特性分析臺灣東北部淺層速度構造

謝偉修¹、溫士忠¹、陳朝輝¹

(1)中正大學地震學研究所

以往為了得到近地表波速，大多使用鑽井、噪聲或是人工震源等方法，這些方法中都需要花費大量時間進行開挖，或是造成土壤環境的破壞，更重要的是需要花費較大量的金錢，且不方便在人口稠密的區域執行，本研究使用前人提出體波極化分析的方法，剛好可以克服上述缺點，減少土壤環境的破壞，以及經費上的支出。本研究使用台灣東北部地區 36 個測站的三分量遠震資料，並使用震央距 30° 到 90° ，地震規模大於 6 的遠震震波記錄，使用體波來計算測站下的極化角度，再透過網格搜索得到最佳的模擬波速。另外對於深度敏感度的問題，本研究發現深度對於頻率的依賴性將可以使我們的結構限制在一個深度範圍內。為了增加體波波速穩定性，本研究加入更多的地震資料，來減少在 S 波極化角度上的不準確，再透過計算來改善壓縮波速模擬不好的問題，從而得到更完整的淺層速度。從研究的結果中可以看出相對低速及高速的地區很好的對應到了中央山脈的變質岩區域，以及近岸邊石灰岩的低速區，此結果亦與 Vs30 和 Z1.0 的結果相呼應。是故，透過此方法可以快速得到測站底下的淺層速度構造，且比起同樣使用遠震的接收函數方法可得到更淺的細部變化，這是使用體波極化分析的優勢。

中文關鍵字：臺灣東北部、極化分析、淺層速度構造、壓縮波速、剪切波速

微震活動在地熱區的行為特徵：以北台灣磺嘴山為例

陳榮輝¹、吳瑋哲¹、蘇建旻¹、溫士忠¹、李奕亨²、廖彥喆²、
彭筱涓²、陳俊榕²、陳朝輝¹

(1)中正大學地震學研究所、(2)工業技術研究院綠能與環境研究所

地熱能源的開發是近年來的熱門議題之一，位於台灣的大屯火山周遭也蘊藏著許多地熱資源，但礙於大屯火山屬於陽明山國家公園的一部份，在開發上有著一定的難度，在 2020 年 5 月 27 號，位於大屯火山群中磺嘴山東北側的金山硫磺子坪地熱示範區正式開鑽，此處剛好位於陽明山國家公園的邊界之外，而且有地熱開發的潛能。為了監測此地熱示範區的背景活動，本研究佈設一微震網紀錄此地熱區的地殼活動。長時間在此處進行微震觀測除了可以更加瞭解地熱區內微震的活動特徵，並可對將來的預設廠址有長期的監控。本研究使用中正大學地震研究所於磺嘴山鄰近地區所佈設之微震觀測網資料，透過所收錄的地震事件進行重新定位及混成震矩張量反演（Hybrid Moment Tensor Inversion）分析，來了解該地熱區微震的活動型態，目前觀察到此地熱區在淺層 1~3 公里的地方，分佈著許多非雙力偶震源的地震，而這些地震屬於膨脹的形式達到 50%~60%，表示此地熱區處於熱水活動活躍的情況，此現象代表著此區的地熱具備開發潛能，除此之外，此監測網亦能成為此區域淺層應力變化的指標。

中文關鍵字：混成震矩張量反演、磺嘴山、微震、地熱潛能

利用後投影法探討新養女湖泥火山區微震訊號

劉子菱¹、溫士忠¹

(1)中正大學地球與環境科學系

本研究目的是利用後投影法呈現微震訊號發生位置，藉此探討泥火山區的構造，因此在泥火山周遭擺設 16 個臨時測站記錄地動訊號。因泥火山底下的訊號會以微震的方式呈現，而微震的振幅小，且 P 波、S 波到時難以辨識，無法使用傳統定位方法進行定位，而後投影法只需要以觀測到的波形、準確的走時就能夠定位訊號來源，因此採用後投影法並運用震源掃描法 (Source-Scanning Algorithm, SSA) 進行定位。因後投影法需仰賴準確走時，故首先以臺灣西南部三維速度構造藉由模擬彎曲波線追跡法 (Pseudo-bending, PB) 反覆疊代，再沿波線路徑分段地將走時最小化，以計算更為精準的 S 波走時，求得此地區地下走時資料庫。接著採用震源掃描法以不同的震源點空間藉由波形的亮度函數進行網格搜索，計算出亮度最大的格點，即為可能的訊號發生的位置。本研究以訊號較強的波段進行定位，從而得知在此區底下有一類似垂直的管狀通道。最後，整合所有微震訊號發生位置，則能得到泥火山底下構造形貌。

中文關鍵字：後投影法、震源掃描法、模擬彎曲波線追跡法、泥火山、微震



TAIGER 南橫炸測是壓垮 2008 年利稻地震的最後一根稻草嗎？

孫郁涵¹、王維豪¹、葉玉蓮¹

(1)中正大學地球與環境科學系

2008 年 TAIGER 計畫 S3P 炸點於 02/27 凌晨 01:32 (UTC+8)炸測，隨後在 20 小時後的 22:07 在台東利稻附近發生一個深度僅 5.4 公里規模 3.2 的地震，由於其深度極淺，且震央位置和炸點相距不遠，故本研究使用 TAIGER 計畫南部測線之測站及氣象局在研究區域附近之寬頻測站的連續波形資料探討炸測與中央山脈南段地震之可能觸發關係。本研究使用 EQTransformer 機器學習程式對 2008/01/01-2008/02/27 連續波形資料進行地震挑選，並將其結果以 HYPOINVERSE 來定位。研究結果顯示，在利稻地震發生在一個月前中央山脈南段小地震分布散亂並未集中於任一處，然而在利稻地震前兩個禮拜開始，在利稻附近已開始出現較多的地震事件，且空間上有往利稻震央附近聚集的現象。而在 TAIGER S3P 炸測過後到地震發生前的 20 小時內，地震幾乎集中出現在震源周邊，數量高達 12 個小地震，此現象與前人研究岩石破裂實驗與在大地震前地震在破裂區時空上的分布演化過程相符。由這兩個月地震時空上的分布可推論在利稻地區既有的弱面在炸測兩周前已經產生應力集中並開始錯動，而炸測所產生的動態應力促使破裂迅速往利稻震源附近群聚，這些群聚的破裂將應力轉移至利稻震源，而最終導致利稻地震的發生。除此之外，本研究也發現在炸測之後出現顫動事件，惟這些事件僅被少數地震站記錄，其發生位置是否也位於利稻震源附近，仍有待後續研究釐清。

中文關鍵字：動態應力、利稻地震、TAIGER 計畫、顫動

花蓮地區孕震構造研究

黃籍億¹、李恩瑞¹

(1)成功大學地球科學系

台灣位於太平洋板塊與菲律賓海板塊交界帶，地震活動頻繁。菲律賓海板塊在台灣東部地區向北隱沒，也因此位於板塊碰撞和隱沒交界帶的花蓮地區，有著更高的地震活動度和複雜的構造系統。在地震活動度方面，根據中央氣象局 (Central Weather Bureau, CWB) 的紀錄，花蓮地區發生了數起致災性的地震事件，其中包含 1951 年 10 月 22 日規模 7.3 的地震事件、2002 年 3 月 31 日規模 6.8 的地震事件以及 2016 年 2 月 6 日規模 6.26 的地震事件。自從 2012 年起，CWB 開始利用連續紀錄來紀錄地震事件，花蓮地區在 2012 年至 2019 年之間，紀錄了高達 59000 個地震事件。而在構造方面，根據前人研究，除了中央地質調查所已經公佈的第一級活動斷層－米崙斷層和第二級活動斷層－嶺頂斷層之外，也有研究指出中央山脈東部斷層和大清水撕裂斷層等可能的構造。

本研究我們採用 Weighted Template Matching Algorithm (WTMA) 的方法來建立一個更完整的地震目錄，WTMA 方法是利用已知的地震波形來當作模板，利用此模板對連續波形進行波形相似度的搜尋並依照信噪比 (Signal-to-Noise Ratio, SNR) 給予權重後疊加，利用這個方式，我們可以找出肉眼無法辨識的地震事件，將地震目錄擴充的更加完整，使我們有更詳細的資料來研究 b 值和地震活動度。為了更加詳細的了解地下構造系統的分佈和判識發震構造，我們利用 GrowClust 重新定位法來進行重新定位。GrowClust 是利用地震的相對位置的重新定位法，利用波形的相似性以及到時差來進行分群並重新定位，之後我們利用重新定位後的地震事件在時間、空間分佈以及震源機制解來進行構造的判識。

我們利用 WTMA 的所搜尋到的小地震以及震源機制解來判別斷層面，也藉由重新定位使地震事件的分佈更加的線性，這有助於我們了解研究區域內的活動構造：米崙斷層、嶺頂斷層、清水斷崖附近的逆斷層、中央山脈東側的高角度西傾逆斷層以及大濁水溪口的逆斷層。

中文關鍵字：花蓮地震、地震目錄、地震重新定位、孕震構造

Ambient noise tomography for northern Okinawa trough OBS array

Ting-Chun Lin¹、Kai-Xun Chen²、Yuancheng Gung¹、Ban-Yuan Kuo³、
Mamoru Nakamura⁴、Shuichi Kodaira⁴、Pei-Ying Patty Lin⁵、

Ching-Ren Lin³

(1)Department of Geosciences, National Taiwan University、(2)Department of Geosciences, National Taiwan University; Institute of Earth Sciences, Academia Sinica, Taiwan、(3)Institute of Earth Sciences, Academia Sinica, Taiwan、(4)JAMSTEC、(5)Department of Earth Science, National Taiwan Normal University

From September 2018 to June 2019, IES, TORI, and JAMSTEC deployed broadband OBSs in the north Okinawa Trough (NOT) and its neighboring sea. Continuous vertical component of data from OBS, F-net stations and five temporary stations are used to extract the empirical Green functions of Rayleigh waves. With the measured dispersion (3-30 seconds) data from the noise-derived Rayleigh waves, we then implement a one-step, wavelet-based multi-scale tomographic technique to invert for 3-D models of both Vs and its azimuthal anisotropy of the upper crust and the shallow mantle structures. Major features in our preliminary model are generally consistent with the local multi-channel seismic model, with structure beneath volcanoes and the OT axis characterized by higher Vs, and fore-arc region characterized by lower Vs. Our models also show that there are clear variations in the fast polarization directions of anisotropy across the trench in the shallow depths, and such variations slowly migrate into a smoother pattern with depth.

Keywords: northern Okinawa trough, NOTOBS, ambient noise tomography, Ryukyu subduction zone

利用福爾摩沙陣列分析大屯火山區倍頻地震訊號之特徵

何其恩¹、陳卉瑄¹、林正洪²、賴雅娟³、史旻弘⁴

(1)臺灣師範大學地球科學系、(2)中央研究院地球科學研究所、國家地震工程研究中心、大屯火山觀測站、(3)國家地震工程研究中心、大屯火山觀測站、(4)中央研究院地球科學研究所、大屯火山觀測站

火山活動的觀測，除了研究噴發史、火山氣體監測、地溫梯度監測等，亦可觀測底下的岩漿活動狀況了解火山的活動性。岩漿庫的活動對應到深部氣體、流體和圍岩的相互作用，可藉由地震波的特徵解讀；而某些特殊的火山微震便是地底下流體活動重要指標。前人研究指出，一般的構造型地震在頻譜上不會有倍頻的特徵出現，通常倍頻訊號的出現，需要流體的運移以及有限而恆定的流體通道。如同水在水管裡快速流動一般，水的速度變化將會產生壓力、在水管裡震盪而形成壓力波，震盪的頻率取決於水管的長度和形狀。這樣的現象發生在火山的岩漿通道，亦可能因壓力的變化產生特定頻率的振動訊號，能量在管道裡傳播形成了駐波的條件，造成倍頻訊號。

大屯火山地區可能發現倍頻訊號嗎？對應到的物理過程和其他已觀測到的單頻和混合訊號是否相同？根據前人文獻，目前對大屯火山地區倍頻訊號，尚未有完整的搜尋和目錄的建置。本計畫的目的，在利用福爾摩沙陣列的資料搜尋大屯火山地區出現的倍頻訊號。我們利用了中央研究院福爾摩沙陣列在 2019 年一至二月的連續資料，在大屯山地區共 14 個測站，目前共找出八個被倍頻事件，持續時間約 15 秒，這些事件在 VO14、VO13、VO10、VO08 四個測站出現了明顯的倍頻特徵。於頻率 2-8 Hz 之間，有特間隔峰值出現（e.g., 3 Hz, 3.8 Hz, 4.6 Hz, 5.4 Hz）的倍頻特徵，以位於七星山東南方的 VO14 測站最為顯著。延續利用這些當時定義的倍頻事件為基準，本研究將改善程式自動搜尋的條件，擴大搜尋的時間範圍至四月，讓大屯火山地區的倍頻訊號有更完整的整理和分析成果。

中文關鍵字：火山倍頻特徵、火山倍頻地震、大屯火山、福爾摩沙陣列

2020 年 12 月 10 日宜蘭外海 M_L 6.6 地震破裂特徵之研究

王聖東¹、黃瑞德¹、林昱全¹、林瓊瑤¹、林采儀¹、黃怡陵²

(1)中國文化大學地質學系、(2)臺灣海洋大學地球科學研究所

本研究利用遠場 P 波逆推和非負解時間域解迴旋探討 2020 年 12 月 10 日宜蘭外海 M_L 6.6 地震的破裂特徵。首先，從遠場 P 波(包含直達 P 波、pP 波和 sP 波)逆推得到此地震的深度為 69 公里、平均震源歷時 4.7 秒、地震矩 1.31×10^{18} Nm (M_w 6.0)和斷層面解 $75^\circ/49^\circ/168^\circ$ 和 $173^\circ/81^\circ/42^\circ$ (strike/dip/slip)。接著，以遠場 P 波逆推的結果在震源處產生不含歷時的直達 P 波當成經驗格林函數，再與觀測直達 P 波進行非負解時間域解迴旋，得到隨測站方位變化的震源時間函數(震源歷時)，其呈現單向破裂特徵，再由破裂方向性分析得到最佳破裂方位 109° 、破裂長度 16.2 公里及破裂速度 3.26 km/s (約是 0.72 倍 S 波速度)。從最佳破裂方位可以確定此地震的斷層面為走向 75° 的面，近似由西往東破裂，此外，從垂直破裂方向的震源時間函數可以確認此地震含有三個子破裂，並非單純的一次破裂，從多重破裂分析顯示由西至東約每 1.2~1.3 秒發生一個子破裂，且每個子破裂的歷時及大小約略相同。

中文關鍵字：遠場 P 波、時間域解迴旋、震源時間函數、破裂速度、多重破裂分析



2019 年秀林(花蓮)地震序列震源歷時與地震矩關係之探討

詹京倍¹、黃瑞德¹、林瓊瑤¹、林采儀¹

(1)中國文化大學地質學系

先前研究已指出 2019 年 4 月 18 日 $M_L 6.3$ 秀林地震餘震序列的地震能量(E_s)與芮氏規模(M_L)間有 $\log E_s \sim 2.0 M_L$ 的關係，但此關係是如何成立呢？在此，本研究將利用震源歷時(T)與地震矩(M_0)之關係來確認 $\log E_s \sim 2.0 M_L$ 成立的原因，除此之外，也可用來探討震源自相似(靜應力降與地震大小無關)的議題。首先，以頻率—波數積分法計算合成波，並調整震源歷時後與觀測波比對，求得最佳的震源歷時，結果顯示秀林地震餘震序列的 M_0 與 T 呈現弱相關，即 $\log T \sim 0.06 \log M_0$ ，此可視為 M_0 與 T 無關，明顯偏離了在震源自相似下的 $\log T \sim (1/3) \log M_0$ 關係，可見秀林地震餘震序列的震源特徵並不符合震源自相似。假設震源時間函數為一等腰三角形，其高(振幅)為 A ，底(歷時)為 T ，此時， $M_0 \sim AT$ 且 $E_s \sim 4A^2/T$ ，也就是 $\log M_0 \sim \log A + \log T$ 和 $\log E_s \sim 2 \log A - \log T$ ，再假設地震規模(M)正比於 $\log A$ ，即 $M \sim \log A$ ，當在震源自相似下會得到 $\log E_s \sim 1.5 \log A \sim 1.5 M$ ，這如同在大地震的 $\log E_s \sim 1.5 M_s$ 關係(M_s : 表面波規模)；反之，當 M_0 與 T 無關，則 $\log E_s \sim 2 \log A$ 。透過 M_0 與 T 的關係探討，本研究得到秀林地震餘震序列的 M_0 與 T 無關，此不符震源自相似條件，也同時得到秀林地震餘震序列 $\log E_s \sim 2.0 M_L$ 關係成立的原因。

中文關鍵字：震源歷時、地震矩、地震能量、芮氏規模、震源自相似性

Correlation between earthquake b value and V_p/V_s ratio in JapanPei-Ying Wu¹、Sean Kuanhsiang Chen¹、Yih-Min Wu²

(1)Department of Geosciences, National Taiwan University、(2)Department of Geosciences, National Taiwan University; Research Center for Future Earth, National Taiwan University; Institute of Earth Sciences, Academia Sinica, Taiwan

Earthquake b value is primarily controlled by differential stress in the crust. Pore pressure has also been reported influencing b value locally. In nature, the effect can only be observed in the subsurface crust by injection wells. It remains unclear whether it can be observed in the entire crust. We assume pore pressure increases proportionally with V_p/V_s ratio to examine the correlation between V_p/V_s ratio and b value. We investigated this correlation in Japan because it is an earthquake-prone country with dense seismic networks and high-quality earthquake catalogs. We calculated b values in the Japan inland region above the 30 km depth using the Japan Meteorological Agency earthquake catalog from 1998 to Feb 2011. We calculated M_c and b value by maximum curvature method and maximum likelihood method in the grids of $0.1^\circ \times 0.1^\circ \times 10$ km with a radius of 30 km from the center of the grids. The b value determination requires the number of earthquakes with magnitudes greater than M_c over 150 within the radius. The V_p/V_s ratios are derived from the National Research Institute for Earth Science and Disaster Resilience. We resampled them to the same grids as b values by either averaging them into the grids or weighting them through a triangular function to the grid's center of b values in depths. We analyzed the b value as a function of the V_p/V_s ratio and binned them within every 0.01 V_p/V_s interval to calculate the means and medians for linear regressions. Our results show little correlation between overall b values and V_p/V_s ratios at the whole study area among different depth ranges. We observed a weak linear negative relation in the binned data at the 10-20 km depth; however, this relation is not likely observed in others depth ranges. We separated the study area into different tectonic regimes and found that the relationship becomes stronger locally. It is consistent with the previous observations that the effect of pore fluid pressure on b value is localized.

Keywords: earthquake b value, V_p/V_s ratio, pore fluid pressure, Japan

Temporal b-value variation before and after $M_L \geq 6.0$ Taiwan earthquakes from 2012 to 2019

Po-Yuan Chen¹、Sean Kuanhsiang Chen¹、Yih-Min Wu²

(1)Department of Geosciences, National Taiwan University、(2)Department of Geosciences, National Taiwan University; Institute of Earth Sciences, Academia Sinica, Taiwan

Recent studies show that earthquake b values gradually decrease before large earthquakes at the epicenters and immediately increase after the earthquakes. Temporal b-value variations may result from crustal stress changes associated with a large earthquake. However, the physical process is rarely observed and remains unclear. Taiwan island is a young orogeny leading to frequent earthquakes with magnitudes greater than $M_L 6.0$, which provides an excellent laboratory to examine the physical process. We calculated b-value variation before and after $M_L \geq 6.0$ Taiwan earthquakes at the epicenters from 2012 to 2019. The period is based on the enhanced earthquake detection capability in Taiwan, which allows the magnitude of completeness (M_c) down to 1.5 in the inland region. We used a relocated earthquake catalog to precisely estimate b value and M_c by the maximum likelihood method and maximum curvature method, respectively. We designed three steps in our research. First, we calculated the b value and M_c at the epicenters of the $M_L \geq 6.0$ earthquakes in overall eight years to know the background seismic activity. Next, we calculated b values and M_c per half year to test the sensitivity between the radius from epicenters (r) and the number of earthquakes with magnitudes greater than M_c (n). Finally, we applied the moving window approach to calculate temporal b-value variations continuously. Our results showed that spatial b values in Taiwan in overall eight years have an average close to 1.0. The b values are systematically lower in the epicenters of $M_L \geq 6.0$ earthquakes from 2012 to 2019. We have determined suitable r and n values for each earthquake. We have observed decreasing and immediately increasing b values before and after the 2018 $M_L 6.3$ Hualien earthquake, respectively, from the relatively stable M_c . We suggest that temporal b-value variations in Taiwan by the $M_L \geq 6.0$ localized earthquakes cannot be observed frequently in our data period.

Keywords: temporal b-value variation, magnitude of completeness, moving window

Station correction of P-Alert network to improve magnitude estimation for earthquake early warning

Yu-Ting Wu¹、Yih-Min Wu²

(1)Department of Geosciences, National Taiwan University、(2)Department of Geosciences, National Taiwan University; Research Center for Future Earth, National Taiwan University; Institute of Earth Sciences, Academia Sinica, Taiwan

Magnitude estimation for earthquake early warning has been shown that it can be achieved by utilizing the relationship among the first three seconds P-wave amplitude, hypocentral distance and magnitude. However, the regression models in previous studies about P-Alert didn't include station correction factors, which may cause non-negligible effects. Thus, to improve the precision of magnitude estimation, we take station corrections into consideration when building the regression model. Station corrections in previous studies are calculated based on empirical interstation difference. Instead, we treat station corrections as missing data and adopt the iteration regression method, which is based on the expectation-maximization algorithm, to determine these unobserved latent variables of the model. By using this method, we are able to approach the values of both the station corrections and the coefficients of the regression model after several iterations. Our results show that after utilizing the iteration regression method, the standard error reduces from 0.273 to 0.257. The station corrections we get range from -0.392 to 0.364, whose distribution is roughly similar to previous study.

Keywords: station correction, ground motion

Effects of crust and mantle heterogeneity beneath the Tatun Volcano Group on synthetic seismograms: A full waveform approach

Chih-Yin Chou¹、Shu-Huei Hung¹

(1)Department of Geosciences, National Taiwan University

The existence of a magma chamber beneath the Tatun Volcano Group (TVG) near the Taipei metropolitan area has recently raised both scientific and public concern but is still under debate. Previous evidence for or against it mostly relies on the ray-based analysis and modeling of P and S arrival times from > 100 km deep earthquakes in the adjacent Ryukyu subduction zone and local earthquake traveltime tomography, thanks to a dense Formosa array of broadband seismographs deployed uniformly across northern Taiwan. On the other hand, with the advent and availability of wave-based numerical methods and high-performance parallel computing, full-waveform modeling and inversion become feasible which leads to resolve the earth's internal structure with much sharper and higher resolution. To explore rich "anomalous" waveform signals resulting from crustal and mantle velocity heterogeneities beneath northern Taiwan, we employ a spectral-element AxiSEM algorithm to simulate seismic wave propagation through 2-D heterogeneous earth models for earthquakes with depth >100 km and $M_w > 4$ occurring in the adjacent subduction zones around Taiwan. The 2-D velocity structure along the great-circle plane is derived from 3-D local tomographic models for the Taiwan region and global models of MIT08 and S40RTS for the region outside of it. The obtained synthetics are benchmarked with those calculated by fully 3-D, but computationally-expensive SPEC-FEM3D_GLOBE and AxiSEM3D methods. By comparing the synthetic seismograms with accuracy up to 5 s for 1D laterally homogeneous and 2D heterogeotneous models with the corresponding observed records at the Formosa and other permanent broadband stations across Taiwan, we will investigate the changes of phase arrival times and waveforms related to the imaged low-velocity bodies beneath the TVG being postulated as the magma reservoir and high-velocity features from the subducted slab.

Keywords: full waveform modeling, AxiSEM, Tatun Volcano Group, Magma reservoir

板塊碰撞轉換至隱沒構造－宜蘭南部地區地震特性

林容辰¹、李恩瑞¹

(1)成功大學地球科學系

台灣地處歐亞板塊與菲律賓海板塊之碰撞造山帶，東北外海有菲律賓海板塊隱沒至歐亞板塊之下而形成的琉球海溝及弧後張裂之沖繩海槽，並在台灣島上擠壓形成貫穿全島中央之脊梁山脈，而東北部陸域即位於兩種構造之轉換帶，其轉換構造與過程至今仍是研究的熱門焦點。

本次研究區域位於宜蘭縣南部，中央山脈最北端之區域，以及其東方海域，其距離台北都會區僅數十公里遠，若在此區域發生較大規模之地震，對台灣政經將產生巨大的威脅，本研究希望從地震數量、分布等，了解此區之孕震構造，對此區域有更進一步的認識。本研究基於中央氣象局自 2012 年至 2019 年間的連續地震觀測資料，進行重新定位後討論區域內的構造分布。在本次研究中利用之重新定位運算方法為 GrowClust，其為相對重新定位法，運用波形、到時差等計算相關性後，再加以分群並進行重新定位。重新定位後之結果與原始地震分布相比，呈現較佳之線性分佈，且有集中的趨勢，對於區域內的構造有更進一步的了解。

另外，本次研究中利用匹配濾波器(Template Matching Algorithm, TMA)建立更完整的地震目錄，TMA 之原理為：使用已知的地震波形作為模板，搜尋連續地震紀錄中類似的波形訊號，以此找尋肉眼難以判別的事件，增加地震目錄的完整性。

中文關鍵字：板塊隱沒、板塊碰撞、地震目錄、模板匹配

Magnitude estimation and on-site earthquake early warning using cumulative absolute velocity in Taiwan

Hao-Yun Huang¹、Yih-Min Wu²

(1)Department of Geosciences, National Taiwan University、(2)Department of Geosciences, National Taiwan University; Institute of Earth Sciences, Academia Sinica, Taiwan

Real-time magnitude determination is one of the critical issues for earthquake early warning (EEW). There are two types of EEW systems, on-site and regional. The on-site EEW system is based on initial P-wave signals to predict ground shakings before destructive waves. Magnitude determination may have a saturation situation using initial seismic signals after an earthquake occurrence. Previous studies utilized eventual cumulative absolute velocity (eCAV) to determine equivalent moment magnitude (M_{ew}) up to 9.0 without any saturation. The eCAV is a good shaking parameter to describe total effective shaking. However, to determine eCAV will be too late for EEW application. To quickly obtain eCAV, 4,754 strong motion records from 64 events with local magnitude (M_L) large than 5.5 in Taiwan are used to establish the relationships between eCAV and integration of five initial shaking parameters (initial CAV, initial cumulative absolute displacement, initial cumulative absolute integral displacement, P_d , and τ_c) for time windows from 1 s to 20 s after P-wave arrival. Our results show that eCAV can be estimated using the integration of five initial shaking parameters. Logarithm linear correlation coefficients vary from 0.77 to 0.97 with standard deviations from 0.25 to 0.10 for time windows from 1 s to 20 s after P-wave arrival. Results show that the correlation coefficient is around 0.91 with a standard deviation is around 0.22 at each time window for magnitude determination. M_{ew} almost follows a 1:1 linear relation with moment magnitude (M_w , Global Centroid-Moment-Tensor) up to 6.8. It is expected that the proposed method can timely estimate M_w for EEW purposes. Additionally, we find that eCAV is a great indicator to describe the intensity of earthquakes similar to peak ground velocity.

Keywords: earthquake, real-time seismology, earthquake early warning, cumulative absolute velocity

利用微地動訊號探討台南台地西緣之地下構造變化

邱連湘¹、吳澄峰¹、周宇廷¹、饒瑞鈞¹

(1)成功大學地球科學系

台南台地位於嘉南平原南端，為一東陡西緩的橢圓形台地，其構造相當特殊，然對於台地的形成機制目前仍存在許多不同的解釋，從過去台南台地地下構造的地球物理資料中，研究主要偏重於東緣後甲里斷層沿線，而有關台地西緣的討論則相對較少。為瞭解台地西緣之地下構造變化，本研究由北至南選定 4 條東西向測線(長 1500~3000 m 不等)，其中，最北端測線位於永康區並橫跨鹽水溪，最南端則位於南區省躬國小附近，每條測線至少以 8 個點進行微地動量測。從單站頻譜比法結果顯示，共振主頻(介於 1.1~1.7 Hz)的變化不大，而同一測線中，放大倍率(介於 1.2~3.7)的變化較為明顯，由台地邊緣西側向東側逐漸增加，且在地表高程 5~15 m 間，放大倍率變化達到最大。為進一步探討在台地邊緣處構造的變化，本研究利用 OpenHVSr 程式反演淺層速度構造，初步結果顯示在台地上方的測站，於淺層 300 m 處，S 波速度達 1000 m/s，此深度可對應至深鑽結果之上部古亭坑層位置(375 m)。另根據所得之二維速度構造剖面，其上部古亭坑的介面深度在測線距離 500-600 m 內，快速由台地邊緣西側(深度~800 m)向東側(深度~300 m)變化，然此一傾斜地層(上部古亭坑介面)的深度於上到台地後變化趨於平緩，此結果與前人利用定年及鑽井資料所繪之剖面相似，而在台地邊緣附近所觀察到之場址放大現象，主要與地下地層厚度與速度的快速變化有關。

中文關鍵字：微地動、台南台地、淺層速度構造

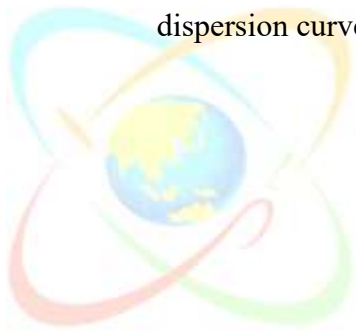
Ambient noise tomography in Southeastern Taiwan

Nguyen Thu Thao¹、Hao Kuo-Chen¹

(1)Department of Earth Sciences, National Central University

Crustal structure in eastern Taiwan is key for understanding the tectonic evolution and interaction between the Philippine Sea and Eurasian plates from subduction to collision. In order to explore the crustal structure in this region in detail, 3-D ambient noise tomography was used with a dense seismic array data set. We deployed 40 temporary seismic stations in southeastern Taiwan in 2019 for about one month. Time series were cross-correlated to construct Rayleigh wave Green's functions. For each station pair, group velocity dispersion curves were picked using a frequency-time analysis and image transformation technique. Then, we applied the direct inversion of surface wave dispersion data to estimate the 3D shear-wave velocity model from these group velocities.

Keywords: Southeastern Taiwan, 3-D ambient noise tomography, group velocity dispersion curves, shallow structure



Study of absorption attenuation of the crust in Kyushu, Japan from the coda of ambient noise cross correlation

Hao-Che Wu¹、Shu-Huei Hung²、Yen-Ting Ko¹

(1)Institute of Oceanography, National Taiwan University、

(2)Department of Geosciences, National Taiwan University

Coda of ballistic waves extracted from ambient noise cross correlation function (NCF) between two stations has been demonstrated to contain multiply-scattered energy whose rate of decay is inversely proportional to the quality factor Q_c , a quantity used to map the scattering and absorption properties of the crust at frequencies <1 Hz. Japan characterized by active volcanoes and frequency earthquakes has established a nationwide high-density seismograph network with continuous seismic recordings for open access. Kyushu in SW Japan is the most seismically and volcanically intensive island sitting in the volcanic front above the subducted Philippine Sea Plate along the Ryukyu trench and Nankai Trough. In 2016, two consecutive earthquakes with magnitude of 6.2 and 7 hit the Kumamoto region within two days in April, and following the eruption of Mount Aso volcano in October. To investigate the absorption attenuation of the crust and possible temporal change impacted by these events, we construct more than 5000 yearly-stacked NCFs between all the available station pairs across Kyushu, using short-period and broadband seismograph records from 2015 to 2017. A strong wavepacket arriving faster than fundamental-mode Rayleigh waves is omnipresent in the NCFs and identified as being generated by a localized stationary noise source from long-period volcanic tremors in Aso volcano. To obtain robust estimates of frequency-dependent Q_c from the coda applied with a series of narrow bandpass filters centered at periods of 2 to 10 s, we exclude these large-amplitude wavepackets and choose the onset time of the coda after the maximum amplitude of the envelope of Rayleigh waves. Besides, the lapse-time dependence of Q_c similar to that estimated by the earthquake coda is also observed and thus the choice of the optimal coda window that yields stable Q_c values needs to be carefully tested.

Keywords: ambient noise cross correlation, coda, seismic attenuation, quality factor

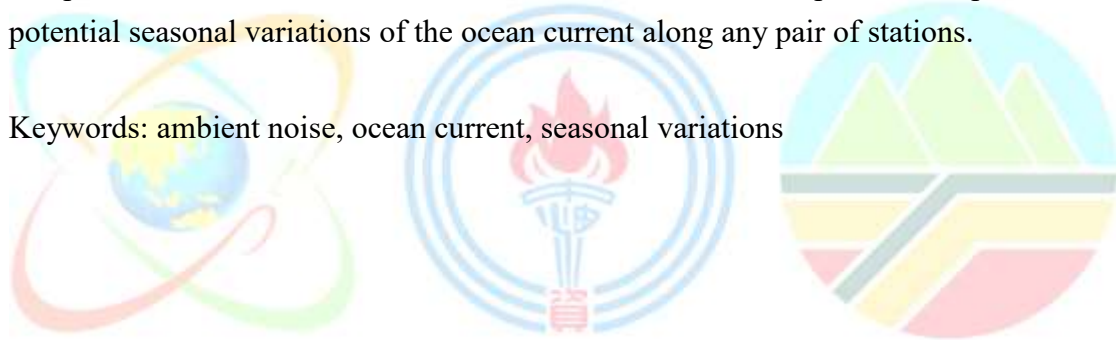
Retrieving the hidden wave signals from oceanic ambient noise

Tony Tsung-Lin Tsai¹、Justin Yen-Ting Ko¹

(1)Institute of oceanography, National Taiwan University

Ambient noise seismic interferometry involving the cross-correlation of continuous signals at different receivers has been widely used to retrieve the Green's functions between any pair of stations. Although many promising results have been demonstrated in recent years, there is no study has been devoted to assessing the possibility for retrieval of ocean waves. The main object of this work is to answer this question whether the technique can be used to obtain the Green's function of the ocean signals. We exploit the ambient noise seismic interferometry to obtain the Green's functions of ocean waves propagating from deep-sea pressure gauges to tide gauge stations deployed in the eastern Taiwan. The preliminary results show that the obtained Green's functions do follow the shallow water equation and can be used to estimate the arrival time of the tsunami propagating from the pressure gauge to the tide stations. The comparison of the Green's function between different stacked periods can provide the potential seasonal variations of the ocean current along any pair of stations.

Keywords: ambient noise, ocean current, seasonal variations



Coseismic velocity reduction and postseismic relaxation of the crust along the Milun fault from ambient seismic noise interferometry

Yi-Ni Chen¹、Shu-Huei Hung¹

(1)Department of Geosciences, National Taiwan University

Coda wave interferometry (CWI) using diffuse ambient seismic noise has been widely applied to monitoring subtle changes of the crustal properties perturbed by tectonic events such as earthquakes, landslides, and volcanism, and seasonal environmental changes such as precipitation, temperature, and atmospheric pressure. In this study, we employ the CWI to investigate coseismic and postseismic velocity variations along the Milun fault, considered as the causative fault of the 2018 Mw 6.4 Hualien mainshock that severely struck the city of Hualien in eastern Taiwan on 6 February 2018. The Python package, MSNoise, is adopted for computing daily-stacked cross-correlation functions (CCFs) of ambient noise recorded by pairs of short-period, strong motion, and broadband stations from CWBSN and BATS and measuring relative time delays (dt/t) and waveform coherence of extracted coda waves between short-term and long-term average CCFs using the Moving-Window Cross-Spectral Method. To enhance the stability of measured dt/t and temporal resolution for continuous monitoring purposes, we apply an adaptive filter based on the S-transform to denoise the daily CCFs and reduce the minimum stacking days for short-term CCFs in secondary microseism frequency band (0.1-0.9 Hz) to be less than 10 days. Preliminary results show sudden increase of dt/t equivalent to coseismic drop in seismic velocity (dv/v) of the crust, most pronouncedly for the station pairs along the Milun fault, and followed by postseismic recovery. In addition, quasi-periodic variation of dv/v is omnipresent, suggesting the seasonal perturbations in the environment probably originated from rainfall and groundwater level fluctuation are substantially detectable. We will dissect the physical causes for these environment fluctuations and remove them from measured dv/v . The remaining dv/v will be further examined for studying the crustal deformation and response to the Hualien earthquake and faulting healing processes.

Keywords: ambient noise, coda wave interferometry, Milun fault, coseismic velocity drop, postseismic relaxation

Ambient noise Full Waveform Inversion along Lanyang River, Ilan Plain, Taiwan– Synthetic tests and application

Fandy Adjil¹、Fanda Fitrianditha¹、How-Wei Chen¹

(1)Department of Earth Sciences, National Central University

Full Waveform Inversion (FWI) is a high resolution method capable of inferring detail subsurface structure and velocity variations. FWI emphasis on utilizing the whole waveform information instead of using first- or reflection arrival time in Travel Time Inversion (TTI). However, FWI may suffer from the potential non-linear nature of the seismic data. The FWI community trying to tackle the high non-linearity problem embedded in FWI through multiscale approach and various objective function formulation. A multiscale FWI approach is performed on the synthetic dataset based on the known Taiwan complex geological fold-bend-fault model provided by CPC to test the capability of the FWI application in central Taiwan area. Synthetic data were generated from the test model. The multiscale approach invert the data with the frequency content of 2, 4, 8, 10, 15, 20 Hz. The result shows promising result as the inverted velocity model are sequentially constructed from smooth-to-detail according to the designated frequency bands. For real data application, ambient noise dataset from Ilan 2004 network is analyzed and studied in this project. The initial model is estimated from the conventional multichannel analysis of surface wave (MASW) inversion. Fifty inter-station cross-correlation gathers were used to construct a 2D profile from Land array data. Preliminary inversion shows wedge-shaped sedimentary basin the Ilan plain thicken from the sea (East) toward mountain (West) direction. To understand its potential generation mechanism, ambient noise data simulation is performed to understand noise generation signatures, effect on the cross-correlation results and compare the synthetic responses with the recorded data. Ambient noise synthetic data are simulated by random source distribution with the random duration and activation time. Data preprocessing including body- and surface waves separation through curvelet transform is necessary before FWI.

Keywords: ambient noise, curvelet, Full Waveform Inversion

Ambient wavefield simulation in ILAN2014 array dataFanda Fitrianditha¹、Fandy Adji Fachtony¹、How-Wei Chen¹

(1)Department of Earth Sciences, National Central University

Ambient noise data is generally attributed to primary or secondary microseisms. The primary microseism is the direct coupling between ocean waves and seafloor. The secondary microseism is the ocean waves once hits the coast, reflect back to the ocean and interacts with another incoming ocean waves and and propagate back to the coast. We simulate the primary and secondary microseisms based on the spectral element method (SEM). The current simulation aims to understand how the coupled acoustic-elastic waves responses while interact with sea-land boundary. Mimic the primary and secondary microseisms along the coastline. Coupled elastic-acoustic waves simulation with excitations occurred inland, ocean, and coastline are studied and analyzed. The 2D model is set to 131x81 km with 1001x621 elements. A total of 163 receivers of ILAN2014 observations are simulated and analyzed through many model setup including model proposed by Su et al, 2019. Different types of sources were initiated along the coastline in a sequential and random manner. Simulating ambient wavefield is challenging for obtaining a reasonable simulation responses within a reasonable computational time. To simulate one-hour ambient noise data, the computational cost is high. Therefore, simultaneous excitation of random sources along the coastline were performed first to obtain the desired 1-hour long records. The simulated data are cross-correlated and stacked to increase the signal-to-noise ratio (SNR). The result shows that the clarity of the extracted high SNR green functions increases as the recording time increases. Simulation also indicate that the body wave arrivals become less visible with the increasing recording time and eventually enhancing surface wave arrivals. The simulation results are consistent with the commonly observed ambient noise records. Such responses are dominated by the wave interferences excited from the Sandiaojiao in the north and Nanfangao-Fenniaolin in the south of Ilan.

Keywords: ambient wavefield, spectral element method, synthetic simulation

利用深度嵌入聚類演算法進行地動訊號分群—以苗栗鹿湖山區為例

王重卿¹、李恩瑞¹

(1)成功大學地球科學系

山崩落石監測系統主要以影像監控搭配邊坡防護欄，一旦偵測到異常即可通知駕駛減速，降低傷亡。然而其方法受到許多限制，例如夜間監測不易、下雨天是落石好發的時段但影像監控的能見度卻不高造成辨識不易，或者崩塌源定位不易，較難及時提出正確警報等等。近幾年落石坍方產生的地表振動訊號能夠被鄰近的地震儀所接收到，落石及崩塌時所產生的地表震動也能夠被地震儀所記錄，地震儀有著連續紀錄且不受氣候影響等優勢，而不同機制（地震、落石、崩塌等等）產生的震動，則會反映在地震儀三分量的記錄上，並且其波形特徵與頻率分佈有肉眼能夠區分的明顯差異。近來已有許多研究成功利用地震波時頻圖(Spectrogram)特徵自動將不同類型的震動源進行分類。而另一方面，隨著近年來機器學習(Machine Learning)相關理論、工具及硬體效能的大幅進步，在地震學領域的應用也展現了巨大潛力，許多研究也嘗試應用機器學習方法於地動訊號的自動辨識中。

目前透過分析山崩、落石所產生的地動訊號搜尋崩塌事件的主要方法為仰賴主觀的人工判讀挑選，此作法除了耗時，更易造成主觀偏誤。苗栗鹿湖山區常有大、小落石崩塌造成道路損毀以及威脅用路人安全。本研究利用架設於該區的四個地震儀測站之地動訊號事件時頻圖進行分析。挑選出可能的地動訊號事件，並以深度嵌入聚類模型(Deep Embedded Clustering)利用非監督式深度學習的自編碼(Autoencoder)學習低維空間的潛在空間並進而學習可能的聚類分佈。自動將訊號類型進行分群並與已知的地震及落石崩塌目錄進行交叉比對加以驗證模型，藉此減少先入為主所造成的主觀偏差並大幅度地降低搜尋崩塌事件的時間。由不同類型地動事件在時頻圖上的特徵差異，藉由非監督式的聚類分析，可以建立出本區域的地動訊號類型特徵，可以讓我們更加的瞭解本研究區域地動訊號的特性。

中文關鍵字：地震學、落石、地震、時頻圖、深度學習、自動編碼器、t-SNE

Ambient seismic wavefield recorded at the seafloor OBS network in the northern Nankai Trough

Hou-Sheng Cheng¹、Emmy T.-Y. Chang¹、Yuancheng Gung²、

Takashi Tonegawa³

(1)Institute of Oceanography, National Taiwan University、(2)Department of Geosciences, National Taiwan University、(3)Japan Agency for Marine-Earth Science and Technology

The ambient seismic wavefield which is mainly excited by oceanic gravity waves can be categorized into three spectral bands: the primary (10-20 s) and secondary (5-10 s) microseisms and infragravity waves (IGWs) (>20 s). Excitation of primary microseisms is converted by nonlinear coupling with local topography between ocean swell and seismic waves on subtle undulation of continental shelves. Whereas, secondary microseisms are derived from storms and wave-wave interaction between ocean gravity waves. The mechanism of IGWs can be explained by the sea-level oscillation affected by the traction force converting from the regional wind field, and are influenced by both offshore leakage and the coastally generated free waves to form the deep-water standing waves. Therefore, the transmitted microseism and IGWs energy depend on ocean wave state and bathymetry. Moreover, the ambient seismic noise converted at the near-shore or from the pelagic areas may exhibit different frequency bands. We provide the spectral analysis of the ambient seismic noise with the data acquired from the Dense Oceanfloor Network System for Earthquakes and Tsunamis (DONET) in the northern Nankai trough. We illustrate the variation of ambient energy with time and space and proceed with the cross-correlation function and cross-correlation beamforming function to discuss its origins and propagations. The spectral analysis shows significant secondary microseisms and IGWs with the DONET data. The secondary microseisms propagated as Scholte waves with velocities of 0.6~0.8 km/s. The peak frequencies of IGWs are in a frequency range of 0.008~0.02 Hz, while they perform a systematical frequency drifting corresponding to the water depth of stations. Besides identifying the potential conversion environment for the ambient seismic noise, our study provides information for the spatial and temporal variation of seafloor noise in the northern Nankai trough.

Keywords: ambient seismic noise, cross-correlation function, cross-correlation beamforming, ocean bottom seismometers

The seismic moment release before-and-after the September 28th, 2018 Mw 7.5 Palu earthquake, Sulawesi, Indonesia

Yopi Ruben Serhalawan¹、Po-Fei Chen¹

(1)Department of Earth Sciences, National Central University

Sulawesi in the eastern Indonesia is a K-shaped island located within a triple junction. There are two slabs (Celebes and Sula) with opposite polarity to the north. The east arm of Sulawesi is categorized as an ophiolitic whereas the southeast arm of Sulawesi is the part of the Australian plate. The west and southwest parts of Sulawesi are the part of Eurasian plate. The central part of Sulawesi exposes the left-lateral Palu-Koro fault and Matano fault with the northwest-southeast direction that associated with extension during the rollback of Banda embayment (Hall, 2012; Hall and Spakman, 2015). On September 28, 2018, the Mw 7.5 earthquake occurred in the Palu-Koro fault with significant left-lateral slip component. This earthquake triggered a tsunami and liquefaction to the city of Palu and the surrounding region with more than 4000 casualties. Before the earthquake, the Palu-Koro fault was considered as a high slip rate (32-45 mm/yr) with low seismicity (Bellier et al., 2001). However, seismicity in Sulawesi is active after the Palu earthquake, including swarm activity in Mamasa region since November 2, 2018 (Supendi et al, 2019), the Mw 6.8 gulf of Tolo earthquake on April 12, 2019, and the Mw 6.2 Majene-Mamuju earthquake which was preceded by Mw 5.7. In this study, we aim at quantifying the seismic moment release of Sulawesi before and after the Palu earthquake. Using data of Global CMT catalog, we divided Sulawesi into boxes of coherent focal mechanism - Mamasa, gulf of Tolo, Majene-Mamuju, etc. We calculated the summation of moment tensors for earthquakes within each box and compare those before and after the Palu earthquake. We expect the results will reveal the seismic behaviour of Sulawesi affected by the Palu earthquake.

Keywords: Palu earthquake, seismic moment release, Palu-Koro fault

Observations of ScS phase by Formosa Array and its applications

Shu-Yun Xie¹、Po-Fei Chen¹

(1)Department of Earth Sciences, National Central University

We examined data of teleseismic events with depth greater than 100 km and magnitude greater than 6.0 as recorded by Formosa Array (FMA), a dense broadband seismic network covering North Taiwan with 140 stations. Among 15 events examined, we found one event (7.06°S, 146.49°E, 146 km, Morro Bay, Papua New Guinea) that exhibits prominent signals of ScS phase. While causes of the clear ScS phase are still under investigation, we calculated the relative arrival time residual (RATR) of ScS for stations of FMA. RATR is a reflection of receiver-side mantle and crust velocity heterogeneity since source-side paths for FMA of one teleseismic event are nearly identical. Resulting pattern of ScS RATR will be examined in the framework of high resolution 3D P-wave velocity model (Su et al., 2019) in conjunction with results of tracing rays by FMTOMO (Rawlinson et al., 2006). Study of the ScS RATR pattern will be expanded to cover whole Taiwan region using data of BATS (Broadband Array in Taiwan for Seismology). Furthermore, the observation of prominent ScS phase not only prompts us to look into the S-to-P conversion (ScSp) at the top of subducting Ryukyu slab for constraint of its geometries. We will also employ a slant-stacking scheme on data of FMA to enhance signals of ScS_{410p} or ScS_{660p} to infer the upper mantle thermal structures beneath NE Taiwan.

Keywords: Formosa Array, ScS phase, relative arrival time residual

Seismic attenuation structures beneath the northeastern JapanChia-Li Yen¹、Justin Yen-Ting Ko¹、Yu-Pin Lin²

(1)Institute of Oceanography, National Taiwan University、

(2)Institute of Earth Sciences, Academia Sinica, Taiwan

Detailed seismic attenuation mapping can provide critical constraints on the thermal evolution of the mantle dynamics. In this study, we investigate the seismic attenuation characteristics beneath northeastern Japan using the regional earthquakes recorded at 343 stations of three different seismic networks (S-net, Hi-net and F-net). Recent deployment of the S-net largely improves the structural resolvability near the trench, in particular at the junction between the Kuril Trench and the Japan Trench. Since the direction of S-net seismometers depends on the layout of marine cables, we correct the rotation angles by multiplying matrices calculated from tilt, rotation, and azimuth before measuring the spectra amplitudes of P and S waves in multiple frequencies using integrals over wavelet transforms. All measurements are referencing to the 1-D synthetics to eliminate the effects from the source and geometrical spreading. We invert the spectra amplitudes for a 1-D frequency-dependent attenuation model. The inverted station residuals, which account for unresolved lateral variations in attenuation structure, suggest stronger attenuation in the volcanic area and the collision region of the Kuril and Japan arcs. On the other hand, for the raypaths passing through the subducting slab are characterized by low attenuation.

Keywords: seismic attenuation, subduction zone, Kuril trench, Japan trench

利用繞射體波探究全球 D'' 區域之速度構造

胡凱傑¹、柯彥廷¹

(1)臺灣大學海洋研究所

自地震學蓬勃發展至今，相對於上部地幔，對於深部地幔速度構造與動力學機制，在不同研究中仍存在相當大的歧異性，特別是位處於核慢邊界的 D'' 區域。科學家認為此區域特別之處在於它有異於其他不連續面的平滑的特徵，存在如同地表大陸與海洋般的高低起伏，以及擁有不同的厚薄分布；近期諸多地震波層析成像的結果顯示，D'' 區域在速度構造上也存在鮮明的差異，快速異常構造多分布於大陸中部與環太平洋地區，慢速異常構造則分布於太平洋中心與非洲大陸西南部區域。前者指示在物質組成與結構上相較於周圍地幔冷而緻密，後者則較為高溫，可能與地幔中的熱柱的湧升及隱沒板塊的沉降有極大的關聯，故研究 D'' 區域能使我們更加了解地球內部的動力機制，一窺地球的奧妙。

為了完整解析 D'' 速度構造之側向變化，本研究蒐集發生在 2005 年至 2020 年規模大於 5.0 的全球深部地震事件傳至全球地震觀測網的資料。雖然我們選擇波相為繞射體波，其波傳路徑大部分伏走於核慢邊界上，保有最多下部地幔的資訊，但並不能排除上部地幔的速度異質性之貢獻。故我們選擇方向來源相近的近震事件來做校正，以確保我們的資料僅保留來自下部地幔的速度特徵。初步檢視我們所下載的資料，繞射核慢邊界的波段均勻分布於全球，高度符合我們所預期的結果，有助於我們檢視全球深部地幔的速度構造。而經過近震校正後的走時殘差與震幅變化，亦更能反映真實下部地幔速度異質性之貢獻。

中文關鍵字：繞射體波、D''、下部地幔、異質性、走時殘差

Application of machine learning for efficient classification on tectonic tremors in Taiwan and Shikoku, Japan

Hao-Yu Chiu¹、Kate Huihsuan Chen²、Kazushige Obara³、Jyr-Ching Hu¹

(1)Department of Geosciences, National Taiwan University、(2)Department of Earth Sciences,

National Taiwan Normal University、(3)Earthquake Research Institute, The University of Tokyo

Tectonic tremor is long-lasting and noise-like seismic signals with the dominant frequency of 2 to 8 Hz. It is generally identified by waveform similarity in envelope with nearly the same arrival at different stations. Without a display of waveforms from multiple stations, discriminating tremors from noises is difficult, especially in the area where the tremors are relatively weak and short such as Taiwan. Is an automatic detection scheme possible across regions? How much the tremor signals can tell us about the source properties and regional differences in physical environment that hosts tremors? This study attempts to explore the signal characteristics of tremors in areas that are naturally separable and different from each other. We used the trained classifier for detecting continuous tremors in Taiwan, eastern and western Shikoku for comparison. Using the tremor waveform from CWBSN in Taiwan identified by Liu et al. (2019) for training data. The tremor events in the Shikoku region were derived from the catalog by Annoura et al. (2016). Here we used the waveform data recorded by Hi-net. To prepare the labeled events composed of the largest number of data, tremors in the catalogs were segmented into 1200-31000 signals with a length of 60 seconds. Using the 60-s-labeled data (1296 tremors in Taiwan; 30888 tremors in Shikoku), we applied k-NN classifier on 29 seismic features to investigate the classification performance. For tremors in Taiwan and eastern Shikoku, the final classification rate is up to 90%; 82.1% for western and eastern Shikoku. This suggests a potential of applying k-NN on tremor detection in different areas. By Fisher's class separability criterion, the optimal feature that allows us to separate tremor in Taiwan from the one in eastern Shikoku is energy of the signals filtered in 0.1-1 Hz. The most distinct feature for tremors in western and eastern Shikoku appears to be energy in the last two-thirds part of the autocorrelation function.

Keywords: tectonic tremors, Shikoku, features, classification rate, k-NN, Fisher's class separability criterion

臺北市區的環境振動特徵

黃宇禎¹、陳卉瑄¹、邱皓瑜²、林正洪³、賴雅娟⁴、史旻弘⁵

(1)臺灣師範大學地球科學系、(2)臺灣大學地質科學系、(3)中央研究院地球科學研究所、國家地震工程研究中心、大屯火山觀測站、(4)國家地震工程研究中心、大屯火山觀測站、

(5)中央研究院地球科學研究所、大屯火山觀測站

近年來，城市地震學備受重視，人們對於非自然起源的微地動訊號備感興趣：人類活動造成的振動可以對應到多大規模的地震？這些振動的時間空間模式和訊號特徵為何？而如何一一釐清振動的起源？藉由分析位於臺北地區的高密度寬頻地震儀 Formosa array 所記錄到的連續地震訊號，可以讓我們探究市區的環境噪音之特徵和起源。利用 2019 年 4 月份在 15 個不同測站的連續資料，我們發現主要頻率分別落在三個區段：1 Hz 以下，3-5 Hz，及 14 Hz。較低頻率 1 Hz 以下，其訊號來源為自然環境的振動。介於 3 Hz 到 5 Hz 的訊號，其來源為重型的交通工具經過或交通工具的來往較不頻繁所引起，然而當交通工具經過較為頻繁時，所產生的頻率約在 14 Hz 左右。不同類別的資料在不同個時段有明顯的人為活動趨勢，各測站間的連續資料相關性，在 <1 Hz 可達到 0.9 的相關係數，而在高頻的區段相關係數大大減低至 <0.5。在該月出現最大振動的，是位於仁愛路附近的 CT08 測站。本研究欲進一步釐清各測站發生異常振動的種類為何？其在訊號特徵的表現與振動起源之關係。

中文關鍵字：城市地震學、環境振動、訊號特徵、高密度寬頻地震儀、臺北市區

The age of Ryukyu subducting slab beneath northern Taiwan inferred from seismic waveform modeling

Yu-Sheng Hung¹、Justin Yeng-Ting Ko¹

(1)Institute of Oceanography, National Taiwan University

The age of Ryukyu subducting slab beneath northern Taiwan inferred from seismic waveform modeling Maxwell Yu-Sheng Hung¹ and Justin Yeng-Ting Ko¹ 1 Institute of Oceanography, National Taiwan University There are two competing scenarios based on the tectonic evolution of western Gagua ridge, believing Huatung Basin (HB) is a trapped piece of an Early Cretaceous ocean basin (125Ma) or is formed in the second spreading era of West Philippine Sea Basin (WPB) (35–50Ma). Therefore the age of the HB plays a critical role in this issue. Scientists endeavor in different aspects to constrain the precise age of HB which includes magnetic field simulation, seismology, thermal modeling and Argon dating. Although there is a general consensus that the birth of HB should be roughly in the Eocene, large uncertainties do exist among different studies ranging from 30 Ma to 125 Ma. In this study, we collected the tele-seismic waveforms with epicenter distance between 30–90 degrees and depth over 100 km recorded by the Broadband Array in Taiwan (BATS). We measure amplitude fluctuations in P-waves comparing to the PREM and characterize the multipathing arrivals caused by the subducting Philippine Sea plate (PSP) from high frequency waveforms. In order to investigate the detailed morphology of the subducting PSP, we use GPU-accelerated Finite-difference method to compute large number of the Green's functions to create a library of the idealized 2D models. We grid search for five model parameters by minimizing the differences in traveltimes, amplitudes and waveform shapes between data and synthetics. The optimal velocity models are converted to thermal structure based on the theorem of Sleep (1973). With a preliminary glance of the simulation results, we suggest that the optimal model would have a better constraint on the slab dynamics and the age of HB. Keywords age, geodynamics, Huatung Basin, morphology, seismology, subducting slab, thermal modeling

Keywords: age, geodynamics, Huatung Basin, morphology, seismology, subducting slab, thermal modeling

TCDP 井下地震儀儀器 15 年長期監測－地震與噪訊

陳文瑜¹、林彥宇¹

(1)中央大學地球科學系

台灣車籠埔鑽探計畫井下地震儀 (Taiwan Chelungpu-fault Drilling Project Borehole Seismometers Array, 簡稱 TCDPBHS) 安裝於 1999 年 Mw 7.6 集集地震最大同震變形 (12m) 之車籠埔斷層北段。井下地震儀所紀錄之高品質地震波形, 許多前人研究已對於此研究區域產生之微地震及斷層帶特性進行深入的分析與探討 (Lin et al., 2012; Wang et al., 2012; Ma et al., 2012; Lin et al., 2016)。TCDPBHS 自 2006 年以來已持續運行近 15 年之久, 本研究分析其長時間之連續波形紀錄的變化, 用以瞭解測站的觀測數據品質在長時間的運行下有無顯著改變。我們分析 15 年間 TCDPBHS 連續波形, 並計算其功率譜密度之機率密度函數 (Probability Power Spectral Density, 簡稱 PPSD), 發現 TCDPBHS 長期噪訊變化並不大, 顯示儀器運作至今依然運作良好。另外, 本研究亦會對監測到之不同類型的微地震, 利用 Lin (2014) 所提出之半自動化的方式進行挑波與分類, 以瞭解 15 年間微地震之活動行為變化, 未來建立 TCDPBHS 之長期完整的地震目錄, 使得這些高品質資料在公開之後能夠更容易地被學界使用。本研究技術將可以直接應用於米崙鑽井計畫之井下地震儀陣列資料分析。TCDPBHS 資料庫預計將於今年在台灣地震科學中心資料庫 (TEC Data Center) 中開放, 歡迎大家多加利用。

中文關鍵字：台灣車籠埔鑽探計畫、井下地震儀、微地震、功率譜密度、機率密度函數

Seismically derived ground tilts induced by the 2010 Chilean tsunami

Jui-Chun Freya Chen¹、Wu-Cheng Chi²、Chu-Fang Yang²

(1)Department of Atmospheric Science, National Taiwan University、

(2)Institute of Earth Sciences, Academia Sinica, Taiwan

We wish to develop new ways to observe tsunami contributes to tsunami research. Tidal and deep-ocean gauges have been used for coastal and offshore observations. However, tsunami-induced ground tilts offer a new possibility. The ground tilt signal induced by 2010 M_w 8.8 Chilean earthquake were observed at a tiltmeter network in Japan. However, tiltmeter stations are usually not as widely installed as broadband seismometers in other countries. Here, we analyzed broadband seismic records from Japan's F-net and found seismically derived ground tilt signals consistent with previously published tiltmeter dataset. We have also included waveforms from broadband seismic networks in other countries, such as Taiwan, as well as an ocean-bottom seismometer, and found similar patterns. In this work, we documented a consistent time sequence of evolving back-azimuth directions of the tsunami waves at different stages of tsunami propagation through beamforming-frequency-wavenumber analysis and particle-motion analysis. Dense broadband seismic networks can provide a useful complementary dataset, in addition to tiltmeter arrays and other networks, to study or even monitor tsunami propagation using arrayed methods.

Keywords: tsunami, ground tilt, broadband seismometer

台南六甲地區孕震構造分析

張筱敏¹、李恩瑞¹

(1)成功大學地球科學系

台南六甲地區在 2020/8/19 單日連續發生 4 起芮氏規模(M_L) 3.8-4.7 的地震，深度皆在 10-11 公里之間，屬於淺層地震。回顧六甲地區的歷史地震事件，以 1862 年的台南大地震最有名，推估的規模可達 6.7，六甲地區一帶之地震活動值得關注。研究資料顯示六甲斷層為一逆衝斷層，全長約 21 公里，傾角約為 30 度向東傾，深度約在 5 至 8 公里，水平抬升速率為 11-12.8 釐米/年，垂直抬升速率為 5.5-6.3 釐米/年，約在 30 萬年前開始活動，目前被列為第一類活動斷層。本研究使用波形交互相關得到之 P、S 波波相相對到時，以 Growclust 重新定位方法，針對此區域內具密集性分布的主餘震序列重新定位，並期望建構更清楚的發震構造樣貌，以了解六甲地區的孕震構造。將六甲地區 2020 年 8 月份的地震資料重新定位後，可發現事件密集分布於地表六甲斷層東側，震源機制解顯示斷層面為北北東至南南西走向，朝東傾約 40 度，而將發震位置依深度投影後發現此區地震事件密集發生於 10-11 公里處，並且呈現 40 度向東傾的趨勢。將研究結果與過去所知的六甲斷層資料作比較，可發現發震深度集中於 10-11 公里之間，並非位於基底滑脫面之上，而傾角（約 40 度與約 30 度）也有明顯的不同。台灣西南部區域以褶皺逆衝帶與覆瓦狀逆衝斷層為主要斷層構造，在麓山帶區域褶皺逆衝帶中，低角度逆衝斷層以造山活動前存在之正斷層的淺層部份作為斷坡向上爬升，透過相關構造觀測與震源資料，推測在更深處可能有造山運動前生成的正斷層影響著此處的活動。六甲地區地震事件在基底滑脫面之下似有另一構造控制著此處的活動，亦有可能為西部斷層活動類型向南延伸分佈的展現，與西南部一帶的褶皺逆衝帶比較，此活動構造可能與造山運動前生成之正斷層有關，而確切構造為何、以及發震的機制與活動則有待進一步的分析與觀測。

中文關鍵字：六甲斷層、地震重新定位、褶皺逆衝帶

深度學習於地震偵測之落地化：連續資料的波相挑選及降低反投影

法之計算開銷

廖勿渝¹、李恩瑞¹

(1)成功大學地球科學系

近來，深度學習算法於地震學之嘗試如雨後春筍冒出，而如何將演算法納入連續，甚至是即時的地震資料處理流程是值得被關注的議題。為了提高模型在動態的波形上偵測地震及波相的穩定性，我們提出了 Marching Mosaic Waveform Augmentation (MMWA)。在模型的訓練資料中加入以不同地震波形拼接而成的資料，並使其隨機前後移動，以模擬多組地震訊號同時出現，以及在判釋的時間窗格內被截切的狀況。本研究以在固定時間窗格內判釋地震 P 波及 S 波到時的模型為例，在時間域上對所有資料點進行移動式的重複判釋，取其中位數以作為模型的穩定輸出。此判釋方式能迫使模型判釋每個資料點時，能同時注意其他資料點隨著時間變化的情形，以模擬人類判釋地震波相到時的行為。反投影法(back-projection)藉由在連續資料上針對多個測站所記錄到的特定訊號（如初達 P 波）建構特徵方程式（如 STA/LTA, Kurtosis 等），在時、空間域進行疊加，以尋找潛在的訊號源。使用傳統的線性方法建構特徵方程式，在連續資料的處理上最大的問題有三：(一)無法分辨 P 波、S 波。(二)無法捕捉在短時間內連續發生之地震，尤其是振幅差異較大之事件。(三)特徵方程式的值無統一單位，偵測閾值設定困難。因此在實務應用上，在地震記錄的三個分量上分別對 P 波及 S 波設計特徵方程式，並使用研究區域的 P 波及 S 波速度模型分別進行演算再疊加是較保守的做法。然而地震波形的變異性甚大，無法以同組參數量化所有地震出現時，所有波相的特徵。本研究以兩百萬餘筆三分量地震記錄(約 5%純噪音，約 25%為 MMWA 所合成的資料)訓練而成的 ARRU (Attention Residual-Residual U-Net) seismic phase picker 進行連續資料的地震偵測及波相判釋，可以很好的緩解上述三個困境。此外，將需要建構並疊加的時間序列函數減少為原本的三分之一，即只輸入模型所產出的 P 波及 S 波偵測函式。其中最大值為 1，最小值為 0，演算法的數值穩定度較高。

中文關鍵字：深度學習、地震偵測、波相挑選、資料增強、連續資料處理

台南左鎮區二寮的海星化石之研究

郭周昱¹、王良傑²、王士偉³、米泓生¹

(1)臺灣師範大學地球科學系、(2)臺南市自然史暨化石研究協會、(3)國立自然科學博物館

本研究透過形態觀察及特徵比較，針對產自台南左鎮地區崎頂層的海星化石進行分類。除了少數標本保存不佳、僅能鑑定至科或屬之標本外，其餘標本皆可鑑定至種；形態特徵為：腕數 5 腕、口面與反口面平坦、體盤相對較小、上緣板(superomarginal)與下緣板(inferomarginal)明顯且對稱、緣板外形呈長方形，板上覆滿顆粒體、帶線(fasciole)明顯、背板較小且呈小柱體狀、腹板呈縱向排列。初步鑑定結果均應歸屬於柱體目(*Paxillosida*)、槭海星科(*Astropectinidae*)、槭海星屬(*Astropecten*)，並且可能皆為同一種；但有些特徵並沒有完整保留下來，例如：腕末端之端板遺失或是留存甚少、背板及腹板殘餘不多、上緣板周圍與體板之間的細棘遺失、第一至第四個上緣板之上側之椎狀棘遺失、從第四個上緣板至腕末端之上緣板中間之小短棘未保存、上緣板與下緣板間之棘刺殘餘甚少，以及篩板遺失。因此鑑定為 *Astropecten cf. vappa*。另，本批化石為目前已知台灣最年輕之海星地質紀錄。

中文關鍵字：化石、海星化石、崎頂層、左鎮



柯式橋石藻 (*Gephyrocapsa kennettii* sp. nov.): 西赤道太平洋

所羅門海域岩芯群發現之中更新世鈣質超微化石橋石屬新化石種

莊智凱¹、魏國彥¹、米泓生²、羅立¹

(1)臺灣大學地質科學系、永續地球尖端科技研究中心、(2)臺灣師範大學地球科學系

我們以高解析影像的場發式掃描電子顯微鏡仔細觀察所羅門海域兩根長岩芯 ODP 1115B 和 MD05-2925 站位的大洋沉積物之鈣質超微化石，發現了一種過去未曾報導過的鈣質超微化石，主要形態特徵在同一個鈣板 (coccolith) 觀察到 *Gephyrocapsa* 屬 (橋石屬) 的橋狀構造及 *Pseudoemiliana* 屬外盤的裂縫特徵，其呈現兩屬之間的過渡形態。由岩芯之有孔蟲氧同位素地層所建立的年代模式，推知此新種的生存年代約為 0.520 - 0.465 Ma。我們將其命名為 *Gephyrocapsa kennettii* (柯式橋石藻)，以彰顯美國加州大學聖塔芭芭拉分校的 James P. Kennett 教授在古海洋學長期的學術貢獻。

本研究以發現於 ODP 1115B 3H2W 90-92cm 的樣本照片中 (氧同位素地層年代約為五十萬年前) 選定了一個 Holotype (正模式標本) 和多個 Isotype (複模式標本)，其形態特徵描述如下：

(1) 鈣板最長軸平均為 3.26 ± 0.22 mm ($n=36$)，短軸平均為 2.71 ± 0.21 mm ($n=36$)，短長軸比例 0.83 ± 0.02 ($n=36$)，大致呈現橢圓形的鈣板形態。

(2) 鈣板外環的裂縫呈鳶形 (不對稱菱形)，不規則分布於外環，裂縫數目為二個到十九個，但多數集中在三到八個之數 (30/36)。屬小型的橋石藻 (鈣板最長軸 < 4 mm)。

(3) 其橋狀構造特徵與鈣板最長軸嚴格呈現僅約 10 度 ($10.5^\circ \pm 1.5^\circ$, $n=36$) 逆時針方向之夾角，與其他橋石屬多呈任意角度分布的夾角不同。

(4) 夾角中心區域為開放式的空心結構，無其他小型橋石屬常見的網狀結構。

柯式橋石藻在鈣質超微化石生物地層和同樣具有不規則數目裂隙之 *Pseudoemiliana* 屬近乎同時絕滅，其生態意義及其在古生物地理上的分布值得再進一步探究。

中文關鍵字：鈣質超微化石、橋石藻、所羅門海

以湖泊泥炭之地球化學特性重建台灣中部自晚全新世之古氣候變遷

連翊豪¹、汪良奇¹、方君而¹、楊育丞¹、徐瑜婕¹

(1)中正大學地球與環境科學系

位於台灣中部濁水溪流域的頭社盆地，為埔里盆地群中晚更新世至全新世的封閉型湖盆；盆地中的連續泥炭沉積，提供了研究古環境變遷的理想材料。先前研究中，以植物孢粉化石分析，重建植被與氣候的變化。故本研究利用多種指標方法分析對其採集的沉積物岩心，包括粒徑、碳屑、燒失量、磁感率等項目。本研究想探討頭社盆地沉積物的特性，與其湖盆周遭的環境變化，在採樣時也提高解析度，以利各指標的交互分析，故採取了總長約 6 公尺的岩心，並以每 2 公分分段，最深處達將近 8 公尺深。

在重建台灣中部山區的古環境變化中，由已完成的放射性碳同位素定年資料得知，此岩心涵蓋範圍約距今 17000~2000 cal BP；由粒徑分析的資料顯示，平均沉積的粒徑在 6.8 μm ，而在 8000~6000 cal BP 期間有幾段明顯的起伏變化出現，出現最小的平均粒徑為 2.1 μm 。本實驗嘗試利用碳屑分析來解釋過去的野火活動與環境變化的關聯，發現在大約 15000 cal BP，有大量的碳屑沉積。先前的研究上，利用燒失量及孢粉資料，得出燒失量低時氣候涼爽、燒失量高時氣候潮濕的結論，本次研究數據平均約有 70%，而在大約 4000~3000 cal BP，出現燒失量低至平均 30%；並且在 9500~5700 cal BP 期間，也有幾次燒失量驟降的情況出現；而在 15000 cal BP~11000 cal BP 中則是平緩的起伏變化。

本研究目的著重在頭社這一萬七千年來的沉積物特性及其環境變遷的分析，利用各指標得到定量的資料，配合詳細的定年結果，得到指標隨時間上的變化，來反映氣候的變化歷史。並探討古氣候的變動特徵或是異常事件。

中文關鍵字：碳屑、野火事件、沉積物

重建一萬一千年來三星妹池之古氣候

劉邦權¹、汪良奇¹、Ludvig Löwemark²

(1)中正大學地球與環境科學系、(2)臺灣大學地質科學系

三星妹池位於宜蘭縣南澳鄉，為三星池旁的濕地。海拔 2100 m，鄰近山地植群隨海拔高度變化明顯分帶。分別為高山植被帶（3500 m 以上）、亞高山植被帶（3000~3500 m）、上部山地植被帶（2000~3000 m）、山地植被帶（1000~2000 m）及下部山地植被帶等。由於百年來森林砍伐，目前三星妹池周圍森林樹種組成以人工造林的紅檜與扁柏為主。

本研究使用三星妹池中 2.5 公尺的沉積物，沉積物中花粉含量豐富，並擁有良好定年控制的 11 個 ^{14}C 定年資料以及 16 個 ^{210}Pb 的定年資料，顯示三星妹池為研究並分析過去一萬一千年來台灣東北部的環境變化的良好地點。其中 ^{14}C 定年使用日曆年校準曲線 INTCAL20，校正後的年代為 cal BP (0 cal BP=1950 AD)。花粉圖譜使用深度對應花粉百分比製作，花粉百分比則是陸生花粉總數為分母。

除了使用花粉資料以外，本研究也使用碳屑資料，根據前人研究，碳屑可以反應當地的火災事件，透過 CharAnalysis，可以將連續碳屑資料中的火災事件以及火災頻率計算出來。

使用 stratigraphically constrained cluster analysis 分析花粉百分比，可劃分為五個孢粉帶，其中 Zone 3 可分為兩個子帶。(Zone 5：11130-10420 cal BP、Zone 4：10420-7960 cal BP、Zone 3-B：7960-4000 cal BP、Zone 3-A：4000-3410 cal BP、Zone 2：3410-790 cal BP、Zone 1：790 cal BP-現代)。結果顯示，三星妹池沉積物內所保存花粉約有 42 種，其中木本植物以 *Alnus*、*Quercus*、*Tusga*、*Pinus*、*Trochodendron* 為常見樹種，草本植物與蕨類則以 *Cyperaceae*、*Poaceae*、*Monolete* 及 *Trilete* 最為常見。

本研究中使用主成分分析花粉百分比，可以得出 PC1 這個指標，代表溫度。根據主成分分析結果、各孢粉帶的組合以及碳屑分析的結果，可以得知在 11140 cal BP 後，氣溫逐漸降低，濕度一直都很低，且有火災事件的發生。直到 10400 cal BP，氣溫持續降低且溼度還是很低，在 9900 cal BP，達到最冷的時期，後持續變暖變濕到 7900 cal BP，而這段時間中都無火災事件。而 7900-4000 cal BP 持續了一段穩定且溫暖且潮濕的時期但這段期間內無火災事件。直到 4000 cal BP 有溫度急遽下降後急遽上升但濕度維持在高值，溫度較 4000 cal BP 之前高，且溼度依然很高，而這段期間內無火災事件。3410 cal BP 後氣溫維持穩定但濕度降至極低，此時火災事件頻率增加，而濕度則是 1620 cal BP 後開始維持定值。到了接近現代，火災事件有大幅增加的趨勢。

中文關鍵字：氣溫、濕度、花粉、孢粉分析、孢粉帶

台灣全新世大炭屑紀錄與火災模式初探

吳妍希¹、劉邦權¹、Ludvig Löwemark²、楊子誠¹、陳豫祥¹、林育仕¹、
汪良奇¹

(1)中正大學地球與環境科學系、(2)臺灣大學地質科學系

沉積物的炭屑分析可重建火災事件並推演氣候狀態，此外自然火災為控制森林演替與全球碳循環的重要因子。炭屑的存在反映人類活動所造成的人為火災，另外自然火災的記錄也可以利用氣候條件的變化去推測火災變化的原因。本研究目的是透過分析宜蘭縣三星妹池、南投縣頭社盆地沉積物的炭屑重建出台灣不同區域完整且連續的火災紀錄。從這兩個地點獲得的岩心分別長 250 公分以及 700 公分，以 1 至 2 公分的深度為間隔，透過分析程式與影像處理計算出各個深度(不同年代)中有多少數量以及面積的炭屑以利去看整體變化的趨勢，可以知道台灣全新世以來的火災歷史。由於這兩個所選地點較少人為擾動，因此其炭屑變化可用來反演台灣全新世氣候乾溼變化，並對台灣不同時間與空間氣候變遷進行比對。

中文關鍵字：炭屑、全新世、火災事件



由地表變形與震度紀錄重建 1839 年緬甸阿瓦(Ava)地震規模

吳昇翰¹、王昱¹、Myo Thant²

(1)國立台灣大學地質科學系暨研究所、(2)Myanmar Geosciences Society

1839/3/23, 緬甸城市阿瓦遭遇震度 9 級的地震(Prachuab, 1988)。該次地震的規模之大, 甚至遠達曼谷也能感受到晃動。歷史紀錄顯示震央應位於阿瓦附近, 幾可確定此次事件的孕震構造是緬甸與巽他地塊間的右移實皆斷層(Sagaing Fault)。實皆斷層以南北向貫穿緬甸, 總長度超過 1000 公里, 持續以約 20 mm/yr 的速率滑移(Maurin et al., 2010)。

實皆斷層沿線在過去 150 年間曾發生多次伴隨地表破裂的災害性地震(如 1930、1931、1946、1956 與 2012 地震), 唯獨密鐵拉至實皆的區段除可能造成 1839 年地震外, 在過去近兩世紀中未有明確的地表同震破裂與地震記錄。以地震再現週期與斷層活動速率而言, 密鐵拉至實皆在過去超過 100 年以上未發生地震, 可能表示該段斷層處於長達數百年的間震期閉鎖之狀態, 並持續累積應力。為了解該地區的斷層活動性質, 本研究試圖確定 1839 地震的地表破裂範圍, 以及透過古地震研究的方法, 嘗試重建密鐵拉區域的斷層活動歷史。

本研究透過高解析度數值地形圖, 標記密鐵拉至內比多附近因斷層活動所造成的地表變形。由地表變形描繪斷層形貌, 判斷研究區域內是否有可作為破裂終點的斷層跡不連續。在斷層跡位置的基礎上尋找錯移量紀錄, 再由錯移紀錄的數值與分布判斷斷層的活動性質。同時檢視區域內的佛寺建築, 從其毀壞狀況與時間推斷是否與地震有關。

透過構造地形判識與野外實查, 本研究發現實皆斷層在密鐵拉至內比多沿線形成 300 公尺寬的斷層錯移帶。於斷層錯移帶中發現數條近乎平行的右移斷層跡與壓力脊、錯斷河、閉塞丘等多種右移斷層常見之活動構造地形。其中可辨識的最小右移量約 1.7 公尺。本研究另於標貝地區找到一開挖露頭, 顯示水平層狀湖相沉積物覆蓋於受擾動且被砂質侵入體貫穿的混亂湖相泥質沉積物之上, 可能與 1839 年地震時斷層破裂所引發的強地動相關。根據 ESI 2007 環境震度分級, 噴砂的尺度說明此事件的震度約可分類在 level IX, 鄰近的斷層應伴隨產生地表破裂。若此紀錄與 1839 年地震地表破裂相關, 1839 年地震的地表破裂範圍應從目前確認的實皆一帶向南延伸至少 150 公里。若加上實皆北方 30 公里 Mingun Pagoda 在 1839 地震中倒塌的紀錄, 我們推論 1839 年阿瓦地震所伴隨的地表破裂最短約 180 km。根據 Wesnousky, 2008 地表破裂長度與地震規模關係經驗公式計算, 最小地震規模應是 Mw 7.6 以上。

中文關鍵字：活動斷層、地震地質、古地震、實皆斷層、緬甸

Shallow rupture pattern of the northernmost Lingding Fault during the 2018 Hualien earthquake: the perspective on aerial photos

Jian-Ming Chen¹、Yu Wang¹、Yu-Ting Kuo²、Shao-Yi Huang³、

James Hollingsworth⁴

(1)Department of Geosciences, National Taiwan University、(2)Department of Earth and Environmental Sciences, National Chung-Cheng University、(3)Institute of Earth Sciences, Academia Sinica, Taiwan、(4)Université Grenoble Alpes

On 6th February 2018, the M_w 6.4 Hualien earthquake occurred near the Hualien City, accompanied with ground deformations along the Milun and Lingding Faults. While post-event field survey provided detailed description and data of the Milun Fault, there was not too much report about the surface rupture and deformations along the Lingding Fault since the surface rupture passed through the Hualien River bed. In order to investigate the shallow rupture behavior of the Lingding Fault during the 2018 earthquake, the pre- and post- earthquake aerial photos are used in this study. We not only map the plausible coseismic surface rupture on the Hualien River bed by visual inspection of the images, but also obtained the surface displacements to determine the spatial pattern and magnitude of offset across the Lingding fault by COSI-Corr. Both approaches reveal clear result within the Hualien River bed, and suggest the 2018 coseismic rupture along the Lingding Fault is dominated by the left-lateral slip, where the displacement decreased from north to south, from $\geq 1.0\text{m}$ near the Hualien River mouth to $\leq 0.4\text{ m}$ south of the Mugua River. Such pattern agrees well to the GNSS RTK field survey result. After that, we conduct a series of half-space fault slip model to fit the sub-pixel correlation data and GNSS RTK survey results. To sum up, the shallow portion of the northernmost Lingding Fault did rupture during the 2018 Hualien earthquake, forming a series of left-lateral surface ruptures with limited fault-normal movement.

Keywords: 2018 Hualien earthquake, Lingding Fault, surface ruptures, aerial photos

由歷史航空照片建置數值地形模型探討 1972 年瑞穗地震瑞穗斷層

向北延伸之活動構造

李應頌¹、王昱¹

(1)臺灣大學地質科學系

台灣東部於 1972 年 4 月 22 日發生規模 6.7(M_w)之瑞穗地震，震源位於瑞穗鄉東方近海深度約 15~29 公里處，為左移逆衝斷層型態破裂。其主震與餘震序列位於 1951 年 10 月花蓮縱谷地震群以南、11 月縱谷地震序列以北，顯示該地震發震斷層可能為 1951 年花東縱谷斷層系統向北破裂之結果。為了解 1972 年瑞穗地震發震斷層與 1951 年縱谷斷層破裂的關聯，以及可能伴隨的地表變形，本研究使用在 1972 年瑞穗地震發生前、後之歷史航照，以運動回復結構(SfM)及多視立體(MVS)之方法建置該地區的歷史數值地表模型(DSM)與正射影像，並透過構造地形判釋及田野調查了解該區域之活動斷層特性與可能的同震地表變形。本研究在海岸山脈西側光復鄉至壽豐鄉一帶，總長約 24 公里的山麓西側發現連續分布之斷層跡，斷層跡沿線可見斷錯河階、斷錯河、閉塞丘、斷層池等多樣的左移活動構造地形；另於東富村阿美族國小等地可見平行排列的活動構造崖與地形抬升，顯示該地區的縱谷斷層系統具有明顯的左移與逆移分量，與 P 波初動法之震源機制解相符。本研究之田野訪談調查結果亦顯示 1972 年瑞穗地震於加里洞至阿托莫地區的地震震度可達改良式麥卡利震度(MMI) VII~VIII 度，暗示 1972 年瑞穗地震為一由南向北傳播的單向斷層破裂所造成。

中文關鍵字：1972 年瑞穗地震、花東縱谷斷層、瑞穗斷層、航空照片、數值地形模型、運動回復結構、多視立體

Reinterpreting Yuli belt serpentinites in eastern Taiwan

Dominikus Deka Dewangga¹、Chin-Ho Tsai¹、Yoshiyuki Iizuka²、
Yui Kouketsu³、Ilona Talvikki Sakaguchi³、Sun-Lin Chung²、Hui-Fen Chen⁴

(1)Department of Natural Resources and Environmental Studies, National Dong-Hwa University、

(2)Institute of Earth Sciences, Academia Sinica, Taiwan、(3)Graduate School of Earth and Planetary
Sciences, Nagoya University, Japan、(4)Institute of Earth Sciences, National Taiwan Ocean University

Serpentinites and metaigneous rocks (metabasalt, metagabbro, and metaplagiogranite) are distributed sporadically in the Yuli belt. These rocks were previously referred to as fragments of dismembered ophiolites (Liou, 1981). The surrounding metasedimentary rocks and some metaigneous rocks were subject to high-pressure (HP) metamorphism. However, the origins and metamorphic conditions of serpentinites are still unclear. This study focuses on serpentinites in the Fengtien (FT), Wanjung (WJ), Tsunkuanshan (TS), and Chinshuichi (CSC) areas. The samples consist of antigorite and magnetite with minor chlorite, olivine, diopside, brucite, talc, and carbonates. Chromian (Cr) spinel is the only relict igneous phase. The compositions of Cr-spinel (Cr#, Mg#, and Fe³⁺%) indicate that the protolith origin of FT and TS serpentinites is abyssal peridotite, whereas WJ and CSC serpentinites are of forearc mantle protolith. Textural features and mineral compositions of olivine (Fo₉₅₋₉₈) and diopside imply a metamorphic origin (cf. Lo et al., 1984). Pseudosection modeling (Perple_X) and the mineral assemblage (atg + mag + chl + ol + di) show that serpentinites from different origins were metamorphosed under similar peak metamorphic temperatures (~550 °C). We assume the pressure conditions of serpentinites according to those of surrounding garnet-bearing metasedimentary rocks (1.4-1.7 GPa; ~550 °C; Yeh, 2019). Serpentinites and surrounding rocks were metamorphosed isofacially (~1.5 GPa; ~550 °C) at great depths (~50 km). This P-T estimation is higher than previously reported (Lan & Liou, 1981). Our results imply that the Yuli belt serpentinites represent materials from a paleo-subduction interface.

Keywords: protolith, Cr-spinel, abyssal, forearc, metamorphism, subduction.

太魯閣帶並非高溫低壓變質帶：來自石榴子石的溫壓新制約

黃韻茹¹、蔡金河¹、葉芝穎¹、Yui Kouketsu²

(1)東華大學自然資源與環境學系、(2)Graduate School of Earth and Planetary Sciences, Nagoya University, Japan

本研究應用近年開發的石榴子石相關地質壓力計，搭配碳質物拉曼光譜地質溫度計(RSCM)，重新計算制約太魯閣帶和平地區泥質片岩之峰期變質溫壓條件。根據變質基性岩的岩石學研究，本變質帶曾經歷綠片岩相至角閃岩相之多期變質作用，最高變質溫度可達約 700 °C，而壓力普遍認為不高於 5 kbar，為一高溫-低壓變質帶(Yen, 1963; Liou et al., 1981; Ernst, 1983; Wintsch et al., 2011)。此變質帶之變質沉積岩因缺乏代表變質相之指標礦物或共生礦物組合，故其經歷之變質溫壓條件尚未釐清。含石榴子石之泥質片岩目前僅知局部出露於和平地區，其峰期變質礦物共生組合為：石榴子石+黑雲母+白雲母+奧長石(An^{27})+石英+碳質物。應用 RSCM 地質溫度計計算石榴子石泥質片岩中的碳質物溫度結果為 510-530 °C，再依此溫度為基準透過石榴石-石英包裹體拉曼光譜壓力計(Enami et al., 2007; Kouketsu et al., 2014)計算得出(包裹礦物殘存)變質壓力為 9-13 kbar。此外，以石榴石-黑雲母地質溫壓計(Holdaway, 2001; Wu, 2019)計算得出變質溫壓分別為 480-500 °C 和 8-10 kbar。計算結果顯示石榴子石泥質片岩的變質壓力明顯高於過去對太魯閣帶的認知，對應形成深度可達 30-40 公里，隱示太魯閣帶或許存在一次與隱沒或碰撞相關之造山運動事件尚待研究。

中文關鍵字：太魯閣帶、變質沉積岩、碳質物、石榴子石、地質壓力計

Structural evolution and active structures of Dezful embayment in Zagros foreland basin deduced from balanced cross section and SAR interferometry

Yu-Ting Tai¹、Jyr-Ching Hu¹、Kuang-Yin Lai²、Ping-Jung Hsieh²

(1)Department of Geosciences, National Taiwan University、

(2)Exploration and Development Research Institute, CPC Corporation

Zagros foreland basin is about 1400 km long, 100-300 km wide, from southeast of Iran to eastern Turkey. This basin was formed since Miocene due to the oblique convergence between Arabian and Eurasian plates. The present-day convergent rate of two plates is about 20-30 mm/yr. The structural development and sedimentary environments greatly contribute to the formation of petroleum system in Zagros basin. At least 60 oil and gas fields have been found by the end of 2009. Therefore, realizing the structural evolution is beneficial to explore petroleum system. Here, we apply Move 2018 to restore the cross section in Dezful embayment to examine the reasonableness and understand the process of structural evolution. In addition, we project the seismic data and GPS data to understand the active structures in this region. Moreover, by using InSAR technique, the surface deformation could be observed appropriately. According to the result of restoration, major faults develop both in-sequence and out-of-sequence thrusting, the shortening is approximately 33 km and the long-term shortening rate would be 1.5 mm/yr parallel to the profile. The most active structure is Mountain Front Fault which accommodated 9.6 km shortening and led Kamarun Anticline to become fault-propagation fold. The GPS result projected to the profile shows Zagros foredeep fault accommodates an insignificant shortening in comparison with whole shortening rate of ~2 mm/yr across the foreland basin. We project earthquake data to correlate the seismicity with the active structures, the high seismicity is located near Mountain Front fault extended to the basement at depth about 20 km. We use multi-temporal InSAR to monitor the deformation patterns in main structures in foreland basin. The preliminary result shows the significant gradient of LOS velocity across the Zagros Foredeep fault, thus we suggest that this structure is active due to the creeping of weak detachment.

Keywords: Dezful embayment, restore cross section, detachment, InSAR, SBAS

Structural evolution and activity of Kirkuk recess in Zagros orogenTing-Yun Lee¹、Jyr-Ching Hu¹、Kuang-Yin Lai²、Ping-Jung Hsieh²

(1)Department of Geosciences, National Taiwan University、

(2)Exploration and Development Research Institute, CPC Corporation

Zagros orogen is part of the Alpine-Himalayan orogenic system and is formed as a result of collision between Arabian Plate and Eurasia Plate with a convergent rate of about 22 mm/yr. Foreland basin of Zagros orogen is one of the most important petroleum-rich area in the world. Kirkuk recess in the northwestern part of the Zagros orogen contains 18% of oil and gas storage of the whole foreland basin. Therefore, a more complete understanding of structural evolution should be helpful to increase the accuracy of oil and gas exploration. This study can be divided into two parts, first we use MOVE 2018 software to restore the balanced cross section in order to investigate the structural evolution of Kirkuk recess. Initial length of the cross section is about 212 km, and gives shortening around 16.3 km after the restoration, 7 km of them being accommodated within the Inner High Folded Zone. The result shows that the deformation propagated from northeast to southwest, which reflects the in-sequence evolution of the low angle basement-rooted thrusts. Because these thrusts don't penetrate the sedimentary cover but connected upward to the basal detachment layer, shortening caused by uplift were propagated to foreland and finally formed detachment folds in sedimentary cover. As the result, deformation style in the study area is characterized by multi-detachment folds detached above a basal detachment level. In the second part of the study, we use Small Baseline Subset (SBAS) technique to deal with D-InSAR data, in order to analyze temporal surface deformation across main fault-related folding within three years. The result shows that hanging wall of Mountain Front Fault have downward movement one year after the 2017 Mw 7.3 earthquake and this implies that Mountain Front Fault continued to slip after the mainshock, thus caused extension on the hanging wall. As the result, we consider Mountain Front Fault is still active nowadays.

Keywords: balanced cross section, Zagros orogen, Kirkuk recess, InSAR, Small Baseline Subset

海岸山脈秀姑巒溪剖面八里灣層之鋁石及磷灰石核飛跡定年研究：

探討源區山脈的剝蝕演化

李政熹¹、陳文山¹、黃奕彰¹

(1)臺灣大學地質科學系

中期中新世以來，海岸山脈從板塊隱沒形成的火山弧，演變為弧陸碰撞的構造環境。前人多針對山脈岩層進行熱定年分析來了解造山帶的時空演化，然而隨著山脈不斷抬升剝蝕，早期出露的岩層已成為碎屑沉積物堆積於盆地中。因此本研究針對海岸山脈秀姑巒溪剖面，採集八里灣層的變質砂岩礫石及砂岩同時進行鋁石核飛跡(ZFT)及磷灰石核飛跡(AFT)定年，輔以砂岩岩象分析，探討脊樑山脈的剝蝕及冷卻歷史。

本研究共分析六個變質砂岩礫石及四個砂岩，礫石年代能反映山脈中特定岩層的抬升冷卻歷史，而砂岩年代頻譜則記錄著源區不同岩層的冷卻年代及剝蝕演化。礫石定年呈現兩種結果：(1) AFT~1.8-1.6 Ma 完全癒合、ZFT~3.4-3.3 Ma 完全癒合；(2) AFT~1.8-1.6 Ma 完全癒合、ZFT 部分癒合；代表源區至少有兩種不同變質度的岩層出露。然而，本研究發現某些砂岩的 AFT 完全癒合峰值~4.0-3.0 Ma，老於同層位礫石的 AFT 年代 ~1.8-1.6 Ma，甚至老於該砂岩的 ZFT 完全癒合峰值，推測此異常的 AFT 年代群應是混合自不同岩層的結果(硬頁岩及板岩)。

砂岩的 ZFT 及 AFT 頻譜皆含有大量完全癒合及部分癒合的年代峰值，且隨著地層層序向上，癒合年代逐漸年輕且含量漸增，顯示 1.5-0.8 Ma 期間山脈已出露大範圍極低度(硬頁岩)至低度變質岩(板岩)，層序上亦呈現反剝蝕現象。此外，根據礫石 ZFT 及 AFT 所記錄的冷卻路徑，源區的變質砂岩層於 3.0-1.5 Ma 開始加速冷卻(剝蝕)，與盆地沉積速率加快的時間相近；由砂岩 ZFT 完全癒合峰值計算的山脈冷卻時間亦向上逐漸減少，顯示在 5.2-0.8 Ma 期間剝蝕速率不斷加快，即源區山脈未達到穩定態。

中文關鍵字：核飛跡定年、鋁石、磷灰石、八里灣層、脊樑山脈、剝蝕歷史

Study of anisotropy of magnetic susceptibility across the southern portion of the Backbone Range, Taiwan

Ya-Chu Tseng¹、En-Chao Yeh¹、Ning-Shan Hsu²、Yu-Ching Chang¹、
Jian-Cheng Lee³、Gong-Ruei Ho³、Ching-Chou Fu³

(1)Department of Earth Sciences, National Taiwan Normal University、(2)Department of Natural Resources and Environmental Studies, National Dong-Hwa University、
(3)Institute of Earth Sciences, Academia Sinica, Taiwan

The Mountain building process is a fascinating and intriguing topic for solid earth research. Taiwan orogen is a classical mountain belt that resulted from on-going arc-continent collision between the Eurasian Plate and the Philippine Sea Plate. The Backbone Range of Taiwan is the oldest geological unit, which is formed and exhumed during subduction and collision. The eastern Backbone Range is commonly composed of the Tananao metamorphic complex and the slate. The former could further be divided into Tarako belt and Yuli belt separated by the Shoufeng shear zone due to the huge age difference between each belt. Although the Tananao metamorphic complex has undergone several deformation events, the mesoscopic mylonitic schists within the Shoufeng shear zone shared the same attitude with the wall rocks of each belt. These observations make difficulty to reconstruct the structural evolution of the Tananao metamorphic complex and examine the role of Shoufeng shear zone. In order to evaluate the deformation imposed on Taiwan orogeny, we plan to explore the different deformation events by investigating the strain pattern across the eastern Backbone Range. This study plans to shed the lights on illustrating deformation domains with the regional strain distribution across the eastern Backbone Range. Anisotropy of Magnetic Susceptibility (AMS) is an efficient tool to analyze the finite strain and characterize petrofabrics and structures. The experiment will measure the principal directions and values of magnetic susceptibility ellipsoid, and further evaluate the mean magnetic susceptibility, the degree of anisotropy, ellipsoid type and strain pattern. Based on the strain distribution inferred from AMS, the changes of deformation across the eastern Backbone Range could be inspected, and the aspects of Shoufeng shear zone can be further characterized.

Keywords: anisotropy of magnetic susceptibility, Backbone Range, Shoufeng shear zone

“梨山斷層”兩側的變質溫度與構造特性

許可亞¹、李元希¹

(1)中正大學地球與科學環境科學系

“梨山斷層”在衛星影像上在眉溪砂岩與廬山層交界附近有明顯的線性構造，大致由東北向西南延伸，經過牛鬥、梨山、霧社、武界等地，全長約 140 公里。但此斷層存在與否仍有爭議，這反映在不同版本的地質圖中有些繪製斷層有些則無。

在支持斷層存在主要證據有“梨山斷層”西側的佳陽層為綠色片岩相，而廬山層為葡萄石-綠纖石變質岩相，存在變質溫度差異，且佳陽層可能為始新世地層而廬山層為中新世地層，存在地層年代差異。近期地震資料的分析似乎亦認為斷層的存在。認為斷層不存在的依據是一些剖面在野外未見重大位移的斷層帶，年代早期斷層位置認為在眉溪砂岩與廬山層間，但此兩地層之間野外並未發現斷層，一些斷層發現於廬山層之中，似乎並不存在重大落差斷層，地層的缺失可能源於不整合。

為釐清此一問題我們初步結合 RSCM 的變質溫度分析、熱定年資料、中視及微視構造討論“梨山斷層”特性。在 RSCM 變質溫度上我們在“梨山斷層”兩側採取密集樣本，分析變質溫度變化，亦在部分剖面進行構造分析。本研究利用拉曼光譜分析岩石薄片中的碳質物，因碳質物具受熱後結晶度提升與結構改變的不可逆性質，以及其分子結構反應出最強一次的熱事件，故常藉此探討變質岩區受熱事件的變質溫度，並將其作為變質溫度分類的依據。當變質溫度夠高時，拉曼光譜的峰值集中在石墨峰 (G)，隨著變質溫度逐漸降低，拉曼光譜的峰值陸續出現缺陷峰 (D1、D2、D3、D4)。依據上述變質溫度所對應的波形特徵，進行峰形分解與擬合曲線等處理，利用 Kouketsu 或 Lahfid 經驗公式，可得相對的變質溫度。

本研究由北至南分別在在中橫(梨山)、霧社、武界採了三組橫跨佳陽層、眉溪砂岩、廬山層的樣本。在中橫剖面，從佳陽層到廬山層接近眉溪砂岩的地區，變質溫度的梯度比起東側的廬山層呈現更大的漸變關係；霧社的研究區域，眉溪砂岩跟廬山層西緣的變質溫度呈現混亂的高低起伏，向東邊驟降後趨於平緩；武界的剖面與霧社的結果較相似，在眉溪砂岩跟廬山層西緣的變質溫度呈現混亂的高低起伏，並且有較大的誤差，向東邊驟降後趨於平緩，並且向西平緩升溫。雖然三個剖面在廬山層西側處都有個降溫梯度較兩側大的區段，變質溫度在約 1-1.5 公里寬下降約 50-70 度。

在武界地區相對露頭較佳，在野外主要要斷層為走向滑移斷層、斷層面向東傾斜逆斷層，若存在“梨山斷層”，應發現斷層面向西的背衝斷層，在微構造亦未見剪切構造發育，因此並未發現“梨山斷層”證據。

在“梨山斷層”附近存在變質溫度梯度較大的變化，但野外未見斷層，我們推測可能於始新世-漸新世的不整合有關，始新世時期為張裂環境，導致較高地溫

梯度，伴隨較高變質溫度，之後始新世地層因正斷層時期的梨山斷層作用抬升侵蝕，之後沉積被動大陸邊緣的中新世地層，此不整合或許是導致變溫溫度梯度變化原因，並非導因於斷層作用。

中文關鍵字：梨山斷層、中橫、霧社、武界、碳質物拉曼光譜、變質溫度



台灣中央山脈東翼玉里帶及板岩帶掘升倒轉及變形歷史研究

楊凱翔¹、李建成²、陳于高¹、何恭睿²

(1)臺灣大學地質科學系、(2)中央研究院地球科學研究所

本研究的目的是，為了更適切地了解台灣中央山脈東翼造山的過程，特別是整個中央山脈發育的扇狀劈理，及中後楔(retro-wedge)的掘升過程。近期的研究指出，中央山脈東翼的玉里帶主要的劈理，可能是在隱沒過程中經歷溫壓峰值 (Peak P/T) 所形成，爾後在掘升(exhumation)過程中，造成了劈理倒轉的現象。在本研究中，我們對沿鹿寮溪及鹿野溪進行了野外調查和薄片分析觀察，並結合近幾年發表的 RSCM 變質溫度，和鉛石鈾鉛定年的資料，提供中央山脈東翼玉里帶及其上覆的板岩帶之構造演化的解釋。

綜合野外調查及薄片觀察的結果，我們將變形作用分為兩期：D1 與 D2，及對應形成的劈理 (S1、S2)。劈理的特徵及位態由西向東的分佈如下：

在玉里帶中的石英雲母片岩，在西側主要是 S0/S1 形成的「向西伸向不對稱褶皺」，及覆蓋其上的「向西傾 (40°-70°) 穿透性最強的 S2」；而玉里帶東側的雲母片岩 (也稱初來層)，主要是 S0/S1 形成的「向東的伸向不對稱褶皺」，及覆蓋其上「向西傾 S2 (30°-40°)」，且 S2 傾角由西向東似乎呈現逐漸變緩的趨勢外，伴隨左移的剪切的伸張線理(220, 10)。

在沈積時期，玉里帶上覆的板岩帶，為中新世隱沒濁流岩中最年輕的地層。其變質度的範圍涵括了由片岩過渡到變質砂岩、千枚岩漸變至板岩。板岩帶在東西向剖面呈現一向西伸向的不對稱褶皺 F1 與伴隨而生的 S1 劈理。在 F1 軸部常可觀察到複褶皺，在翼部則偶可發現發育後期褶皺急折帶 F2 及對應的 S2 劈理，由於是局部發育，顯示 F2 褶皺及 S2 劈理發育的過程，板岩與玉里帶比較是處在相對低溫的環境；而在南北向剖面的褶皺則發育出後期(secondary)的劈理。

在薄片分析結果，玉里帶的早期劈理 S1，明顯的被穿透性的 S2 截穿，在垂直 S2 面 (XZ 面) 觀察到左移剪切；而板岩帶在 S1 褶皺軸部偶有後期的 S2 劈理發育，而 S1 面發育右剪的黃鐵礦型態壓影構造，垂直 S1 面 (XZ 面) 以純剪伸張為主。

綜合構造分析及其他年代學結果，本研究提出以下中央山脈東翼的構造演化。從玉里帶在隱沒初期 (~10-7 Ma)，濁流岩產生褶皺 (D1) 並伴隨 S1 劈理發育。爾後玉里帶持續向東隱沒並開始受到菲律賓海板塊的聚合擠壓 (~7-5 Ma)，產生了第二期的褶皺(D2)，並伴隨了第二期 S2 劈理 (向東傾)。同時上覆濁流岩 (板岩帶) 也開始受變形變質作用並發育第一期的褶皺及板劈理 S1。玉里帶和板岩帶兩者對應近年發表 RSCM 峰值溫度(深度)，分別為 450-500°C (15-20 km) 及 300-375°C (10-12 km)。在持續的板塊聚合過程中，玉里帶及板岩帶開始快速掘升伴隨橫向的左移剪切 (3-0 Ma)，並使 S2 由原本向東傾倒轉成向西傾，同時板岩帶 S1 也受擠壓，發育後期的褶皺 (D2) 與伴隨的急折帶。

中文關鍵字：玉里帶、東板岩、劈理、掘升倒轉



臺灣北部脊樑山脈板岩層年代與地體構造演化 -

利用碎屑鋁石鈾鉛定年法

張秋蓮¹、許緯豪¹、陳文山¹

(1)臺灣大學地質科學系

臺灣北部脊樑山脈的大南澳片岩與上覆的板岩層，兩者以不整合（E 礫岩）或斷層接觸，由於化石的缺乏，上覆板岩層的年代仍有爭論。以往認為板岩層的年代最老為中生代，部分學者推測為始新世或中新世。近期的研究顯示不整合面上覆的變質石灰岩層，含有始新世以來的珊瑚化石，顯示不整合面上覆的板岩層，時代應為始新世或年輕於始新世。此外，一般認為臺灣自中生代晚期以來的碎屑性沉積物是由來自西側華南提供的碎屑沉積物推積而成，然而，近期的研究表示 E 礫岩是侵蝕來自東側大南澳片岩和變質花崗岩的碎屑沉積物推積而成。因此，E 礫岩上覆的板岩層的沉積物來源與當時的地體架構是值得重新討論的議題。本研究藉由採集自和平溪上游板岩層中所夾變質砂岩與變質凝灰岩樣本，利用碎屑鋁石鈾鉛定年法，探究板岩層的年代，並藉由碎屑鋁石頻譜討論板岩原岩沉積物的來源，進而描繪古近紀以來臺灣地體架構演變。

利用碎屑鋁石鈾鉛定年法，得到板岩層的碎屑鋁石頻譜結果，分別落在鋁石年齡族群三角圖（ternary diagram）的白堊紀、始新世-漸新世與中新世範圍內，無法呈現確切沉積年代，表示板岩層原岩的沉積物來源不單只源自西側華南，還包括東側大南澳片岩的物源供應。此外，板岩層中所夾的變質凝灰岩層，最年輕峰值為 34.5 ± 0.2 Ma，顯示始新世-漸新世時期的張裂活動伴隨著部分火成活動，且板岩層原岩的沉積時代可能始於此時期。綜合碎屑鋁石鈾鉛定年結果，顯示古近紀早期，發生張裂活動，基盤（大南澳片岩和變質花崗岩）形成地壘高區（古中央山脈），受到侵蝕進而沉積變質礫岩層（E 礫岩），地塹產生納積空間，堆積始新世-漸新世的沉積物，並伴隨著火成岩類的侵入。古近紀晚期至新近紀早期，整個區域受熱沉陷作用而下沉，堆積中新世以來的碎屑性沉積物。

中文關鍵字：大南澳片岩、E 礫岩、板岩層、碎屑鋁石鈾鉛定年

以熱變質度解析台灣中部雪山－脊梁板岩帶邊界構造運動模式

陳尚謙¹、陳致同¹

(1)中央大學地球科學系

在台灣造山帶中，板岩帶為被動大陸邊緣不同部位沉積物之深埋、隱沒、變質，最終掘升至地表之結果，其中以梨山斷層為界，可再劃分為雪山板岩帶與脊梁板岩帶，二者之地質年代、變形行為、變質度皆有所落差。因此若要對板岩帶，以至於台灣造山歷史有更一步的剖析，作為界線斷層的梨山斷層有不可忽略的研究價值。本研究以拉曼碳質物光譜(Raman Spectroscopy of Carbonaceous Material, RSCM)進行板岩帶變質巔峰溫度(T-peak)高密度量測。RSCM 為一高精度 T-peak 溫度計，其樣本間誤差值可低至 10-15°C，對區域的 T-peak 變化能有更精準的結果。本研究區域於中橫梨山段向北延伸至啞口一帶，界定出雪山-脊梁交界處 T-peak 有約 45-60°C 的陡降。此外預計將 T-peak 結果結合薄片微構造觀察及野外斷層擦痕資料，推論梨山斷層可能的位置、運動模式及變形歷史。

中文關鍵字：拉曼碳質物光譜、梨山斷層、雪山山脈、脊梁山脈板岩帶



台灣西北部竹苗地區找齊正斷層與逆衝斷層銜接及演化關係

吳佩庭¹、楊耿明¹、柯孝勳²、柯明淳²、方星尹²

(1)成功大學地球科學系、(2)國家災害防救中心

台灣西北部新竹苗栗地區為台灣重要科技產業所在地，該區域的活動斷層研究更為重要。本研究區域內依照中油地質圖所繪製之斷層，由北而南分別為東—西走向的新竹斷層與斗煥坪斷層，和東北—西南走向的新城斷層、竹東斷層、北埔斷層與鹿廚坑斷層；其中新城斷層伴隨寶山背斜，並且在地下分之維兩條斷層，北端以新竹斷層為界，南端以斗煥坪斷層為界；而鹿廚坑斷層位於斗煥坪斷層的南側伴隨永和山背斜，斗煥坪斷層向東延伸又連接竹東—北埔斷層及其上盤的竹東背斜。

本研究目的在探討竹苗地區早期正斷層與後來發育之逆衝斷層兩者相互銜接關係，以及斷層面上下盤地層截切線的變化，並提出演化順序模型。本研究結合前人研究與本研究所繪製平衡剖面，並運用 SUKA-GOCAD 建置斷層及地層地下三維模型，提出以下結論：

一、新城斷層以低角度的斷層面連接高傾角新竹斷層，向東分出兩條斷層，且分支點從近地表開始，往南越來越深，最南端再合併為一條斷層，並以低傾角斷層截止於高傾角的作為撕裂斷層之斗煥坪斷層；鹿廚坑斷層則以 S 型連接斗煥坪斷層，並以斗煥坪斷層作為其側斷坡滑移斷層；斗煥坪斷層在東邊連接帶有低角度逆衝斷層特性的北埔斷層與竹東斷層。

二、新城斷層與鹿廚坑斷層地下三維斷層型貌和滑移量本就不一致，顯示兩條斷層為獨立發育的斷層。新城斷層上盤地層背斜型貌較為和緩，且未受到竹東—北埔斷層的影響，和竹東—北埔斷層上盤的竹東背斜為獨立的構造。鹿廚坑斷層上盤背斜東翼則可視為深部獅頭山構造的延伸，形成緊密的向斜，且未見鹿廚坑斷層滑移過側斷坡所形成的背斜。

三、綜合上述特性，可判斷本研究區域演化順序如下：東—西向的斗煥坪斷層及新竹斷層早於竹東—北埔斷層，後鹿廚坑斷層於斗煥坪斷層南邊向北發育，並以斗煥坪斷層作為側斷坡，且部分鹿廚坑層間斷層受到深部獅頭山構造的影響；新城斷層未受到竹東—北埔斷層的影響，於斗煥坪斷層北邊向南北發育，以新竹斷層作為側斷坡、斗煥坪斷層作為撕裂斷層。

中文關鍵字：西部麓山帶、三維地層構造模型、GOCAD 軟體、正斷層再活動

利用數值模型探討中寮隧道之高密度泥貫入體形成之機制

林佳勳¹、王維豪¹

(1)中正大學地球與環境科學系

位於高雄市田寮區的中寮隧道北端出口，剛好位於旗山斷層與龍船斷層之間，自從開通以來便因地表抬升作用而導致道路被嚴重破壞。旗山斷層與龍船斷層為東北-西南走向之逆斷層，但是近幾年的大地測量資料顯示旗山斷層下盤與龍船斷層上盤之間 450 公尺內的同時具有水平伸張與壓縮的地形變，且垂直抬升速率高達 10 cm/yr。然而，此抬升區域為重力異常高區，並非一般低密度貫入體的形成機制。因此本研究使用 2-D 黏彈塑數值模型，希望藉由模擬出符合觀測資料之地表速度以探討此區地形變得形成機制。

本研究模型中包含：古亭坑層、高孔隙流體壓泥層、烏山層以及旗山斷層。根據前人研究，我們認為在古亭坑層深處會因低滲透率、甲烷氣的生成與黏土礦物脫水而形成高孔隙流體壓力。本研究模擬結果顯示，當古亭坑泥岩受到造山運動的推擠後，靠近旗山斷層的高壓泥層開始累積應變，並上抬升，使其上方的古亭坑層產生局部的應力集中，形成斷裂。此時底部的高孔隙流體進入破裂的泥岩，使得斷層因含水與高流體壓而進一步的弱化作用，形成弱面，進而促使高壓泥岩上升形成泥貫入體。隨著破裂面的增長與弱化，泥貫入體上升速度也逐漸增加。綜上所述，本研究認為壓密、脫水與脫氣作用使得超高壓泥岩在中寮隧道地下約 3-5 公里處產生，而造山運動的擠壓使得其上方的泥岩產生破裂，部分的水與天然氣沿著新生的斷層溢出，並弱化泥質斷層面，同時也增加原高壓層的密度。而殘留孔隙壓力仍足以抬升高密度的泥岩，並形成重力高區與異常的抬升速率。

中文關鍵字：中寮隧道、旗山斷層、古亭坑層泥岩、泥貫入體、數值模擬

台灣北部大屯火山溫泉之硫同位素分布特性

洪清宏¹、游鎮烽¹、鍾全雄¹、畢如蓮²、李曉芬³

(1)成功大學地球科學系、(2)中正大學地球與環境科學系、(3)中央研究院地球科學研究所

大屯火山群為台灣唯一的活火山，火山活動造就大屯火山含有豐富的溫泉資源，硫為溫泉中含量最為豐富的元素之一。在火山熱液上升過程中硫同位素會與圍岩作用產生顯著同位素分化，其同位素比值能夠作為熱液系統的來源指標。為區分不同溫泉中熱液系統的來源，本研究分析溫泉硫酸鹽的硫同位素組成，討論硫的來源與分化之現象，並綜合前人研究之其他同位素資料，探討該區域熱液的來源。

本研究的樣本，在大屯火山溫泉地區共有九處，其中以大埔溫泉離海最近，地熱谷溫泉則距海最遠。樣品分別以感應耦合電漿光譜儀（ICP-OES）與感應耦合電漿質譜儀（ICP-Q-MS）測定其主要元素和微量元素濃度；使用陰離子交換樹脂萃取溫泉水之硫元素，最後利用多接收器感應耦合電漿質譜儀（MC-ICP-MS）進行硫同位素分析。初步結果顯示，大屯火山群之溫泉水的硫同位素成分落在-5.2‰~+29.1‰。大埔溫泉與地熱谷溫泉分別為+29.1‰與+26.0‰，具有非常重的硫同位素比值，而四礮坪則是-5.2‰有相對輕的硫同位素比值。其中大埔溫泉的鈉與鎂濃度相對於地熱谷溫泉來得高且接近沿海地區，認為有海水來源的注入。根據硫酸根離子與碳酸鈣濃度，該區域的溫泉水分為酸性硫酸鹽泉與中性碳酸鹽泉。藉由硫同位素比值與主要元素及微量元素變化，搭配前人文獻噴氣口氣體成分，認為大屯火山溫泉中有二次酸化泉生成的可能性。

中文關鍵字：大屯火山溫泉、硫同位素、主要元素

海水蒸發結晶過程元素與硼同位素分化特徵研究

陳柏達¹、游鎮烽¹、鍾全雄¹

(1)成功大學地球科學系

穩定硼同位素因其對不同環境因素的分化差異和特性，在地球科學領域已經被廣泛應用於追蹤滷水及岩鹽形成過程。過去研究大多聚焦於地層中的蒸發岩類相關研究，由於對當時環境因子掌握不足，無法釐清主導硼同位素分化的機制。為解析環境因素對硼同位素分化之影響，本研究以自然開放環境進行海水蒸發實驗，在實驗過程中獲取在強蒸發環境下不同結晶模式的氯化鈉樣品，分析其硼同位素組成，進一步去探討不同蒸發環境條件和氯化鈉結晶型式對硼同位素的分化程度。

為得知海水蒸發鹽在不同蒸發條件和不同結晶形式對硼同位素分化機制，本研究在春季(3月)和夏季(5月)於四草安順鹽場採集各個蒸發池中逐步濃縮的滷水及鹽樣品，以感應耦合電漿光學發射光譜儀(ICP-OES)、離子層析儀(IC)分析其元素組成，並以微昇華純化分離樣品的硼，使用多接收器感應耦合電漿質譜儀(MC-ICP-MS)進行同位素分析。初步結果顯示，在夏季的高蒸發條件下出現浮於蒸發池表面的氯化鈉結晶，其化學特徵符合二維結晶作用(Two-dimensional crystallization)所形成之晶體，在沉澱時間早於池水底部粗鹽，且其鉀含量高。而二維結晶的氯化鈉容易有液包體使其氯化鈉濃度降低，在本次研究的樣品含量僅約70%左右鹽度。而硼濃度可高達18 ppm，為同時期的粗鹽樣品含硼濃度3倍。而兩季粗鹽含硼濃度亦有差異(春季11.5 ppm，夏季6.61 ppm)，將再進一步利用硼同位素了解其關聯性。

中文關鍵字：硼同位素、滷水、蒸發鹽

利用鋰同位素探討降雨強度影響流域系統化學風化之變化情形

許哲維¹、游鎮烽¹、鍾全雄¹、劉厚均¹、陳一菁²

(1)成功大學地球科學系、(2)成功大學生命科學系

矽酸鹽化學風化過程中會消耗大氣中的二氧化碳，是調節長期地球氣候的重要反應，因此了解矽酸鹽化學風化是重要的課題。河流逕流水的主要來源來自降雨及流域內地層中的水，包含地下水、土壤水等，這些水會和矽酸鹽進行水岩反應，因此水的化學組成可提供來自這些水岩反應的訊息。在矽酸鹽中，鋰(Lithium)是一易遷移元素，其同位素組成可作為了解矽酸鹽水岩反應及次生礦物形成過程的指標。台灣位於西太平洋颱風行經路徑上，颱風侵襲常伴隨強降雨事件。為了探討不同降雨強度時，不同風化來源對逕流水中溶解物質的貢獻，本研究針對濁水溪流域中游及上游區域附近的雨水、土壤水以及中游河水進行採樣，分別以 ICP-OES、ICP-QMS、IC 及 MC-ICP-MS 分析樣品的主要元素、微量元素、陰離子濃度以及鋰同位素值($\delta^7\text{Li}$)。

根據樣品之 Sr/Na、Li/Na 的相關性，河流中的鋰在一般時期時，來自上游土壤水的貢獻較大；在高流量時期則主要來自附近的土壤水、雨水及地下水。前人對河水鋰同位素研究指出，一般時期及強降雨時期的 $\delta^7\text{Li}$ 可初步估計上游區域土壤水具有較低的 $\delta^7\text{Li}$ 值，中游則具有較高的 $\delta^7\text{Li}$ 值，顯示上游 $\delta^7\text{Li}$ 的分化程度較中游低。進一步使用雷利分化模型(Rayleigh fractionation model)評估上游土壤水，可由分化係數推估形成次生礦物的程度及種類。根據本研究的鋰同位素值預計能夠區分濁水溪在不同降雨強度時的風化來源及不同次生礦物提供的訊號。

中文關鍵字：矽酸鹽化學風化、鋰同位素、風化來源、土壤水

臺灣東部綠島之火山岩相與火山演化初探

唐懷昱¹、宋聖榮¹

(1)臺灣大學地質科學系

建構臺灣的弧陸碰撞歷史，釐清島弧火山的演化至關重要。海岸山脈、綠島與蘭嶼為呂宋島弧北延的部分，呈現時間與空間上的島弧火山演變序列，提供絕佳的研究題材。不同於海岸山脈已受到弧陸碰撞的影響發生強烈擠壓、抬升以致複雜的變形與侵蝕，綠島雖受到侵蝕，但尚未發生強烈變形，火山噴發物的紀錄仍完整保存。然而前人對於綠島研究多著墨於火山岩的岩象、年代與化學特徵，鮮少提及這些噴發物所代表的火山作用以及弧陸碰撞過程中島弧演化的意義。鑒於上述原因，本研究於綠島進行野外地質調查，檢視與釐清火山岩分佈與產狀，並進行岩象與岩相分析，配合彙整前人研究結果建立火山層序並探討火山演變。

野外調查顯示，綠島東側柚子湖與海蔘坪一帶有放射或水平之柱狀節理熔岩流出露；島的南側(龜灣鼻)至東北側(燕子洞)海岸沿線，有數層可側向追蹤的火山碎屑流、再積性火山角礫岩、凝灰岩層，其岩層的位態走向大致上以柚子湖為中心，向北側呈現 N85°E/30°N，向南呈 N60°W/25°S；露頭常見到錯移距離 0.5~5 m 不等的正斷層，斷層面位態走向並沒有一致的趨勢。分析結果指示綠島東側的火山岩相展現近火山口相之組合特徵，岩層位態顯示東側曾經有一個古地形高區，但於現今地形已不復見。位處弧陸碰撞帶的綠島就大地構造尺度而言，應屬於擠壓的應力環境，卻於島上東側野外露頭可見到許多正斷層；這些正斷層可能與火山噴發與垮塌作用有關，指示有大規模噴發與崩塌事件曾經發生，其與綠島東側的地形高區消失是否有關連，需進一步調查釐清。

中文關鍵字：弧陸碰撞、北呂宋島弧、綠島、垮塌作用

Temporal variation of permutation entropy in seismic noise during three eruption cycles at Shinmoedake volcano, Japan

Diah Ayu Rahmalia¹ 、 K. I. Konstantinou¹

(1)National Central University

Permutation entropy (PE) is a simple complexity parameter for time series that is useful in the presence of observational noise. This study investigated PE variation during three eruptions in 2011, 2017, and 2018 at Shinmoedake volcano. Shinmoedake had its first magmatic eruption in January 2011 and after 6 years, a new activity began in October 2017 and it was followed by another eruption in March 2018. The frequency range 1-7 Hz was used to infer the temporal change of randomness in time series data. Permutation entropy calculation considered the embedding dimension ($m=5$) and embedding delay ($L=2$) in a 20 minutes time window length. The results showed that PE values decreased before each eruption occurred. Decreasing PE values indicated a reduction of complexity that is associated with magma migration to the shallower depth and caused attenuation of seismic waves. Besides, PE also exhibited increasing behavior and suddenly decreased just before the eruption events in 2011, 2017, and 2018. We also analyzed the correlation between tremor depth location and PE values that depicted a negative correlation in each eruption period. PE values would decrease when tremor occurred at a shallower depth and PE values would increase when tremor migrated to larger depths.

Keywords: permutation entropy, Shinmoedake volcano, eruption, Tremor depth location

**Remnant forearc preserved in a paleo-subduction complex?
A new inference from HP metaigneous rocks in eastern Taiwan**

Wen-Han Lo¹、Chin-Ho Tsai¹、Sun-Lin Chung²、Hao-Yang Lee³、

Qiu-Li Li⁴

(1)Department of Natural Resources and Environmental Studies, National Dong-Hwa University、
(2)Institute of Earth Sciences, Academia Sinica, Taiwan; Department of Geosciences, National Taiwan
University、(3)Institute of Earth Sciences, Academia Sinica, Taiwan、(4)State Key Laboratory of
Lithospheric Evolution, Institute of Geology and Geophysics, Chinese Academy of Sciences, Beijing,
China

High-pressure (HP) metaigneous rocks are sporadically exposed in the metasedimentary Yuli belt. Recent studies suggest that the HP rocks were subject to subduction zone metamorphism at depths of ~ 45 to 55 km (e.g. Keyser et al., 2016). The metaigneous rocks, including metabasalt, metagabbro, and metaplagiogranite, together with serpentinite, are interpreted as fragments from dismembered ophiolites with unknown origin (Liou, 1981; Lin et al, 1984). As the remnant of an ancient oceanic lithosphere, these fragments provide an invaluable opportunity to investigate tectono-magmatic-metamorphic evolution of subduction zones. To address this issue, we report the first SIMS U-Pb zircon dates coupled with whole-rock geochemical constraints from the metaplagiogranite and metagabbro in the Chinshuichi area of the southern Yuli belt. Our results show that (1) the SIMS U-Pb zircon analyses of all samples yielded consistent magmatic ages of ~ 17 Ma, which are coeval with the timing of subduction initiation of the South China Sea lithosphere (cf. Shao et al., 2015; Lai et al., 2017); and (2) whole-rock trace element compositions are characterized by negative Nb-Ta and positive Th anomalies, indicating a supra-subduction zone environment (oceanic forearc or volcanic arc). On the basis of available data, we argue that these HP metaigneous rocks represent a remnant from a nascent forearc section during the early Miocene subduction initiation.

Keywords: subduction initiation, high-pressure metamorphism, U-Pb zircon dating, forearc, ophiolite

泰國新生代火成岩之地球化學特徵與岩石成因

徐雅容¹、彭君能²、鍾孫霖³

(1)臺灣大學地質科學系、(2)中央研究院地球科學研究所、(3)中央研究院地球科學研究所、臺灣
大學地質科學系

中南半島各國均受到不同程度晚新生代板內火山活動之影響，產生分布廣泛的玄武質岩石。其中，在泰國的新生代火山岩零星出露，與在越南南部、寮國南部及柬埔寨的新生代火山岩成強烈對比，這現象到底跟岩漿源區或熔融程度有關，跟地體構造及其作用的差異性有關，還是跟岩漿分化的程度有關？此外，綜觀整個中南半島，泰國則是少數有前人研究報導中酸性火山岩的地方，那些分異程度較高的火山岩成因為何？它們與玄武岩的關係又如何？探討以上問題除有助於更了解板內岩漿系統的形成與噴發機制外，對整個東南亞地區的地體構造或許有重要啟示。因此，本研究分析了 61 個採集自泰國不同地區的新生代火山岩，其中包含 Barr and Macdonald (1981)和 Barr and James (1990)所提供的 26 個樣本，進行系統的岩象描述與地球化學分析。

岩象觀察表明，大多樣本受到蝕變的影響有限，保留相對新鮮的斑晶與基質，多數玄武質岩石樣本具有斑狀結構，少數為無斑隱晶質。根據 CIPW Norm，樣本分為鹼性玄武岩、橄欖石拉斑玄武岩、石英拉斑玄武岩及中酸性岩四大類，其中鹼性玄武岩可進一步細分為強鹼性和弱鹼性兩種。鹼性玄武岩和橄欖石拉斑玄武岩具有相似於洋島玄武岩的微量元素特徵，富集大離子親石元素(從原始地函的 20 到 110 倍不等)與輕稀土元素(從原始地函的 70 到 350 倍不等)，重稀土元素相對虧損(從原始地函的 0.5 到 5 倍不等)，相較於不相容性相近的微量元素，鈮、鉭與鈦均沒有呈現負異常，表明岩漿不曾受到地殼混染，或許跟岩漿在地殼上升的過程較為迅速有關。此外，多數樣本呈現鉀的負異常($K/La = 58-384$)，指示岩漿源區可能含有金雲母或角閃石的殘餘相，若此推測屬實，則岩漿的產生可能為曾遭受交代換質之岩石圈地函來源為主。石英拉斑玄武岩微量元素特徵較不一致，元素分布趨勢多在富集型中洋脊玄武岩與洋島玄武岩之間，主因或許跟地函部分熔融程度有關，另一可能的解釋為不同程度的玄武質岩漿與地函圍岩的相互作用。本研究初步排除地殼混染為泰國新生代火山岩岩漿分化機制之一，未來將進一步利用主要元素與微量元素制約岩漿在地函源區形成的過程，並配合待進行的 $^{40}\text{Ar}/^{39}\text{Ar}$ 定年學與 Sr-Nd 同位素測定，試圖提出泰國新生代火山岩最合理的形成機制。

中文關鍵字：泰國、新生代、板內火成岩、鹼性玄武岩、地球化學

印尼爪哇西部新生代火山岩之年代學與地球化學特徵

梁瑋琪¹、賴昱銘¹、李皓揚²、辛怡儒³、Lediyantje lintjewas¹、

Iwan Setiawan⁴、Long-Xiang Quek¹

(1)臺灣師範大學地球科學系、(2)中央研究院地球科學研究所、(3)臺灣大學地質科學系、

(4)Research Center for Geotechnology, Indonesian Institute of Sciences (LIPI)

東南亞地區位於三大板塊，歐亞板塊、菲律賓板塊和印度—澳洲板塊聚集邊緣的交匯處，同時也包含了數個活躍的板塊隱沒帶，並有著許多由早期岡瓦納古大陸(Gondwana)分裂的地殼，歷經古生代至新生代的地質構造活動後聚集至現今東南亞位置。爪哇島位於巽他古陸(Sundaland)的南緣，為一平行於巽他-班達隱沒帶(Sunda-Banda Subduction Zone)之島嶼，依照大地構造的分布可分為西爪哇、中爪哇、東爪哇三個地塊。西爪哇以新生代火山島弧為主，其北部為巽他古陸大陸基盤，中、東爪哇以白堊紀增積的蛇綠岩體及島弧岩石為主，南部殘存的部分太古代大陸地殼則平行分布於爪哇全島。針對西爪哇研究的部分，前人在定年工作上有數個第三紀的鉀氬定年結果，並初步討論新生代火山在空間上的分佈；地球化學部分，前人工作僅有全岩主要元素的分析，因此本研究將於西爪哇地區採樣並進行了更詳細的定年與地球化學分析，從而試取得西爪哇地體演化架構相關線索，以及西爪哇各期火山活動之年代。

本研究於西爪哇採集了新生代之火山岩(共 55 個)，並依照火山和地理位置把樣本分成五群(Danau 火山體、Bayah Dome 北部、Bayah Dome 南部、Gede 火山體、Ciemas 火山體)，進行鋁石鈾鉛定年分析與全岩地球化學分析。鋁石鈾鉛定年初步結果可將西爪哇的火山岩分兩期，分別為中期中新世(11~17 Ma) 到晚期中新世(5.4~9.9 Ma)及更新世(小於 1 Ma)。空間上的分布：中期到晚期中新世出露在整個 Bayah Dome 地區(南、北部)；更新世火山岩為整個西爪哇最年輕的火山岩體，主要出露在 Danau 火山體、Bayah Dome 北部和 Ciemas 火山體；從初步結果可得知第三紀的岩漿活動具有由西爪哇南部向北部，呈現年代愈趨年輕的現象並呼應前人使用鉀氬定年結果之相同推論。另外，在 Bayah Dome 北部具有白堊紀年代約 140 Ma 之繼承鋁石紀錄，並可對比至蘇門答臘同時期的岩漿活動，顯示此岩漿活動由蘇門答臘南延至西爪哇北部。全岩地球化學中，主要元素指出此區域火山岩主要為鈣鹼質的玄武岩至石英安山岩 ($\text{SiO}_2 = 45\sim 69 \text{ wt.}\%$)；微量元素部分，輕稀土元素對重稀土元素有相對較富集的現象和微銷負異常，並且呈現高場強元素 (high field strength elements, HFSEs) 虧損，特別是鈮、鉍及鈦(TNT)等元素，以及大離子親石元素(large ion lithophile elements, LILEs)富集，呈現典型的島弧岩漿地球化學特徵。

本研究發現印度—澳洲板塊在西爪哇地區呈現多階段的隱沒作用，並可將島弧火山的空間分布與噴發時間相聯結，地化部分還有待後續的全岩鋁鈹同位素與鋁石鈾同位素資料獲得後，做更進一步的岩石成因的探討。

中文關鍵字：印尼爪哇、巽他島弧、新生代火成岩、鋁石鈾鉛定年法、全岩地球化學

